

UNIVERSITAT ROVIRA I VIRGILI

TWO-DIMENSIONAL INFRARED CORRELATION SPECTROSCOPY AND MULTIVARIATE CURVE RESOLUTION

METHODS: APPLICATION TO QUANTITATIVE MONITORING OF CURING PROCESS

Nicolas Spegazzini

ISBN:978-84-693-4049-3/DL:T.998-2010

TWO-DIMENSIONAL INFRARED CORRELATION SPECTROSCOPY AND MULTIVARIATE CURVE RESOLUTION METHODS

Application to quantitative monitoring of curing process

Doctoral thesis

Nicolas Spegazzini

Tarragona, 2010



UNIVERSITAT
ROVIRA I VIRGILI

DEPARTMENT ANALYTICAL CHEMISTRY
AND ORGANIC CHEMISTRY



CHEMOMETRICS, QUALIMETRICS
AND NANOSENSORS GROUP

UNIVERSITAT ROVIRA I VIRGILI

TWO-DIMENSIONAL INFRARED CORRELATION SPECTROSCOPY AND MULTIVARIATE CURVE RESOLUTION

METHODS: APPLICATION TO QUANTITATIVE MONITORING OF CURING PROCESS

Nicolas Spegazzini

ISBN:978-84-693-4049-3/DL:T.998-2010

UNIVERSITAT ROVIRA I VIRGILI

TWO-DIMENSIONAL INFRARED CORRELATION SPECTROSCOPY AND MULTIVARIATE CURVE RESOLUTION

METHODS: APPLICATION TO QUANTITATIVE MONITORING OF CURING PROCESS

Nicolas Spegazzini

ISBN:978-84-693-4049-3/DL:T.998-2010

UNIVERSITAT ROVIRA I VIRGILI

TWO-DIMENSIONAL INFRARED CORRELATION SPECTROSCOPY AND MULTIVARIATE CURVE RESOLUTION

METHODS: APPLICATION TO QUANTITATIVE MONITORING OF CURING PROCESS

Nicolas Spegazzini

ISBN:978-84-693-4049-3/DL:T.998-2010

Cover's: Ramos Russo family

Editor: N. Spegazzini (Thank you N. Bhatt!!!)

Typesetting: L^AT_EX 2_ε

TWO-DIMENSIONAL INFRARED CORRELATION SPECTROSCOPY AND MULTIVARIATE CURVE RESOLUTION METHODS

Application to quantitative monitoring of
curing process

Doctoral Thesis

Department
Analytical Chemistry and Organic Chemistry



UNIVERSITAT ROVIRA I VIRGILI

Tarragona
2010

UNIVERSITAT ROVIRA I VIRGILI

TWO-DIMENSIONAL INFRARED CORRELATION SPECTROSCOPY AND MULTIVARIATE CURVE RESOLUTION

METHODS: APPLICATION TO QUANTITATIVE MONITORING OF CURING PROCESS

Nicolas Spegazzini

ISBN:978-84-693-4049-3/DL:T.998-2010

TWO-DIMENSIONAL INFRARED CORRELATION SPECTROSCOPY AND MULTIVARIATE CURVE RESOLUTION METHODS

Application to quantitative monitoring of
curing process

Dissertation Presented by
Nicolas Spegazzini
to Obtain the Degree of Doctor from the
Universitat Rovira i Virgili

Supervisors: Prof. María Soledad Larrechi García
and Dr. Itziar Ruisánchez Capelástegui

Department
Analytical Chemistry and Organic Chemistry



UNIVERSITAT ROVIRA I VIRGILI

Tarragona
2010

UNIVERSITAT ROVIRA I VIRGILI

TWO-DIMENSIONAL INFRARED CORRELATION SPECTROSCOPY AND MULTIVARIATE CURVE RESOLUTION

METHODS: APPLICATION TO QUANTITATIVE MONITORING OF CURING PROCESS

Nicolas Spegazzini

ISBN:978-84-693-4049-3/DL:T.998-2010



UNIVERSITAT
ROVIRA I VIRGILI

DEPARTAMENT DE QUÍMICA
ANALÍTICA I QUÍMICA ORGÀNICA

C/ Marcel·lí Domingo s/n

Campus Sescelades

43007 Tarragona

e-mail: secqaqo@urv.cat

Dr. María Soledad Larrechi García, Professor and Dr. Itziar Ruisánchez Capelástegui, Associate professor of the Department of Analytical Chemistry and Organic Chemistry at the Universitat Rovira i Virgili,

CERTIFY:

That the Doctoral thesis entitled:

**“TWO-DIMENSIONAL INFRARED CORRELATION
SPECTROSCOPY AND MULTIVARIATE CURVE
RESOLUTION METHODS**

**Application to quantitative monitoring of curing
process”, submitted by**

Nicolas Spegazzini to obtain the degree of Doctor from the Universitat Rovira i Virgili, has been carried out under our supervision in the Chemometrics, Qualimetrics and Nanosensors research group at the Universitat Rovira i Virgili, and all results presented in this thesis were obtained in experiments conducted by the mentioned Doctoral student.

Tarragona, February 2010

Dr. María Soledad Larrechi García _____

Dr. Itziar Ruisánchez Capelástegui _____

UNIVERSITAT ROVIRA I VIRGILI

TWO-DIMENSIONAL INFRARED CORRELATION SPECTROSCOPY AND MULTIVARIATE CURVE RESOLUTION

METHODS: APPLICATION TO QUANTITATIVE MONITORING OF CURING PROCESS

Nicolas Spegazzini

ISBN:978-84-693-4049-3/DL:T.998-2010

*La intelectualidad
es un pañuelo al aire,
tan ilógica como el Ático
frente a los xilófagos.
El roble habla un idioma
que no rehúye el viento,
pero la biblioteca
sí.
(El Hombre es simplemente
un estornudo.)
J. Ramón Couchet*

*“The Ancient Japanese
considered the Go board to be a
microcosm of the universe.
Although when it is empty it
appears to be simple and
ordered, in fact, the possibilities
of gameplay are endless. They
say that no two Go games have
ever been alike. Just like
snowflakes. So, the Go board
actually represents an extremely
complex and chaotic universe...”
- Max Cohen’s mentor Sol
Robeson, in π*

UNIVERSITAT ROVIRA I VIRGILI

TWO-DIMENSIONAL INFRARED CORRELATION SPECTROSCOPY AND MULTIVARIATE CURVE RESOLUTION

METHODS: APPLICATION TO QUANTITATIVE MONITORING OF CURING PROCESS

Nicolas Spegazzini

ISBN:978-84-693-4049-3/DL:T.998-2010

UNIVERSITAT ROVIRA I VIRGILI

TWO-DIMENSIONAL INFRARED CORRELATION SPECTROSCOPY AND MULTIVARIATE CURVE RESOLUTION

METHODS: APPLICATION TO QUANTITATIVE MONITORING OF CURING PROCESS

Nicolas Spegazzini

ISBN:978-84-693-4049-3/DL:T.998-2010

To my family

In memory of

Matilde

and

J. Ramón Couchet

UNIVERSITAT ROVIRA I VIRGILI

TWO-DIMENSIONAL INFRARED CORRELATION SPECTROSCOPY AND MULTIVARIATE CURVE RESOLUTION

METHODS: APPLICATION TO QUANTITATIVE MONITORING OF CURING PROCESS

Nicolas Spegazzini

ISBN:978-84-693-4049-3/DL:T.998-2010

Acknowledgments

UNIVERSITAT ROVIRA I VIRGILI

TWO-DIMENSIONAL INFRARED CORRELATION SPECTROSCOPY AND MULTIVARIATE CURVE RESOLUTION

METHODS: APPLICATION TO QUANTITATIVE MONITORING OF CURING PROCESS

Nicolas Spegazzini

ISBN:978-84-693-4049-3/DL:T.998-2010

During this thesis I was supervised by Prof. María Soledad Larrechí García and Dr. Itziar Ruisánchez Capelástegui and the work was undertaken in the Chemometrics, Qualimetrics and Nanosensors Research Group, from the Analytical and Organic Chemistry Department at the Universitat Rovira i Virgili in Tarragona, Spain. I would like to thank my supervisors for their constant support and their advices during this period. I also want to thank the head group, Prof. F. Xavier Rius, and all the members from the Chemometrics, Qualimetrics and Nanosensors Group for the pleasant moments we shared together. I don't have to forget Prof. Virginia Cádiz, Prof. Angels Serra and Prof. Ana Mantecón from the Polymer Research Group.

I must also thank Dr. Michael Amrhein for his excellent condition, either human and professional and Prof. Dominique Bonvin for giving me the possibility to stay in the Automatic Control Laboratory, Swiss Federal Institute of Technology at Lausanne (EPFL). A special thanks to Nirav Bhatt, Patrice Müller.

Finally, the Spanish Ministry of Education and Science (MEC) for the doctoral fellowship AP2006-04172.

UNIVERSITAT ROVIRA I VIRGILI

TWO-DIMENSIONAL INFRARED CORRELATION SPECTROSCOPY AND MULTIVARIATE CURVE RESOLUTION

METHODS: APPLICATION TO QUANTITATIVE MONITORING OF CURING PROCESS

Nicolas Spegazzini

ISBN:978-84-693-4049-3/DL:T.998-2010

Invoco al recuerdo (cuasi cristalino) cuando Liliana me recomendaba a través de Pablo, para realizar un doctorado, en la Univeritat Rovira i Virgili. Debo y agradezco a ellos el cambio de paradigma, que fui recogiendo a lo largo de estos años.

Soy consciente de mi insolencia y juventud...

Alguien dijo una vez

“Soy tristemente consciente que esta es la única parte atractiva de una tesis, lo único que será leído” “La tesis es el epílogo de los agradecimientos”

Yo diría el prefacio, más que nada. Reflexiono en que es la seducción y atracción de lo íntimo, y sentimental de la propiedad privada, que por instantes roza lo banal. Creo que es parte de la condición humana, sería un ingenuo no pensarlo.

Recibí, y sigo recibiendo. Intento devolver correspondiendo. En verdad, a través de pequeños artilugios, ya que las palabras se vuelven superfluas a estas horas... pero (siempre) con la grandeza de lo casi exacto y tal vez casi puro.

Por eso quiero nombrar la confianza y libertad, por momentos casi ciega de María Soledad Larrechi García y Itziar Ruisánchez Capelástagui, permitiéndome explorar, a veces con ciertas limitaciones propias del aprendizaje, y el hecho de conocer las limitaciones de mi propia limitación e inexperiencia de la juventud, mi camino en la investigación, como también de lo inverosímil que es esta.

Hago uso de la razón; que he hecho honor y justicia a la confianza y libertad depositada, llegando hasta al final de mis fuerzas en busca de lo que a mi pesar, es un suceso fuera de lo común.

De los tantos pensamientos este fue el único que me consiente (hasta el momento), satisface mi sed y puedo exteriorizar en cierta parte, después de mucha reflexión.

Algunos dicen que tenemos vacío interior, al menos yo lo poseo... transitamos y basamos nuestra existencia en la búsqueda del saber ¿cómo? llenarlo.

Algunos con la superación del “todos los días”, como individuo y/o como integrante de un inconsciente colectivo.

Dos *vacíos* me aquejan, uno *real* y otro *tácito*...

Realmente, espero cancelar esa deuda pendiente con mis padres, que solo será paga a través de mis acciones a generaciones futuras. El resto lo guardo en antologías kafkianas.

Tácitamente, siento que debo disculpas a gente por mis actitudes, infiero que es parte de mi personalidad, acompañado de la torpeza, desazón y obsesiva búsqueda por momentos insana, de valores éticos. Desearía poder tener mi redención, pero no es el momento, ni la ocasión. Porque carezco aún de esa contundencia, exactitud, sofisticación y el minimalismo de la madurez trabajada desde la experiencia.

Puedo decir que he formado parte de un grupo, de mis amistades y fundamentalmente de una familia. Y no puedo dejar de pensar como estos últimos años me han cambiado la cosmovisión del mundo. Doy gracias a todos.

No quedo exceptuado de culpa y cargo...

Scope

UNIVERSITAT ROVIRA I VIRGILI

TWO-DIMENSIONAL INFRARED CORRELATION SPECTROSCOPY AND MULTIVARIATE CURVE RESOLUTION

METHODS: APPLICATION TO QUANTITATIVE MONITORING OF CURING PROCESS

Nicolas Spegazzini

ISBN:978-84-693-4049-3/DL:T.998-2010

The curing process of epoxy resin directly affects the properties of the final polymer [2-3], so it is of great interest to develop analytical methods that make it possible to determine the pathway of the curing processes. Numerous studies have examined the evolution of the curing process and the quantification of the corresponding kinetic parameters using various techniques, such as differential scanning calorimetry (DSC) [4], differential scanning calorimetry with temperature modulation (MTDSC) [5], thermogravimetric analysis (TGA) [6], fluorescence [7], Raman spectroscopy [8], nuclear magnetic resonance (NMR) [9], high-resolution liquid chromatography (HPLC) [5,10], Fourier transform infrared spectroscopy (FTIR) [11,12] and near-infrared spectroscopy (NIR) [13-18]. Most studies use model reactions because it is very difficult, and sometimes even impossible, to isolate the intermediate products that are involved in the curing process. This thesis aims to explore the possibilities of two-dimensional correlation spectroscopy for the quantitative monitorization of curing processes by means of infrared spectroscopy and curve resolution methods. The thesis focuses on a complex reaction in which several side reactions might take place, most or all of them almost simultaneously.

This main goal is pursued as follows:

1. Analysis of generalized two-dimensional correlation spectroscopy and perturbation-correlation moving-windows two-dimensional correlation spectroscopy as a tool for obtaining information about the reaction pathway.
2. Analysis of sample-sample two-dimensional correlation spectroscopy as a tool for obtaining concentration profiles of the chemical species involved in the curing process.
3. Use of global phase angle generalized two-dimensional correlation spectroscopy to determine the optimal number of iterations in the optimization-step for the quantitative resolution by means of multivariate curve resolution - alternating least squares (MCR-ALS).

UNIVERSITAT ROVIRA I VIRGILI

TWO-DIMENSIONAL INFRARED CORRELATION SPECTROSCOPY AND MULTIVARIATE CURVE RESOLUTION

METHODS: APPLICATION TO QUANTITATIVE MONITORING OF CURING PROCESS

Nicolas Spegazzini

ISBN:978-84-693-4049-3/DL:T.998-2010

Structure

UNIVERSITAT ROVIRA I VIRGILI

TWO-DIMENSIONAL INFRARED CORRELATION SPECTROSCOPY AND MULTIVARIATE CURVE RESOLUTION

METHODS: APPLICATION TO QUANTITATIVE MONITORING OF CURING PROCESS

Nicolas Spegazzini

ISBN:978-84-693-4049-3/DL:T.998-2010

The thesis is structured in several chapters, as set out below.

Chapter 1 presents the background to this thesis, highlighting the current interest in studying epoxy resins. The theory of two-dimensional spectroscopy analysis is briefly reviewed and the relevant chemometric tools (multivariate curve resolution methods) are presented. This chapter also discusses the novelties introduced in the thesis and provides references for the underlying basic concepts.

Chapter 2 concerns the experimental work. The instrumental analytical techniques used to monitor the curing process are briefly described. The experimental conditions and setup of two main curing reactions are described: a reaction between phenyl glycidyl ether (PGE) and γ -butyrolactone monitored by NIR, and copolymerization between diglycidyl ether of bisphenol A (DGEBA) and γ -valerolactone by FTIR/ATR. The conditions of the DGEBA homopolymerization are also presented. Finally, the ^1H and ^{13}C NMR experimental conditions for obtaining the spectrum of the final product in the first reaction between PGE and γ -butyrolactone are described.

Chapter 3 presents the results of the experimental work that has been carried out. This chapter cites five published works, each introduced with a brief description of the study's main goal and content. The five articles are presented in sequential order according the main goal of the thesis.

Chapter 4 contains the conclusions and describes the goals achieved.

UNIVERSITAT ROVIRA I VIRGILI

TWO-DIMENSIONAL INFRARED CORRELATION SPECTROSCOPY AND MULTIVARIATE CURVE RESOLUTION

METHODS: APPLICATION TO QUANTITATIVE MONITORING OF CURING PROCESS

Nicolas Spegazzini

ISBN:978-84-693-4049-3/DL:T.998-2010

CONTENTS

Acknowledgments	i
Scope	vii
Structure	xi
1 BACKGROUND	1
1.1 Cationic curing of epoxy resins	3
1.2 Two-dimensional spectroscopy analysis	5
1.2.1 Generalized two-dimensional correlation spectroscopy (variable-variable 2DCOS)	5
1.2.2 Global phase angle	9
1.2.3 Sample-sample two-dimensional correlation spectroscopy (SS-2DCOS)	9
1.2.4 Perturbation-correlation moving-windows two- dimensional correlation spectroscopy (PCMW2D)	10
1.3 Multivariate curve resolution method	12
1.3.1 Multivariate curve resolution - alternating least squares (MCR-ALS)	12
1.3.2 Two-dimensional spectroscopy analysis and multivariate curve resolution - alternating least squares	15
2 EXPERIMENTAL	19
2.1 Instrumental techniques	21
2.2 Cases studied	24
2.2.1 Monitoring reaction between phenyl glycidyl ether and γ -butyrolactone by NIR	24
2.2.2 Curing reaction of diglycidyl ether of bisphenol A with γ -valerolactone by FTIR/ ATR	25

2.2.3	Curing reaction of diglycidyl ether of bisphenol A homopolymerization by FTIR/ ATR	26
2.3	Other measurements	27
2.3.1	¹ H and ¹³ C NMR spectra of the final product in the reaction between phenyl glycidyl ether and γ-butyrolactone	27
3	RESULTS	29
3.1	Quantitative resolution of a model epoxy reaction us- ing wavelength-wavelength two-dimensional NIR corre- lation spectroscopy and MCR-ALS	31
3.2	Study of a curing reaction using wavenumber - wavenumber two-dimensional FTIR correlation spec- troscopy and evolving factor analysis (EFA)	53
3.3	Quantitative resolution of a curing reaction using global phase angle spectroscopy and MCR-ALS	81
3.4	Methodology to estimate concentration profiles from sample-sample two-dimensional covariance spectroscopy	105
3.5	Study of mechanisms involved in the cationic curing process by perturbation-correlation analysis and a curve resolution method	127
4	CONCLUSIONS	149
	REFERENCES	153
A	Appendix	159
A.1	Papers Presented	161
A.2	Meeting Contributions	163
B	Predoctoral Formation	165
B.1	Master	165
B.2	Stay Abroad	165

Chapter 1

BACKGROUND

UNIVERSITAT ROVIRA I VIRGILI

TWO-DIMENSIONAL INFRARED CORRELATION SPECTROSCOPY AND MULTIVARIATE CURVE RESOLUTION

METHODS: APPLICATION TO QUANTITATIVE MONITORING OF CURING PROCESS

Nicolas Spegazzini

ISBN:978-84-693-4049-3/DL:T.998-2010

1.1 Cationic curing of epoxy resins

Epoxy resins have many applications in coatings, adhesives and composites. The chemistry of epoxides and the wide range of resin materials commercially available for use as pre-polymers allows for a variety of properties in the final product (i.e. co-polymer). The first commercial epoxy resin to be developed was DGEBA[18], and it remains one of the most widely used resins in the industry. Diglycidyl resins are usually cross-linked with primary diamines but they can also be cured by cationic or anionic initiators by the ring-opening polymerization mechanism.

When epoxy resins are cured by initiators, a three-dimensional polyether structure is formed and the thermosets obtained have certain drawbacks, such as: fragility, contraction during the curing process, and a lack of recyclability or degradability. In the materials field, several methods have been developed to solve some of these problems. One such method is based on curing epoxy resin/lactone mixtures, which can copolymerize in the presence of a Lewis acid as a cationic initiator. In this copolymerization process, the density of cross-linking is reduced by the introduction of linear structures from the lactone unit, which increases the flexibility of the network, thus reducing fragility.

The introduction of ester groups makes the material more degradable, which allows materials coated in this material to be recovered or recycled. The complex mechanism of this copolymerization also reduces shrinkage in the last stages of curing, in which the material has a low mobility. This sharply reduces stress and leads to a material with better characteristics.

The Polymer Group of the Analytical and Organic Chemistry Department of Rovira i Virgili University, has extensive experience working with epoxy resins. In recent years, this group [19-23] has developed new curing agents such as rare-earth metal triflates. These compounds are Lewis acids, stable in aqueous media, frequently used in organic reactions [24-28] and considered environmentally favorable. Three different rare-earth triflates are used in this thesis: scandium, ytterbium and lanthanum. The Lewis acidity and Pearson hardness of these triflates decrease in the following order: $\text{Sc}(\text{OTf})_3 > \text{Yb}(\text{OTf})_3 > \text{La}(\text{OTf})_3$

[28]. The thermosets are three-dimensional polymers that cannot be dissolved in organic solvents.

The reaction mechanisms therefore cannot be studied by means of nuclear magnetic spectroscopy, so FTIR is usually the best tool for this purpose. Due to the complex mechanism adopted in copolymerizations of this type, two-dimensional correlation spectroscopy together with multivariate curve resolution - alternating least squares could be powerful chemometric tools for analyzing these curing processes.

1.2 Two-dimensional spectroscopy analysis

An intriguing idea was put forward in the field of NMR spectroscopy about 35 years ago: spreading the spectral peak over the second dimension. Following this conceptual breakthrough, an impressive amount of progress has been made in the branch of the science now known as two-dimensional (2D) spectroscopy. In the last decade or so, perturbation-based generalized two-dimensional correlation spectroscopy has become a surprisingly powerful and versatile tool for the detailed analysis of various spectroscopic data. This seemingly straightforward idea of spreading the spectral information onto the second dimension by applying the well-established classical correlation analysis methodology, primarily attaining clarity and simplicity by sorting out the convoluted information content of a highly complex chemical system, has turned out to be very fertile ground for the development of a new generation of modern spectral analysis techniques.

1.2.1 Generalized two-dimensional correlation spectroscopy (variable-variable 2DCOS)

Two-dimensional correlation spectroscopy (2DCOS) was first developed in the late 1980s and early 1990s by Isao Noda in a series of papers in which he described the basic principles of this technique and its application to polymer systems using infrared spectroscopy [29-32]. In a 2D infrared experiment, the sample is subjected to an arbitrary environmental perturbation, such as a change in concentration, temperature, pH, pressure, etc., which causes a physical or chemical modification in the sample, which in turn leads to a measurable change of some sort in the resulting spectrum. The system's response to the perturbation often manifests itself as a set of characteristic variations in the spectrum, known as a *dynamic spectrum*. In a typical 2D experiment, a series of perturbation-induced dynamic spectra are collected in some sequential order. Such a set of spectra may be readily manipulated mathematically, using simple scheme correlation analysis, to yield the desired 2D correlation spectra [31,32]. Figure 1 shows the basic scheme for a 2DCOS experiment based on external perturbation [31,32]. In traditional spectroscopy measurement, the interaction between electromagnetic radiation and the constituents of the sample are analyzed in order to elucidate detailed information about the sample.

In 2DCOS, an additional external perturbation is applied during the spectroscopic measurement to stimulate the system of interest.

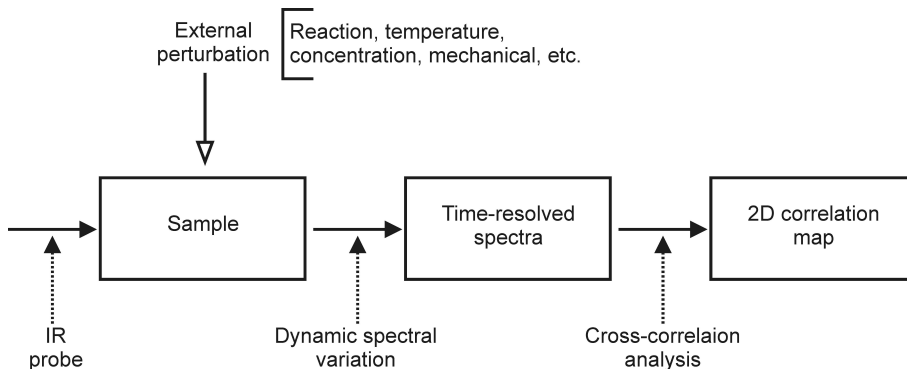


Figure 1: General scheme for obtaining perturbation-based 2D correlation spectra.

The spectral variations induced by the applied perturbation are referred to as dynamic spectra in 2D correlation. The variations in intensity of individual spectral frequencies are then mathematically cross-correlated to produce contour plots called two-dimensional correlation maps, in which several peaks appear. The positions and signs of those peaks can be related to the effect of the applied perturbation.

In this thesis, the system under study is the chemical reaction and the perturbation is the curing process over time.

The *dynamic spectrum* $\tilde{y}(\nu, t)$ of a system induced by the application of an external perturbation is formally defined as follows:

$$\tilde{y}(\nu, t) = \begin{cases} y(\nu, t) - \bar{y}(\nu) & \text{for } T_{min} \leq t \leq T_{max} \\ 0 & \text{otherwise} \end{cases} \quad (1)$$

where $\bar{y}(\nu)$ is the *reference spectrum* of the system that is commonly the average spectrum, calculated as follows:

$$\bar{y}(\nu) = \frac{1}{T_{max} - T_{min}} \int_{T_{min}}^{T_{max}} y(\nu, t) dt \quad (2)$$

In some applications, however, the reference spectrum could be a spectrum at the beginning of the experiment, or at the end, or in some cases it could even be set to zero. The choice of the reference depends on the specific 2D correlation analysis being applied.

The fundamental concept governing 2DCOS is a quantitative comparison of the spectral intensity variations along the perturbation (t) observed at two different spectral variables, ν_1 and ν_2 , over some finite observation interval between T_{min} and T_{max} . The similarity or dissimilarity of spectral $X(\nu_1, \nu_2)$ measured at two different spectral variables, ν_1 and ν_2 , during a fixed interval can be evaluated by means of Equation (3):

$$\mathbf{X}(\nu_1, \nu_2) = \langle \tilde{y}(\nu_1, t) \cdot \tilde{y}(\nu_2, t') \rangle \quad (3)$$

where the symbol $\langle \rangle$ denotes the cross-correlation function.

Mathematical $\mathbf{X}(\nu_1, \nu_2)$ can be expressed as a complex number function [31,32].

$$\mathbf{X}(\nu_1, \nu_2) = \Phi(\nu_1, \nu_2) + i \Psi(\nu_1, \nu_2) \quad (4)$$

comprising two orthogonal (real and imaginary) components known as the *synchronous* $\Phi(\nu_1, \nu_2)$ and *asynchronous* $\Psi(\nu_1, \nu_2)$ 2D correlation intensities, respectively. The correlation intensity in the 2D synchronous and asynchronous maps reflects the relative degree of in-phase or out-of-phase response, respectively.

Synchronous and asynchronous 2D correlation intensities are calculated using Equation 5:

$$\Phi(\nu_1, \nu_2) + i \Psi(\nu_1, \nu_2) = \frac{1}{\pi (T_{max} - T_{min})} \int_0^\infty \tilde{Y}_1(\omega) \tilde{Y}_2^*(\omega) d\omega \quad (5)$$

The term $\tilde{Y}_1(\omega)$ is the forward Fourier transform of the spectral intensity variations $\tilde{y}(\nu_1, t)$ observed at a given spectral variable ν_1 , with respect to the external variable t . It is given by:

$$\tilde{Y}_1(\omega) = \int_{-\infty}^\infty \tilde{y}(\nu_1, t) e^{-i\omega t} dt = \tilde{Y}_1^{Re}(\omega) + i \tilde{Y}_1^{Im}(\omega) \quad (6)$$

where $\tilde{Y}_1^{Re}(\omega)$ and $\tilde{Y}_1^{Im}(\omega)$ are, respectively, the real and imaginary components of the Fourier transform (the real component $\tilde{Y}_1^{Re}(\omega)$ is an even function of ω , while $\tilde{Y}_1^{Im}(\omega)$ is an odd function). The Fourier frequency ω represents the individual frequency component of the variation of $\tilde{y}(\nu_1, t)$ traced along the external variable t . According to Equation (1), the above Fourier integration of the dynamic spectrum is actually bound by the finite interval between T_{min} and T_{max} .

The conjugate of the Fourier transform $\tilde{Y}_2^*(\omega)$ of the spectral intensity variation $\tilde{y}(\nu_2, t)$ observed at another spectral variable ν_2 , is given by:

$$\tilde{Y}_2^*(\omega) = \int_{-\infty}^{\infty} \tilde{y}(\nu_2, t) e^{+i\omega t} dt = \tilde{Y}_2^{Re}(\omega) - i\tilde{Y}_2^{Im}(\omega) \quad (7)$$

Once the appropriate Fourier transform of the dynamic spectrum $\tilde{y}(\nu, t)$ defined in the form of Equation (1) is carried out with respect to the variable t , Equation (5) will directly yield the synchronous and asynchronous correlation spectra, $\Phi(\nu_1, \nu_2)$ and $\Psi(\nu_1, \nu_2)$.

A modification of the generalized method was introduced by Noda to simplify the calculations using the discrete Hilbert-Noda transform in place of the complex Fourier transform [33-35]:

$$\Phi = \frac{1}{n-1} \tilde{\mathbf{D}}^T \tilde{\mathbf{D}} \quad (8)$$

$$\Psi = \frac{1}{n-1} \tilde{\mathbf{D}}^T \mathbf{N} \tilde{\mathbf{D}} \quad (9)$$

Equations (8) and (9) are used to directly compute the synchronous and asynchronous correlation intensities, respectively, for a discrete data set \mathbf{D} (of dimensions $n \times m$ corresponding to the n spectra recorded in each experiment at the wavelength or wavenumber m), where $\tilde{\mathbf{D}}$ denotes the mean-centered matrix of \mathbf{D} , n represents the number of the spectrum and \mathbf{N} is the discrete Hilbert-Noda transformation matrix defined as follows:

$$\mathbf{N} = \frac{1}{\pi} \begin{bmatrix} 0 & 1 & 1/2 & 1/3 & \dots \\ -1 & 0 & 1 & 1/2 & \dots \\ -1/2 & -1 & 0 & 1 & \dots \\ -1/3 & -1/2 & -1 & 0 & \dots \\ \vdots & \vdots & \vdots & \vdots & \ddots \end{bmatrix} \quad (10)$$

Two-dimensional synchronous spectra are symmetric with respect to the diagonal line in the correlation map. Intensity maxima appearing along the diagonal are called autopeaks and are always positive. Intensity maxima located at off-diagonal positions are called cross peaks. The cross peaks may be positive or negative.

Two-dimensional asynchronous spectra are antisymmetric with respect to the diagonal line in the correlation map. Only cross peaks

located at off-diagonal positions appear in asynchronous spectra; a pair of cross peaks consists of two intensity maxima/minima, one of which is necessarily positive and the other necessarily negative.

The synchronous and asynchronous maps provide complementary information about the spectral bands. In the synchronous spectra correlation $\Phi(\nu_1, \nu_2)$, the cross peaks indicate the correlation between spectroscopic variables. Under the same perturbation, the increase or decrease is simultaneous. More information can be obtained from the corresponding asynchronous correlation spectra $\Psi(\nu_1, \nu_2)$, where the cross peaks develop only if the intensities of two dynamic bands change asynchronously. Also, the sign of an asynchronous correlation peak, $\Psi(\nu_1, \nu_2)$, provides information about the sequential order of intensity variations between bands ν_1 and ν_2 . According to Noda and Ozaki, when $\Phi(\nu_1, \nu_2) > 0$, if $\Psi(\nu_1, \nu_2)$ is positive, band ν_1 varies before band ν_2 , and, if $\Psi(\nu_1, \nu_2)$ is negative, band ν_1 varies after ν_2 . If $\Phi(\nu_1, \nu_2) < 0$, the inverse rules apply [31,36,37].

1.2.2 Global phase angle

The global phase angle (Equation 11) represents the ratio between the asynchronous and synchronous correlation intensities at given spectral coordinates [38]. The coherence of signals [39,40] is used in this thesis to find a reference value, which in turn is used to determine the optimal number of iterations in the optimization step in MCR-ALS.

$$\Theta = \arctan \left(\frac{\Psi}{\Phi} \right) \quad (11)$$

1.2.3 Sample-sample two-dimensional correlation spectroscopy (SS-2DCOS)

Over the past decade, two-dimensional correlation analysis has been extended to analysis among sample variations. The basic concept of the sample-sample correlation was originally proposed by Zimba [41]. The idea is based on a simple exchange of the rows and columns of a data matrix when 2D spectra are calculated by means of matrix algebra.

The interesting idea of sample-sample correlation was later refined and utilized extensively by Šašić et al. [42]. A conventional wavenumber–wavenumber synchronous spectrum can be related to a

covariance matrix. The synchronous sample-sample correlation enables the pairwise comparison of spectral similarity of two samples by taking inner products of spectral vectors. Šašić et al. pointed out that, although equivalent forms of matrices are found in chemometrics corresponding to synchronous spectra, no such equivalent form exists for asynchronous spectra [42].

The sample-sample 2D covariance matrix of the experimental data \mathbf{D} centered along rows $\tilde{\mathbf{D}}$ is calculated using Equation 12:

$$\Phi = \frac{1}{m-1} \tilde{\mathbf{D}} \tilde{\mathbf{D}}^T \quad (12)$$

Each point in the sample-sample covariance matrix represents the covariance between a given pair of samples measured at different reaction times. Each vector or slice spectrum in this matrix gives information about the evolution of each sample in the matrix \mathbf{D} . Thus, if we correlate these slices, we can detect the point of maximum dissimilarity or maximum variability.

1.2.4 Perturbation-correlation moving-windows two-dimensional correlation spectroscopy (PCMW2D)

The concept of autocorrelation-based moving-windows 2D correlation analysis was originally introduced by Thomas and Richardson [43]. In this case, correlation analysis is applied to a window of spectra from data matrix \mathbf{D} . The autopeaks are detected on the correlation map. Successive correlation maps are found by incrementing the position of the window along the perturbation axis. A waterfall plot of autopeaks is generated as a function of the wavenumber and perturbation variable. Moving-windows 2D analysis is especially useful for the rapid identification of the characteristic zone of spectral intensity changes along the perturbation axis. PCMW2D correlation spectroscopy [44] is a powerful variant form of the moving- windows analysis derived from the generalized 2DCOS [31,32] and moving-windows 2D correlation analysis [44]. This method is characterized by a synchronous Π_Φ and asynchronous Π_Ψ correlation spectra spread on a 2D plane defined by the spectral variable axis (wavenumber) and the perturbation variable axis (reaction time). Because the correlation intensities are calculated in a sub-divided matrix named "moving-windows" along the

perturbation directions, it is necessary to define the size of the window ($2m + 1 = \text{size}$). The correlation between the spectral variation and perturbation variation of the windows is calculated. According to the study of Morita et al. [44], the synchronous $\mathbf{\Pi}_{\Phi}$ and asynchronous $\mathbf{\Pi}_{\Psi}$ PCMW2D correlation spectra are proportional to the first derivative and the opposite sign of the perturbation second derivative, as shown in Equations (13) and (14), respectively.

$$\mathbf{\Pi}_{\Phi}(\nu, p_j) = \frac{1}{2m} \sum_{J=j-m}^{j+m} \tilde{A}(\nu, p_J) \cdot \tilde{p}_J \sim \left[\frac{\partial A(\nu, t)}{\partial t} \right]_{\nu} \quad (13)$$

$$\mathbf{\Pi}_{\Psi}(\nu, p_j) = \frac{1}{2m} \sum_{J=j-m}^{j+m} \tilde{A}(\nu, p_J) \sum_{K=j-m}^{j+m} N_{JK} \cdot \tilde{p}_K \sim - \left[\frac{\partial^2 A(\nu, t)}{\partial t^2} \right]_{\nu} \quad (14)$$

where A is absorbance (spectral intensity) as a function of wavenumber ν and perturbation p and N_{JK} is the discrete Hilbert-Noda transformation. This method makes it possible to extract information about the variation of the spectral gradient along the reaction [44,45,46].

1.3 Multivariate curve resolution method

Self-modeling curve resolution was first introduced by Lawton and Sylvester [47]. The method, as first reported, resolved two-component mixture spectra into non-negative concentration profiles and non-negative absorption spectra of the pure constituents without any prior knowledge. Of the various different approaches that have been used, this thesis focuses on the MCR-ALS algorithm that was first introduced by Karjalainen [48] and later expanded by Tauler [49-52].

1.3.1 Multivariate curve resolution - alternating least squares (MCR-ALS)

This section, first presents the general scheme for obtaining the concentration and spectroscopic profiles of the chemical species involved in a reaction by means of alternating least squares. Afterwards, the methodology developed in this thesis, which considers 2DCOS information before or during the application of MCR-ALS, is presented. Following the methodology depicted in Figure 2, various multivariate analysis techniques (EFA, SIMPLISMA, etc.) can be used for the MCR-ALS decomposition indicated in Equation 15. Because they are widely known and covered extensively in the literature, these techniques not described in this thesis.

Multivariate curve resolution-alternating least squares (MCR-ALS) [49-52] aims to decompose the raw data matrix \mathbf{D} into two submatrices according to Equation (15).

$$\mathbf{D} = \mathbf{C}\mathbf{S}^T + \mathbf{E} \quad (15)$$

where \mathbf{D} is the data matrix (in our case containing the raw spectra monitored during the process), \mathbf{C} contains the concentration profiles of the chemical species and \mathbf{S}^T contains the pure spectra. \mathbf{E} is the residual matrix after decomposition.

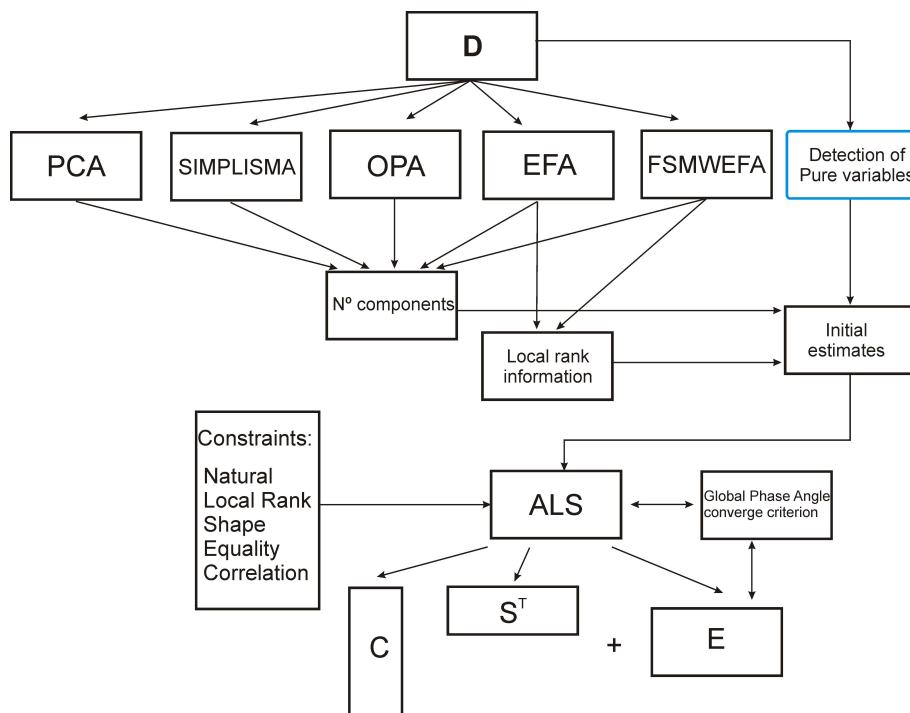


Figure 1

The MCR-ALS operating procedure can be summarized in five steps:

1) Determination of the number of components (i.e. rank determination).

2) Generation of an initial estimate of \mathbf{C} or \mathbf{S}^T .

3) Constrained least-squares calculation of \mathbf{S}^T using the \mathbf{C} estimate.

$$\mathbf{S}^T = \mathbf{C}^+ \mathbf{D}$$

4) Constrained least-squares calculation of \mathbf{C} using the calculated \mathbf{S}^T .

$$\mathbf{C} = \mathbf{D}(\mathbf{S}^T)^+$$

5) Reproduction of \mathbf{D} from $\mathbf{C}\mathbf{S}^T$. Then, takes place an iterative process starting from step 3 is implemented. In this process, ALS es-

estimates the pure variables \mathbf{C} and \mathbf{S}^T until convergence is achieved by minimizing the error criterion of the sum of squared residuals (SSR). $SSR = \|\mathbf{D} - \mathbf{CS}^T\|$.

The procedure requires an initial estimate of either concentration profiles (\mathbf{C}) or spectra (\mathbf{S}^T), which, as mentioned above, can be estimated by means of several multivariate analysis techniques. The solutions of MCR-ALS (\mathbf{C} and \mathbf{S}^T) are subject to ambiguities [50]. Constraints are therefore used to limit the number of possible solutions, e.g. by forbidding negative concentrations. Non-negativity is applied to concentration values, but other constraints can also be used, such as unimodality, closure or local rank information [51,52].

Non-negativity: can be applied to all profiles of concentration and some types of instrumental responses (i.e. UV spectra, infrared, etc.). This restriction imposes that all values of a profile (of concentration or response) must be greater than or equal to zero [51,52].

Closed system: This restriction imposes that the sum of the concentrations of species present in a system (or systems) must be constant at all times [51,52].

Unimodal: This restriction imposes the presence of a single maximum (absolute maximum) in the profiles [51,52,53]

The goodness of the MCR-ALS model can be evaluated by testing for lack of fit:

$$lof = \sqrt{\frac{\sum_i \sum_j (d_{ij} - \hat{d}_{ij})^2}{\sum_i \sum_j d_{ij}^2}} \quad (16)$$

where d_{ij} represents each element of the experimental matrix \mathbf{D} and \hat{d}_{ij} represents the elements calculated by the \mathbf{CS}^T product.

Another parameter that provides similar information, is the percentage of explained variance given by the \mathbf{CS}^T product:

$$R^2 = \frac{\sum_i \sum_j \hat{d}_{ij}^2}{\sum_i \sum_j d_{ij}^2} \quad (17)$$

Moreover, to evaluate the quality of the estimated profiles (concentration and spectra), their correlation with the real profiles can be

calculated using Equation (18). To do this, obviously, it is necessary to know the real profiles, and this is not always possible.

$$r = \cos \gamma = \frac{\mathbf{s}_i^T \hat{\mathbf{s}}_i}{\|\mathbf{s}_i\| \cdot \|\hat{\mathbf{s}}_i\|} \quad (18)$$

where γ is the angle defined by the vectors associated with the recovered MCR-ALS ($\hat{\mathbf{s}}_i$) profile and the real profile (\mathbf{s}_i), for a given studied species i .

1.3.2 Two-dimensional spectroscopy analysis and multivariate curve resolution - alternating least squares

The following flowchart presents the strategy employed in this thesis. The key point is the consideration of 2DCOS information before or during the application of MCR-ALS

This correlation information is used for different purposes:

a) To determine the number of components, variable-variable 2DCOS is employed as explained in Section 1.2.1.

b) To find concentration profiles, sample-sample two-dimensional correlation spectroscopy analysis (SS-2DCOS) is employed as explained in Section 1.2.2. To find the most representative profiles, to be used later as initial estimates in the application of MCR-ALS, the value of the **correlation coefficient** is employed. This procedure is described in detail below.

The correlation coefficient ρ between two vectors or slices (**i** and **j**) calculated from SS-2DCOS is defined in Equation 19. With values ranging from +1 to -1, it is a measure of the similarity of the two vectors or slices.

$$\rho_{ij} = \frac{\text{cov}(\mathbf{i}, \mathbf{j})}{SD_i \cdot SD_j} \quad (19)$$

The concentration profiles of a reaction R (reactive) \rightarrow P (product) can be represented by two symmetric profiles, corresponding to each of the species involved. For reactions of this sort, the value of the correlation coefficient between the two profiles is -1. When intermediate compounds take part in the reaction, i.e. R (reactive) \rightarrow I

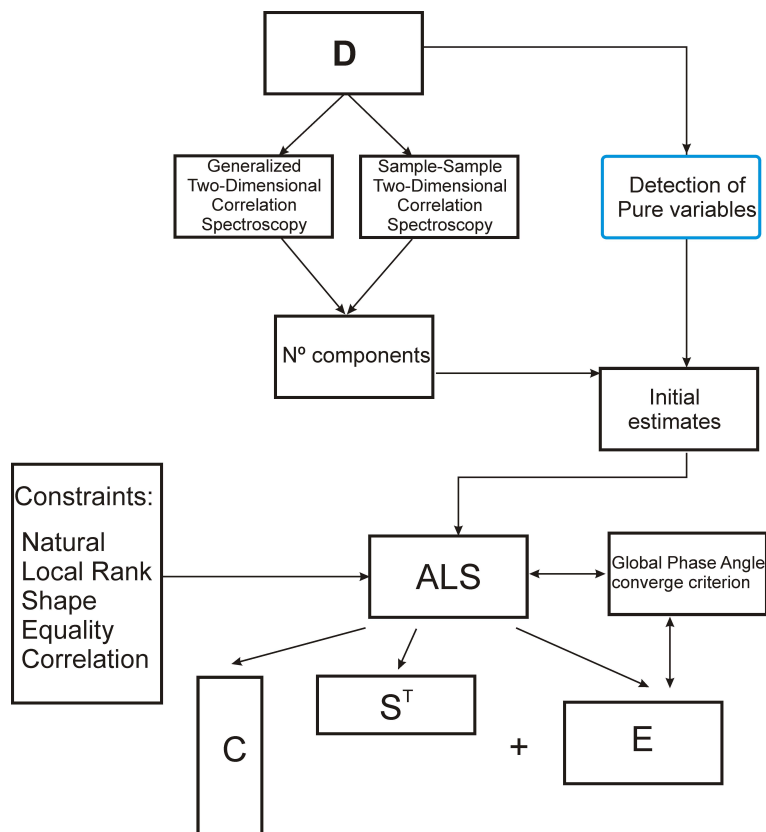


Figure 2

(intermediate)→P (product), several different concentration profiles can be found to represent the dynamic evolution of the system depending on the reaction kinetic. In reactions of this sort, when the correlation coefficients are calculated between all profiles, an interval between +1 and -1 is found, with the zero value corresponding to the point of maximum dissimilarity between the profiles.

c) To determine the optimal number of iterations during the optimization step according to ALS, the global phase angle is employed as explained below.

The global phase angle convergence criterion is a good strategy for balancing the purely mathematical model with the physical model underlying the system. The criterion is defined as the sum of the squared residuals between the global phase angle of the original spectra **D** and

the reconstructed spectra $\hat{\mathbf{D}} = \mathbf{C}\mathbf{S}^T$.

$$\text{SSR}_{\Theta} = \|\Theta - \hat{\Theta}\| \quad (20)$$

where $\hat{\Theta}$ is the global phase of the reconstructed spectra $\hat{\mathbf{D}}$.

If this criterion is to be used, the optimal value of SSR_{Θ} must be identified during the ALS iteration process. ALS minimizes SSR by a sequential matrix rotation process, and SSR gradually decrease with the increase in the number of iterations. The error criterion based on global phase angle, is a reflection of the underlying physical model [58].

UNIVERSITAT ROVIRA I VIRGILI

TWO-DIMENSIONAL INFRARED CORRELATION SPECTROSCOPY AND MULTIVARIATE CURVE RESOLUTION

METHODS: APPLICATION TO QUANTITATIVE MONITORING OF CURING PROCESS

Nicolas Spegazzini

ISBN:978-84-693-4049-3/DL:T.998-2010

Chapter 2

EXPERIMENTAL

UNIVERSITAT ROVIRA I VIRGILI

TWO-DIMENSIONAL INFRARED CORRELATION SPECTROSCOPY AND MULTIVARIATE CURVE RESOLUTION

METHODS: APPLICATION TO QUANTITATIVE MONITORING OF CURING PROCESS

Nicolas Spegazzini

ISBN:978-84-693-4049-3/DL:T.998-2010

This chapter describes the experimental work that has been done: the main curing reactions, the experimental conditions and the reaction schemes.

2.1 Instrumental techniques

This section describes theoretical concepts related to the practical application of the instrumental techniques used in the aforementioned research.

Near-infrared (NIR) spectroscopy

Near- infrared (NIR) spectroscopy measurements were carried out in the transreflectance mode. In the transreflectance mode, radiation passes through the sample to a reflective surface (which may be ceramic, gold or stainless steel), is reflected, and returns back through the sample to reach the detector (Figure 3 and Figure 4). The absorbed radiation is proportional to the concentration and follows the Beer-Lambert law if there are no particles in the sample that cause turbidity or scattering of radiation [59]. The measurements were taken using a NIR spectrophotometer (Bran+Luebbe InfraAlyzer 500).

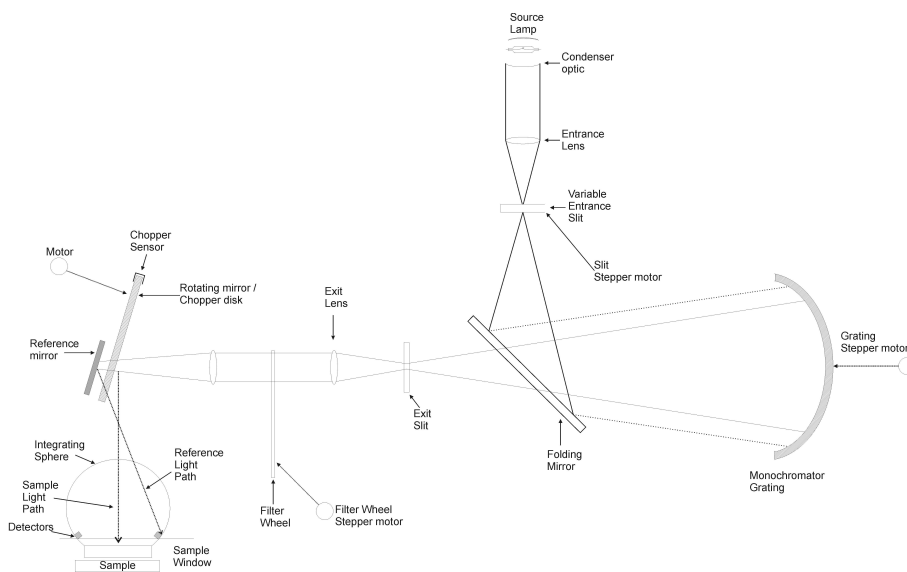


Figure 3: Schematic optical path of a NIR instrument.

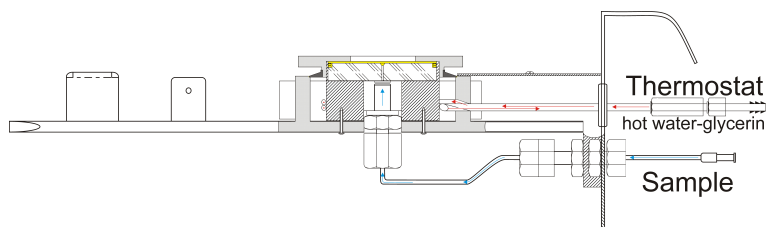


Figure 4: Schematic liquid cell in the NIR measurement.

Fourier transform infrared spectroscopy-attenuated total reflection (FTIR/ATR)

Attenuated total reflection (ATR), also known as internal reflection spectroscopy (IRS), is a versatile, nondestructive technique for obtaining the infrared spectrum of the surface of a material. In this technique, the sample is placed in contact with the internal reflection element (Figure 5) where the light is totally reflected, several times, and the sample interacts with an evanescent wave [60]. The internal reflection element was made from diamond, in the ATR cell (Specac Golden Gate) . The curing reactions were done under control temperature. The FTIR/ATR spectra recorded during the monitoring of the curing reaction were obtained with an FT-IR 680 PLUS JASCO spectrometer (Figure 6).

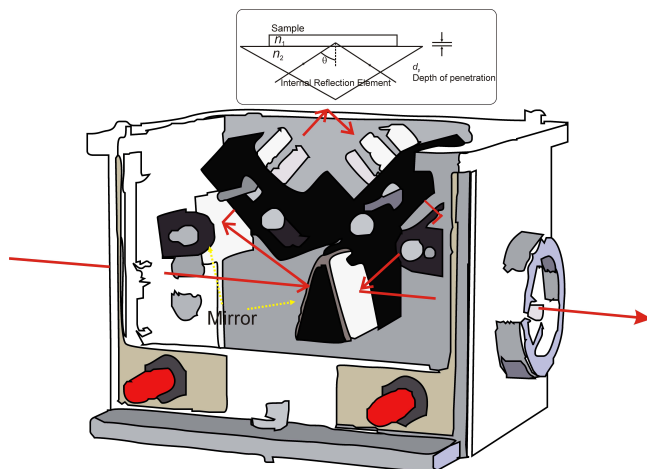


Figure 5: Schematic ATR cell in the FTIR measurement.

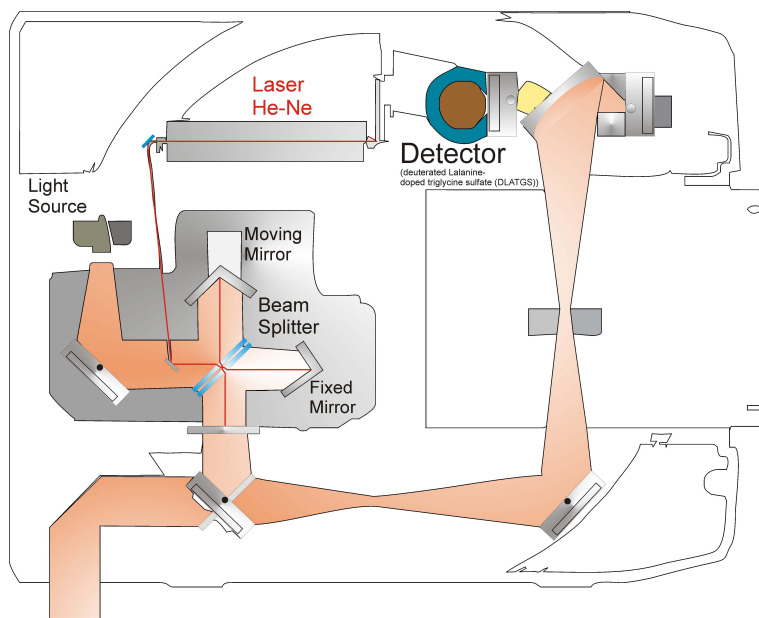


Figure 6: Schematic diagram of a FTIR instrument.

Nuclear magnetic resonance (NMR)

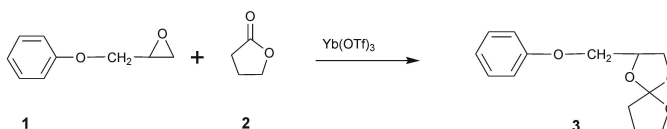
This technique was employed to confirm the presence of a final product. NMR spectra (^1H , 400 MHz; ^{13}C 100.6 MHz) were recorded using a Varian Gemini 400 spectrometer with Fourier transform, with deuterated chloroform (CDCl_3) used as the solvent and tetramethylsilane (TMS) used as the internal standard.

2.2 Cases studied

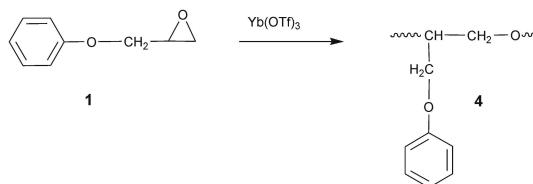
2.2.1 Monitoring reaction between phenyl glycidyl ether and γ -butyrolactone by NIR

Scheme 1 shows the possible reactions between PGE (1) and γ -butyrolactone (2). The first reaction (a) corresponds to the formation of spiro-orthoester (SOE) (3), the second reaction (b) corresponds to the homopolymerization of PGE (4), and the third reaction (c) is the copolymerization of PGE and SOE to obtain the copolymer (5).

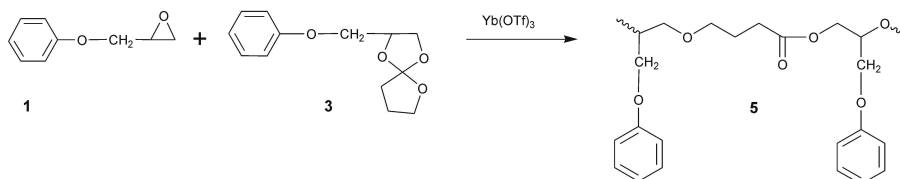
(a) Reaction of Phenylglycidylether with γ -butyrolactone



(b) Homopolymerisation of Phenylglycidylether



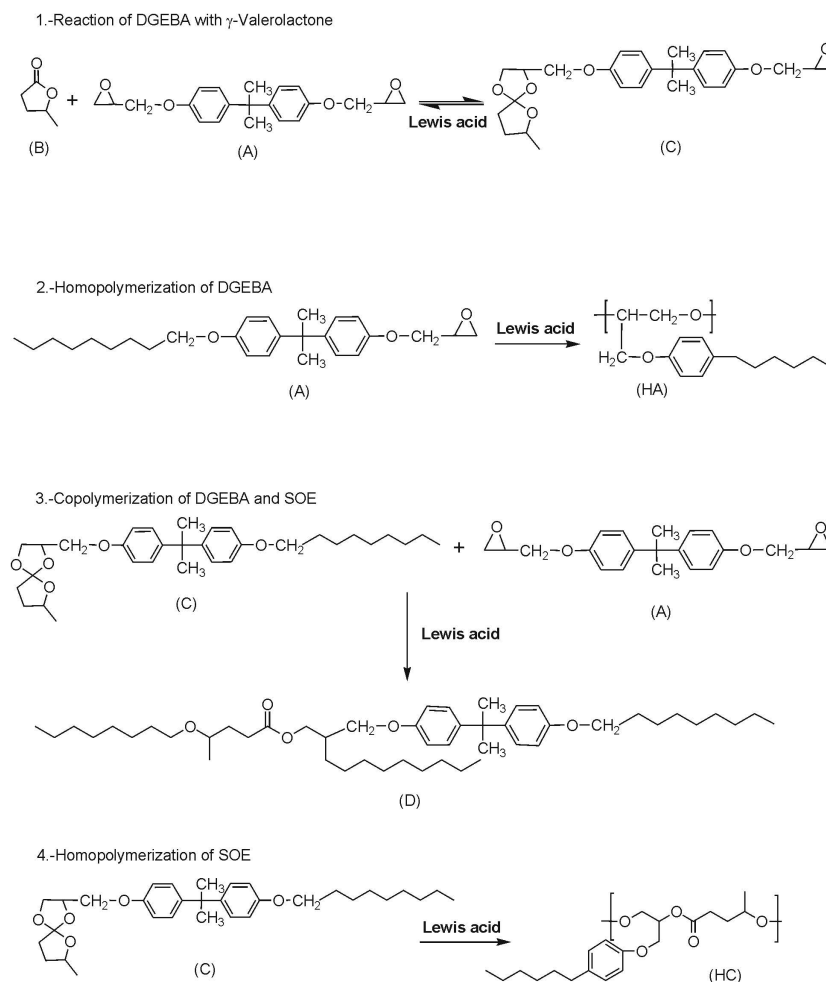
(c) Copolymerisation of Phenylglycidylether and Spiroorthoester



Scheme 1: reaction between phenyl glycidyl ether and γ -butyrolactone (1:1) at 95°C .

2.2.2 Curing reaction of diglycidyl ether of bisphenol A with γ -valerolactone by FTIR/ATR

The curing reaction of DGEBA with the γ -valerolactone (γ -VL) mixture involves several reactions (Scheme 2). The first reaction corresponds to the formation of an intermediate SOE. The second reaction corresponds to the DGEBA homopolymerization. The third reaction corresponds to the copolymerization of the SOE with epoxide. Finally, the fourth reaction corresponds to the homopolymerization of SOE.

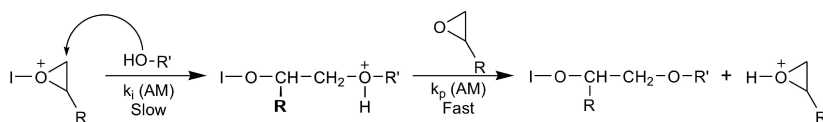


Scheme 2: reaction of diglycidyl ether of bisphenol A with γ -valerolactone (2:1) at 160°C.

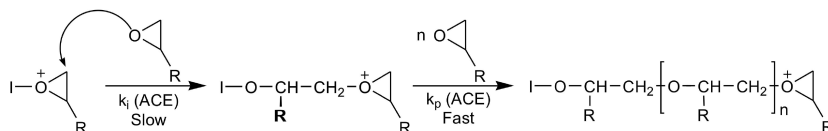
2.2.3 Curing reaction of diglycidyl ether of bisphenol A homopolymerization by FTIR/ATR

In this process, the only reaction that takes place is the second reaction of Scheme 3. The curing reaction of the homopolymerization of DGEBA is a cationic ring opening of epoxides, and it can proceed through two different mechanisms: activated monomer (AM) and active chain end (ACE). Both mechanisms, which can coexist, are shown in Scheme 3.

Activated monomer mechanism (AM)



Activated chain end mechanism (ACE)



Scheme 3: cationic ring opening of epoxides, and it can proceed through two different mechanisms: activated monomer (AM) and active chain end (ACE).

2.3 Other measurements

2.3.1 ^1H and ^{13}C NMR spectra of the final product in the reaction between phenyl glycidyl ether and γ -butyrolactone

NMR spectra (^1H , 400 MHz; ^{13}C , 100.6 MHz) of the product were obtained after 100 minutes of reaction, with Fourier transform, CDCl_3 as the solvent, and tetramethylsilane (TMS) as the internal standard.

UNIVERSITAT ROVIRA I VIRGILI

TWO-DIMENSIONAL INFRARED CORRELATION SPECTROSCOPY AND MULTIVARIATE CURVE RESOLUTION

METHODS: APPLICATION TO QUANTITATIVE MONITORING OF CURING PROCESS

Nicolas Spegazzini

ISBN:978-84-693-4049-3/DL:T.998-2010

Chapter 3

RESULTS

UNIVERSITAT ROVIRA I VIRGILI

TWO-DIMENSIONAL INFRARED CORRELATION SPECTROSCOPY AND MULTIVARIATE CURVE RESOLUTION

METHODS: APPLICATION TO QUANTITATIVE MONITORING OF CURING PROCESS

Nicolas Spegazzini

ISBN:978-84-693-4049-3/DL:T.998-2010

3.1 Quantitative resolution of a model epoxy reaction using wavelength-wavelength two-dimensional NIR correlation spectroscopy and MCR-ALS

In order to validate the methodology proposed in this thesis, the first study was done with a model reaction representing a cationic curing reaction.

The model reaction was the epoxy reaction between PGE and γ -butyrolactone. On the basis of an analysis of the spectra set recorded during the reaction by two-dimensional NIR correlation spectroscopy, only one reaction is postulated. The chemical species involved in this reaction are the reactant and the final product (SOE). The concentration and spectra profiles of this species were obtained by MCR-ALS.

In a previous study by the Rovira i Virgili University Polymer Group, the SOE was isolated and the NIR spectrum of this product was recorded. This spectrum was compared to the estimated spectral profiles found by MCR-ALS.

UNIVERSITAT ROVIRA I VIRGILI

TWO-DIMENSIONAL INFRARED CORRELATION SPECTROSCOPY AND MULTIVARIATE CURVE RESOLUTION

METHODS: APPLICATION TO QUANTITATIVE MONITORING OF CURING PROCESS

Nicolas Spegazzini

ISBN:978-84-693-4049-3/DL:T.998-2010

Spectroscopic and Quantitative Analysis of Spiroorthoester Synthesis by Two-Dimensional Correlation and Multivariate Curve Resolution Methods of NIR Data

Analyst, 133, (2008), 1028

Nicolás Spegazzini,^a Itziar Ruisánchez,^a M. Soledad Larrechi^a
Virginia Cádiz,^b Judit Canadell^b

^aChemometrics, Qualimetrics and Nanosensors Group, ^bPolymer's
Research Group, Department of Analytical and Organic Chemistry,
Rovira i Virgili University. Marcel·lí Domingo s/n, 43007, Tarragona,
Spain

Abstract

The spiroorthoester synthesis include several and competitive reactions. A way of determining the reactions that are taking place and their sequential order, is presented. The reaction between the phenylglycidylether and γ -butyrolactone to obtain a spiroorthoester has been monitored by near-infrared spectroscopy (NIR). In addition to the formation of the corresponding spiroorthoester, some parallel processes can occur. By means of Two-Dimensional Correlation Analysis, only one reaction is postulated, the one corresponding to the spiroorthoester formation. This was confirmed by recording the NMR spectra of the final product. Applying Multivariate Curve Resolution - Alternating Least Squares (MCR-ALS) to the NIR spectra obtained during the reaction, has been possible to obtain the concentration values of the species involved in the reaction. The recovered spectra were compared with the

experimentally recorded spectra for the reagents (phenylglycidylether, γ -butyrolactone) and the final product (spiroorthoester) and the correlation coefficients were, in all cases, higher than 0.990. The maximum and minimum limits associated with the ALS solutions were calculated making possible to limit to a considerable extent the ambiguity that is characteristic of these curve resolution methods.

1 Introduction

Epoxy resins have a good combination of attractive properties such as moisture, solvent and chemical resistance, toughness, superior electrical and mechanical properties, and good adhesion to many substrates [1]. However, the curing of epoxy resins is generally accompanied by shrinkages of 4-5% because the covalent bonds, which form between chains, increase the density of the materials. This shrinkage is a major problem in industrial applications because it leads to the formation of microvoids and microcracks, which reduce the durability of material and worsen the properties.

One way of solving this problem is to copolymerise the epoxy resins with the so-called “expanding monomers” [2], which are monomers that lead to zero shrinkage or even positive expansion during polymerisation [2-5]. The most useful cyclic monomers are spiroorthoesters which lead by cationic homopolymerisation to poly(ester-ether) chains and it is reported to maintain their volume or actually expand during the double ring-polymerization. Spiroorthoester can be readily synthesized from epoxides and lactones [6,7] and undergo cationic ring-opening polymerisation by Lewis acid catalysts. In addition to the formation of the corresponding spiroorthoester, some parallel processes can be expected: the homopolymerisation of the epoxide and the copolymerisation of the spiroorthoester with epoxide.

This work focused in the study of the different reactions which can take place and the quantitative contribution of the chemical species involved using two chemometrics methods, the 2D correlation and multivariate curve resolution of the spectra recorded during the reaction. This methodology has been used to obtain the pure spectra and profiles concentration of the polystyrene, methyl ethyl ketone and deuterated

toluene obtained in the solvent evaporation process of their mixture using the FTIR spectra [8] and to analyze the Raman spectra recorded from the reaction of malonitrile with KOH carried out in the ionic liquids [9]. In this work the reaction studied is an advance owing to the possibility of competing side reactions. It has been demonstrated that near infrared spectroscopy (NIR) with multivariate curve resolution methods, such as multivariate curve resolution-alternating least squares (MCR-ALS), is a useful tool to obtain the spectra and concentration profiles of the chemical species involved in a reaction [10].

A previous and very important step, in the optimization process of MCR-ALS applied to the NIR spectra obtained in reaction monitoring, is to find the chemical rank of the spectra data matrix. Ideally, this rank is the same of the number of chemical species involved in the reaction. Several algorithms based on factor analysis [11] are used to calculate this number. The chemical interpretation of this step requires an accurate analysis of the spectral changes observed in the recorded spectra. This stage becomes more difficult when the different chemical species involved in the reaction have the same functional groups and the observed changes in the spectra can be assigned to more than one species and in addition, several reactions simultaneously can coexist.

In this work the reaction between the phenylglycidylether and γ -butyrolactone in presence of ytterbium triflate, as cationic initiator, has been monitored by NIR. Two-dimensional correlation spectroscopy (2D correlation) analysis and MCR-ALS have been applied to elucidate the mechanism of this reaction. The analysis of the correlation map (synchronous and asynchronous) allows the establishment of unambiguous assignments of bands. Thus, only one reaction, the spiroorthoester formation, is postulated when phenylglycidylether and γ -butyrolactone react. This was confirmed by recording the NMR spectra. This is also in accordance with the significant number of values calculated by singular value decomposition (SVD) of the chemical rank of the spectra data matrix.

In these conditions, the problem of rank deficiency usually found in the application of MCR-ALS to the data matrix of chemical reactions monitoring, was detected. This problem of rank deficiency is overcome by using the chemical information of the reagents. The MCR-ALS results are evaluated by the residuals and parameters such as lack of fit, the percentage of explained variance and the coefficient of similarity

between the recovered spectra and the spectra of the pure species. The maximum and minimum limits of the solutions found by ALS, in accordance with the method established by Tauler et al. [12], are included. To our knowledge, this work is the first attempt of describing, in a comprehensive way, the involved reactions in the spiroorthoester formation.

2 Experimental

2.1 Reaction conditions and procedure

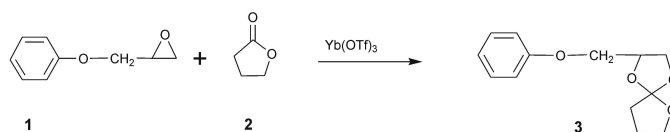
Scheme 1 shows the possible reactions between phenylglycidylether (**1**) and γ -butyrolactone (**2**). The first reaction (a) corresponds to the formation of spiroorthoester (**3**), the second reaction (b) to the homopolymerisation of phenylglycidylether to obtain the phenylglycidylether homopolymer (**4**), and the third reaction (c) is the copolymerisation of phenylglycidylether and spiroorthoester to obtain the copolymer (**5**). Note that, as γ -butyrolactone does not homopolymerise for thermodynamic reasons, therefore this reaction does not appear in Scheme 1.

The reaction between phenylglycidylether and γ -butyrolactone (1:1 mol/mol), in the presence of 1 phr (parts of initiator per 100 part of mixture, w/w) of ytterbium triflate was carried out in isothermal conditions at 95°C. The experimental procedure involves mixing 1051.2 mg of phenylglycidylether and 601.5 mg of γ -butyrolactone at room temperature to obtain the molar ratio (1:1). Immediately after, 1 ml of this mixture is injected into the liquid cell of the NIR spectrophotometer which is kept under controlled temperature of 95°C by recycling hot water-glycerin.

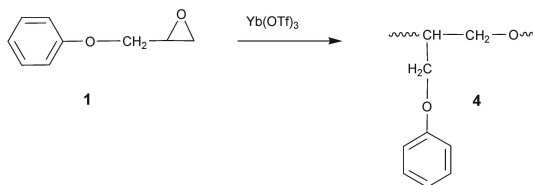
2.2 Data acquisition and pre-treatment of NIR spectra

The data correspond to the NIR spectra recorded every 4 nm between 1600 nm and 2400 nm in an InfraAlyzer 500 Bran+Luebbe spectrophotometer. The instrument is design to measure the reflectance of the samples using as reference, when the radiation is reflected over a stainless steel disk. For each experiment, data at intervals of 2 minutes until the end of the reaction were acquired. The band at 2208 nm,

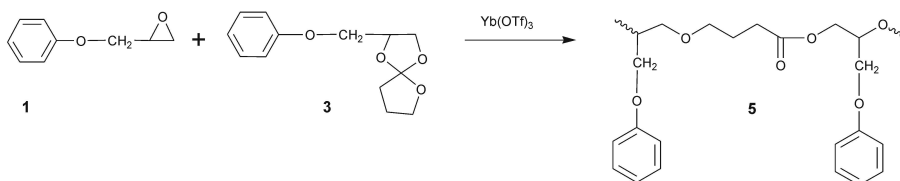
(a) Reaction of Phenylglycidylether with γ -butyrolactone



(b) Homopolymerisation of Phenylglycidylether



(c) Copolymerisation of Phenylglycidylether and Spiroorthoester



Scheme 1: Chemical reaction of phenylglycidylether with γ -butyrolactone (1:1) at 95°C . (1) phenylglycidylether, (2) γ -butyrolactone, (3) spiroorthoester, (4) phenylglycidylether homopolymer and (5) copolymer.

which is characteristic of the oxirane group [1], was chosen as a reference. Thus, the reaction was considered to be completed when this band disappeared (see Figure 1). In this way, we considered that the reaction ended after 100 minutes. In this time, 50 spectra were obtained. NIR spectra of the pure reactants were also recorded in the same experimental conditions. Also, the NIR spectrum of the synthesized spiroorthoester [13] was recorded to compare it to the results discussed below.

Spectra were exported and converted into MATLAB binary files [14]. Experimental data corresponding to the reaction were arranged in a matrix **D** of (50 x 201), whose rows were the number of recorded spectra and whose columns were the $\log(1/R)$ (R = reflectance) values

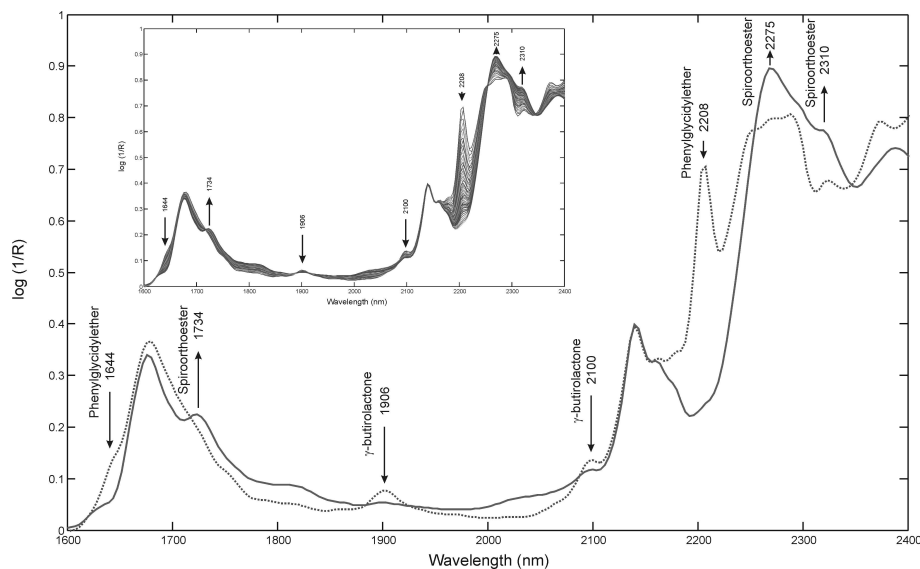


Figure 1: NIR spectra, N⁰ 1 (solid line) and N⁰ 50 (dotted line).

at different wavelengths. All the original spectra were pre-treated with offset correction [15] to eliminate any vertical shift in the spectra caused by using a NIR spectrophotometer with only one light beam.

2.3 NMR spectra

NMR spectra (¹H, 400 MHz; ¹³C, 100.6 MHz) of the product obtained after 100 minutes of the reaction, were recorded using a Varian Gemini 400 spectrometer with Fourier transform CDCl₃ as the solvent, and tetramethylsilane (TMS) as internal standard.

¹H NMR δppm) of the synthesized spiroorthoester[13]: 2.02 (2H,m), 2.19 (2H,m), 3.95 (4H,m), 4.06 (1H,m), 4.24 (1H,t), 4.63 (1H,m), 6.91 (2H,m), 7.28 (1H,m), 7.28 (2H,m).

¹³C NMR δppm) of the synthesized spiroorthoester[13]: 24.17 (t), 32.65 (t), 66.36 (t), 67.27 (t), 67.86 (t), 73.60 (d), 114.43 (d), 121.09 (d), 129.30 (d), 129.59 (s), 158.35 (s).

2.4 Data analysis

2.4.1 Two-dimensional correlation analysis

To minimize the noise effect [16-18], two-dimensional correlation maps were calculated using the data reconstructed from the two first principal components of the original data matrix D [19]. The percentage of the recovered variance was 99.98%.

Synchronous and asynchronous 2D NIR correlation spectra were calculated using an algorithm based on a numerical method developed by Noda and Ozaki [20-23]. The 2D correlation calculations, using the data reconstructed, were preceded by subtracting from the normalized data the average spectrum considered as reference spectrum of the system, obtaining of this way the dynamic spectrum. For sake of clarity, the maps were constructed in two wavelength intervals: 2250-1600 nm and 2400-1850 nm, using in both only six spectra (the number 1, 10, 20, 30, 40 and 50, in the reconstructed matrix, that are evenly spaced in time and corresponding to the time reaction of 0, 20, 40, 60, 80 and 100 min, respectively). Synchronous and asynchronous maps provide complementary information about the spectral bands. In the synchronous spectra correlation $\Phi(\nu_1, \nu_2)$ the cross peaks indicate the correlation between spectral variables (wavelength). Under the same perturbation, the increase or decrease is simultaneous. More information can be obtained from the corresponding asynchronous correlation spectra $\Psi(\nu_1, \nu_2)$, where the cross peaks develop only if the intensities of two dynamic bands change asynchronously. Also, the sign of an asynchronous correlation peak, $\Psi(\nu_1, \nu_2)$, provides information about the sequential order of intensity variations between band ν_1 and ν_2 . According to the Noda and Ozaki [21] publications, if the synchronous cross peak is positive, $\Phi(\nu_1, \nu_2) > 0$, and the asynchronous peak is positive, $\Psi(\nu_1, \nu_2) > 0$, ν_1 varies before ν_2 . If the asynchronous peak is negative, $\Psi(\nu_1, \nu_2) < 0$, the band ν_2 varies before ν_1 . When the synchronous cross peak is negative $\Phi(\nu_1, \nu_2) < 0$, and the asynchronous peak is positive, $\Psi(\nu_1, \nu_2) > 0$, ν_2 varies before ν_1 . If the asynchronous peak is negative, $\Psi(\nu_1, \nu_2) < 0$, the band ν_1 varies before ν_2 . Two-dimensional correlation analysis was performed using "2D shige" of Shigeaki Morita [24].

2.4.2 Multivariate curve resolution-alternating least squares (MCR-ALS)

of the MCR-ALS method is to transform the theoretical solution obtained by factor analysis of the experimental data matrix \mathbf{D} , in order to obtain matrices \mathbf{C} and \mathbf{S}^T which have a real chemical significance, according to eqn (1):

$$\mathbf{D} = \mathbf{C}\mathbf{S}^T + \mathbf{E} \quad (1)$$

in which matrix \mathbf{C} ($n \times c$) has column vectors corresponding to the concentration values of the c pure components for each sample (n = number of recorded spectra), that are present in matrix \mathbf{D} . The row vectors of matrix \mathbf{S}^T ($c \times m$) correspond to the spectra between the wavelength λ_1 and λ_m , of the c pure components, and \mathbf{E} is the matrix of the residuals. First, the number of compounds present in \mathbf{D} that have chemical information, is estimated from the “chemical rank” associated with the data matrix \mathbf{D} . This determination is performed by Singular Value Decomposition (SVD)[25], knowing that singular values associated with chemical compounds are larger than singular values associated with noise and experimental error.

The detected problem of the rank deficiency was overcome appended the NIR spectra of reagents to the data matrix \mathbf{D} as a new row vectors. A new augmented matrix \mathbf{M} is obtained. In the optimization process, in which ALS is applied to the matrix \mathbf{M} , several constraints were imposed: non-negativity for the concentrations profiles to be resolved in matrix \mathbf{C} and to the spectral profiles in matrix \mathbf{S}^T , and closure for the concentrations profiles. Likewise, a local rank constraint of selectivity and equality was imposed at the starting point of the reaction.

The percentage of variance explained by the product of $\mathbf{C}\mathbf{S}^T$ and the lack of fit were used as parameters to evaluate the performance of the model. The initial estimates found by MCR-ALS were used in the optimization process indicated in eqn (2), to define the bands in which the real profiles are found. Initial matrix \mathbf{T} is the identity matrix, of the same dimensions as \mathbf{C} . The restrictions mentioned above were used

$$\begin{aligned} \mathbf{D} &= \mathbf{C}_{\text{inic}} \mathbf{S}_{\text{inic}}^T = \mathbf{C}_{\text{inic}} \mathbf{T}_{\text{min}} \mathbf{T}_{\text{min}}^{-1} \mathbf{S}_{\text{inic}}^T = \mathbf{C}_{\text{min,k}} \mathbf{S}_{\text{min,k}}^T = \\ &= \mathbf{C}_{\text{inic}} \mathbf{T}_{\text{max,k}} \mathbf{T}_{\text{max,k}}^{-1} \mathbf{S}_{\text{inic}}^T = \mathbf{C}_{\text{max,k}} \mathbf{S}_{\text{max,k}}^T \end{aligned} \quad (2)$$

Theory and application of MCR-ALS have been described in detail [26,27] and freely available subroutines of MATLAB by R. Tauler was

used for MCR-ALS analysis [28].

3 Results and discussion

3.1 Infrared analysis

Fig. 1 shows the first and the last spectra recorded in the experiment. As can be seen all spectra are also inserted in the figure, to show that along the reaction the changes in the absorption bands always go in the same direction, either the bands decrease or increase. To facilitate the analysis of the observed changes, we will only refer to the first and later spectra.

The principal changes correspond to the following vibrations: decrease of the absorption bands intensities at 2208 nm and 1644 nm characteristics of oxirane group present in phenylglycidylether (**1**, Scheme 1). The same happens with the absorption bands at 1906 nm and 2100 nm characteristics of the C=O group present in γ -butyrolactone (**2**, Scheme 1) and in the copolymer (**5**, Scheme 1). As the intensity of these bands always decreases, it can be an indication that in the mentioned experimental conditions, the copolymerisation reaction between phenylglycidylether and spiroorthoester has not taken place, or if this copolymerisation reaction took place the production of copolymer would be at a much slower rate than consumption of γ -butyrolactone. Also, an increase of the absorption bands intensities at 1734 nm, 2275 nm and 2310 nm is observed. These bands are characteristics of the stretching vibrations of the C-H bond of the CH₂ groups, presents in all chemical species of the Scheme 1. So, it could be due to the **3**, **4** and **5** in Scheme 1.

3.2 Two-dimensional correlation analysis

The two dimensional correlation spectroscopy analyses can help in the interpretation of the chemical reactions. Fig. 2A and 2B show the synchronous correlations maps between 2250 nm and 1600 nm and between 2400 nm and 1850 nm, respectively. As it was expected, negative cross peaks are observed between the characteristics bands of product and reagents (**1** and **2**): in (Fig. 2A), (1734, 2208) nm of (spiroorthoester, phenylglycidylether), (1734, 1644) nm of (spiroorthoester, phenylglycidylether), (1734, 1906) nm of (spiroortho-

ester, γ -butyrolactone); and in (Fig. 2B), (2275, 2208) nm of (spiroorthoester, phenylglycidylether), (2310, 2208) nm of (spiroorthoester, phenylglycidylether), (2310, 2100) nm of (spiroorthoester, γ -butyrolactone), (2275, 1906) nm of (spiroorthoester, γ -butyrolactone).

These maps provide information about the simultaneous changes which occur in the NIR spectra of the reaction. If phenylglycidylether homopolymerisation reaction should take place, the changes at 1734 nm, 2275 nm and 2310 nm will not be simultaneous to the changes at 2100 nm and 1906 nm which are characteristic of γ -butyrolactone, and synchronous peaks will not be observed in the synchronous map (Fig. 2A and 2B). Moreover, if the production of copolymer (**5**, Scheme 1) took place the positive synchronous peaks would not be observed between the bands of both reagents, phenylglycidylether (2208 nm) and γ -butyrolactone (1906 nm). Because there is a positive peak this reaction must not take place or only in a non significant extension.

Cross peaks are also observed between the characteristics bands of reagents (phenylglycidylether and γ -butyrolactone) and products in the asynchronous map (Fig. 2C and 2D) where changes out phase are detected. Applying the Noda rules (Table 1), additional information about the sequential order of the changes observed can be obtained. Relative to the above mentioned peaks, the sequential order is the one expected. The characteristics bands from the reagents change before the characteristics bands from products. It must be noted that the band at 1906 nm, band characteristic of γ -butyrolactone, changes before than the one at 2208 nm, band characteristic of oxirane group of phenylglycidylether. So, it can be attributed to the fact that the reaction is initiated by the formation of a coordination compound, between of γ -butyrolactone and the catalyst, which further facilitates the oxirane ring opening. This behaviour is the usual in presence of a Lewis acid catalyst [29]. This fact indicates that the phenylglycidylether homopolymerisation, which must produce intensity decrease at 2208 nm, is less favoured than the reaction between phenylglycidylether and γ -butyrolactone. As conclusion of the above spectral analysis, we can postulate that in these experimental conditions, the only significant reaction that takes place is the one of spiroorthoester formation.

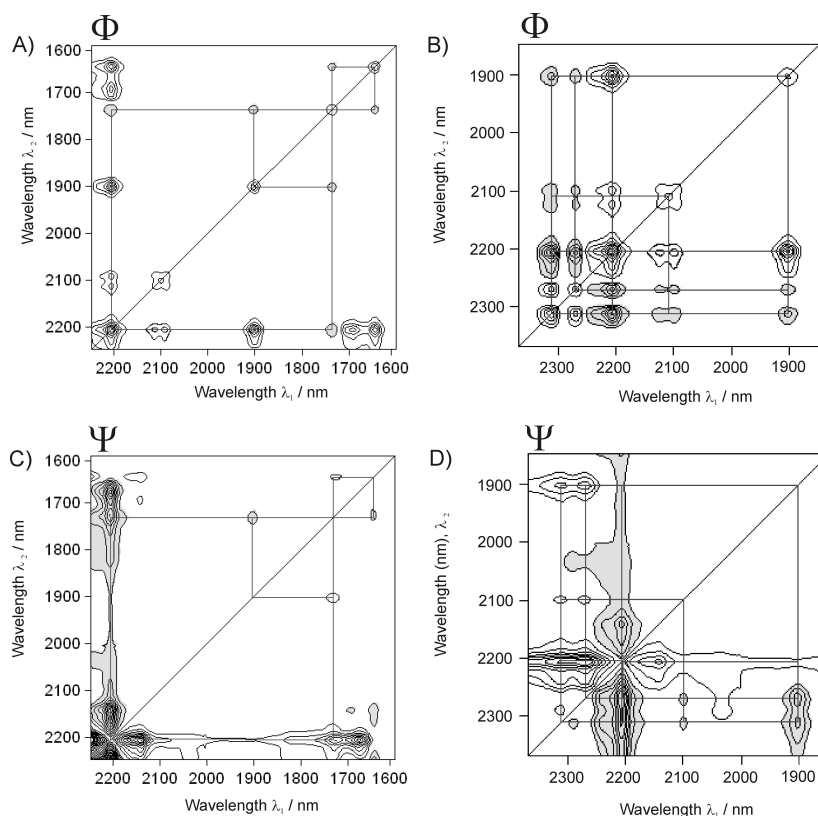


Figure 2: Synchronous spectra 2D NIR correlation map, (A and B) and asynchronous spectra map 2D NIR correlation map (C and D). Positive cross peaks in white contour, negative cross peaks in grey contour. Between 2250 and 1600 nm (A and C) and between 2400 and 1850 nm (B and D).

3.3 NMR analysis

Fig. 3A and 3B shows the ^1H and ^{13}C NMR spectra, respectively, of the products obtained after 100 minutes of reaction, with all the assignments. As can be seen all signals correspond unequivocally to spiroorthoester. These results confirm the postulated above that the only product obtained in the studied reaction is the spiroorthoester.

Table 1 Synchronous, Asynchronous 2D correlation intensities and order of intensities variations between bands in the characterization of (1) phenylglycidylether, (2) γ -butyrolactone, and (3) spiroorthoester.^a

Number	Φ	Ψ	Assignment	Order
1	Φ (1906,2208) >0	Ψ (1906,2208) > 0	2 (C=O), 1 (CH of epoxv)	1906 before 2208 nm
2	Φ (2310,1906) <0	Ψ (2310,1906) >0	3 (CH of CH ₂), 2 (C-O)	1906 before 2310 nm
3	Φ (2310,2100) <0	Ψ (2310,2100) >0	3 (CH of CH ₂), 2 (C=O)	2100 before 2310 nm
4	Φ (2310,2208) <0	Ψ (2310,2208) >0	3 (CH CH ₂), 1 (CH of epoxy)	2208 before 2310 nm
5	Φ (2275,1906) <0	Ψ (2268,1906) >0	3 (CH), 2 (C-O)	1906 before 2275 nm
6	Φ (2275,2208) <0	Ψ (2268,2208) >0	3 (CH), 1 (CH of epoxy)	2208 before 2275 nm
7	Φ (1734,1644) <0	Ψ (1734,1644) >0	3 (CH of CH ₂), 1 (epoxv)	1644 before 1734 nm
8	Φ (1734,1906) <0	Ψ (1734,1906) >0	3 (CH of CH ₂), 2 (C-O)	1906 before 1734 nm
9	Φ (1734,2208) <0	Ψ (1734,2208) >0	3 (CH of CH ₂), 1 (CH epoxv)	2208 before 1734 nm

^a v_1 after (before) v_2 means the intensity change of the band.

3.4 Multivariate curve resolution-alternating least squares (MCR-ALS)

Table 2 shows the information from the rank analysis of experimental matrix **D** (50 x 201). Only the five first values of the singular values calculated by SVD are shown. A visual analysis of them shows that only two factors can be considered significantly different from the others. This is in agreement with Amrhein *et al.* [30] who report that the number of significant factors corresponds to the number of independent reactions plus one. This agrees with the postulation that only the reaction of spiroorthoester formation takes place.

The strategy followed to overcome the rank deficiency is to append, as new row vectors (column-wise augmented data matrix), the pure spectra of phenylglycidylether and γ -butyrolactone. So, the new matrix **M** contains 52 spectra. The results of the rank analysis of this **M** matrix are also shown in Table 2. Now, there was a considerable increase in the third singular value, whose magnitude was similar to the second singular value of the **D** matrix. The rank deficiency, therefore, is broken and an attempt can be made to resolve the system satisfactorily. In accordance with the previous discussion, the initial estimates of the profiles required to apply MCR-ALS were: the spectra of pure of phenylglycidylether and γ -butyrolactone and for the product (spiroorthoester) the later spectra recorder in matrix **D**. In the optimization process, in which ALS is applied to the **M** matrix, two constraints were imposed; non-negativity for the concentrations profiles to be resolved in matrix **C** and for the spectral profiles in matrix **S**^T, and closure for the concentrations profiles. Likewise, a local

Table 2 Rank analysis of the matrix **D** and the column-wise augmented matrix **M**.

Number of factors	Singular value of the D matrix	Singular value of the M matrix
1	100.3893	100.6812
2	4.7608	4.8530
3	0.3424	2.1014
4	0.1658	0.3721
5	0.1088	0.3173

rank constraint of selectivity zone was imposed at the starting point of the reaction so that the concentration of the product associated with spiroorthoester was zero. This constraint is an approximation of reality because the first spectrum was recorded immediately after the two reagents were mixed. Also, constraint of equality was imposed at the stating point of the concentration values associated whit the reagents phenylglycidylether and γ -butyrolactone. The percentage value of total mass mixture corresponding to each reactive was imposed at the stating point of the concentration profile.

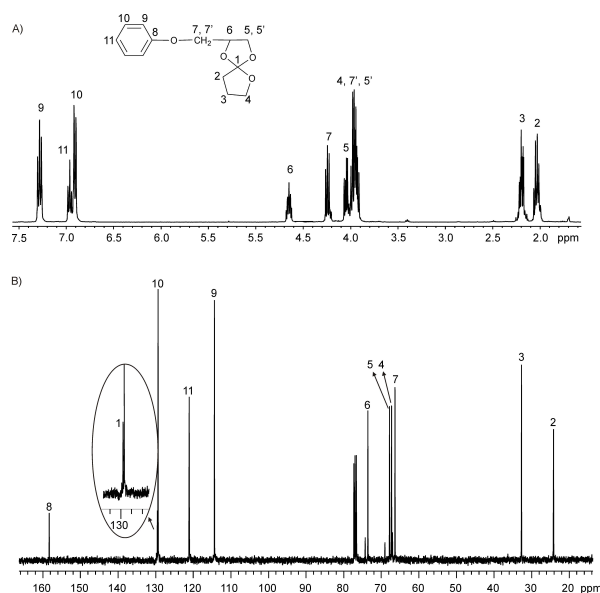


Figure 3: Shows the ^1H and ^{13}C (A and B) NMR spectra of the spiroorthoester obtained by cationic polymerisation. This result confirms the previous analysis, where only reaction that takes place is the one of spiroorthoester formation.

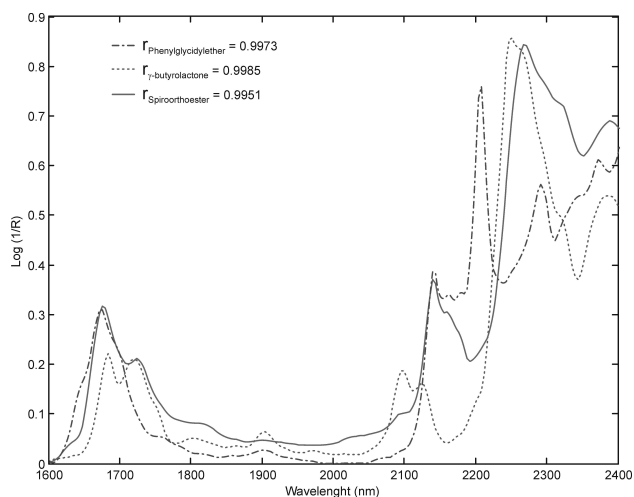


Figure 4: Spectra of the species recovered by MCR-ALS. phenylglycidylether (solid line), γ -butyrolactone (dotted line) and spiroorthoester (dash-dot line).

The found results during the optimization process gave rise to matrix \mathbf{C} (52×3), which contained the concentration profiles for the three compounds and \mathbf{S}^T matrix (3×201) which contained the corresponding spectra profiles. The product of both matrices, in accordance with eqn (1), accounts for 99.99 % of the variance associated with the augmented experimental \mathbf{M} matrix. The percentage of lack of fit was 0.96 %, which in quantitative terms means that it explains practically all the variability of the experimental data as a product of the found spectral and concentration profiles. However, this fit parameter provides an overall measure of the residual.

Fig. 4, shows the recovered spectral profiles for the species that are involved in the chemical reaction. The goodness of the spectral profiles was determined, in quantitative terms, using the similarity coefficient (r) between the recovered spectra and the experimental spectra. To calculate the r value for spiroorthoester, the recovered spectrum of spiroorthoester was compared to the spectrum corresponding to a sample of pure spiroorthoester synthesized by us [11]. The r values calculated were: 0.9973 for phenylglycidylether, 0.9985 for γ -butyrolactone and 0.9951 for spiroorthoester, indicating that all the recovered profiles have a high degree of concordance with the original ones.

Fig. 5, shows the concentration evolution of the chemical species. ALS results are expressed in mass units, so the corresponding values in moles were obtained by dividing each concentration profile by the corresponding molecular weight, assuming that each species and their molecular weight are known. In overall terms, this is a good reflection of the one expected, because independently of the catalyst effect on γ -butyrolactone, the result is a stoichiometric reaction. In the same way, as the reagent concentrations decrease the product concentration increase.

A more detailed analysis shows that, at the beginning of the reaction, the mol number for the reagents is the same and its value correspond to the mol number of the mixture. This situation was expected as equality constraints were applied in the optimization process. But, while the reaction is taking place, the evolution of the concentration profiles of γ -butyrolactone and phenylglycidylether are different being at the end of the reaction, the phenylglycidylether concentration zero while there is still some γ -butyrolactone. This can be explained if we take into account that the found solution is only one of the many that are possible. These solutions are to be found within the bands that include the possible values that minimize the **E** matrix eqn (1). Fig. 6 shows the limits associated with these possible solutions for the concentration profiles. These bands explains the discrepancies observed in the case of the unique solution shown in Fig. 5. To calculate these bands, the same constraint of selectivity and equality above indicated were imposed at the starting point of the reaction. For this reason, the ambiguity of the solution is more evident as the reaction goes on.

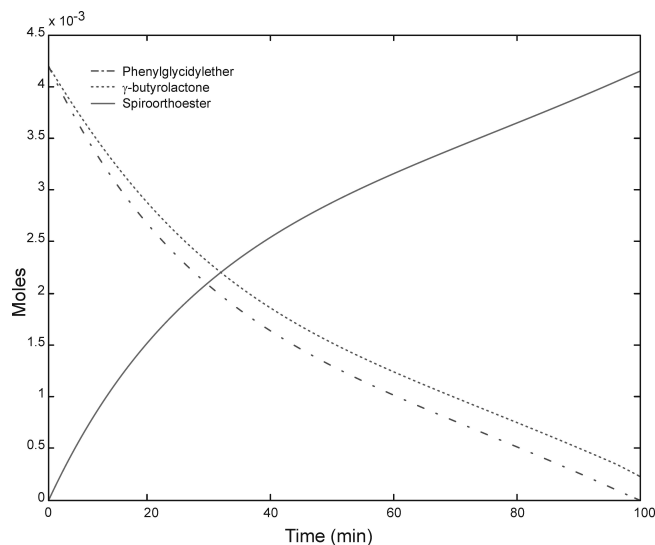


Figure 5: Concentration profiles of the species recovered by MCR-ALS. phenylglycidylether (solid line), γ -butyrolactone (dotted line) and spiroorthoester (dash-dot line).

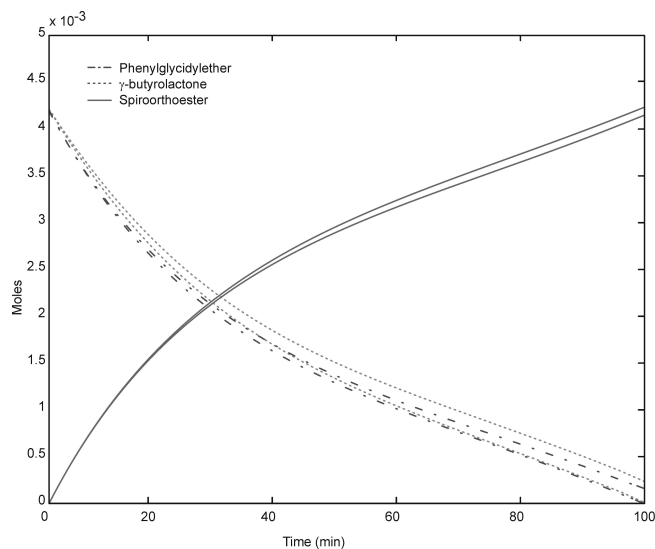


Figure 6: Maximum and minimum limits associated with the values of the concentration profiles by MCR-ALS. phenylglycidylether (solid line), γ -butyrolactone (dotted line) and spiroorthoester (dash-dot line).

4 Conclusions

In this study we have shown that generalized 2D NIR correlation is a powerful technique for identifying the sequential order in a cationic reaction, where different and competitive processes can occur, from phenylglycidylether and γ -butyrolactone. In the experimental conditions only one reaction is postulated, the one corresponding to the spiroorthoester formation. This was confirmed by recording the NMR spectra. This is also consistent with the values found in the rank analysis of the data matrix.

Applying MCR-ALS to the NIR spectra recorded during the reaction, allows to obtain the concentration values of the species that are involved. Also, the recovered spectrum for the final product (spiroorthoester) is in good agreement with the one obtained when spiroorthoester is isolated in more complex experimental conditions. As rotational and intensity ambiguities exist, the MCR-ALS solution found is one of a number of possible solutions, despite the restrictions imposed on the system. Finding the unique solution may involve other strategies such the combination of hard-modeling and soft-modeling.

These methodologies break new ground in the quantitative study of the reactions involved in the formation of the spiroorthoester, where successive steps and competitive reactions are involved.

Acknowledgements

The authors would like to acknowledge the economic support provided by the MCyT projects CTQ2007-61474/BQU and MAT2005-01593 and the CICYT (Comisin Interministerial de Ciencia y Tecnologia)

References

- [1] T. F. Mika and R. S. Bauer, Epoxy resins: chemistry and technology, ed. C. A. May, Marcel Dekker Inc., New York, 2nd edn., 1988, pp. 481.
- [2] H. J. Booth, In Expanding Monomers: Synthesis Characterization and Applications, ed. R. K. Sadhir, M. R. Luck, CRC Press, Boca Raton FL, 1992, pp. 208.

- [3] R. E. Smith, C. S. Pinzino, C. C. Chappelow, A. J. Holder, E. L. Kostoryz, J. R. Guthrie, M. Miller, D. M. Yourtee, J. D. Eick, *J. Appl. Polym. Sci.*, 92, (2004), 62.
- [4] T. Hino, T. Endo, *Macromolecules*, 36, (2003), 5902.
- [5] H. Nishida, H. Morikawa, N. Takeshi, T. Ogata, K. Kusumoto, T. Endo, *Polymer*, 46, (2005), 2531.
- [6] K. Bodenbenner, *Justus Liebig Ann*, 625, (1959), 183.
- [7] M. Fedtke, J. Houfe, E. Kahlert, G. Müller, *Angew. Makromol. Chem.*, 255, (1998), 53.
- [8] Y. M. Jung, S. B. Kim, I. Noda, *Appl. Spectrosc.*, 57, (2003), 1376.
- [9] M. López-Pastor, A. Dominguez-Vidal, M. J. Ayora-Cañada, M. Valcárcel, B. Lendl, *J. Mol. Struct.*, 799, (2006), 146.
- [10] M. S. Larrechi, F. X. Rius, *Appl. Spectrosc.*, 58, (2004), 47.
- [11] H. R. Keller, D. L. Massart, *Chemom. Intell. Lab. Syst.*, 12, (1992), 209.
- [12] R. Tauler, *J. Chemom.*, 15, (2001), 627.
- [13] J. Canadell, A. Mantecón, V. Cádiz, *Macromol. Chem. Phys.*, 208, (2007), 2018.
- [14] Matlab version 6.5., Mathworks Inc., Natick, MA, USA, 2002.
- [15] J. J. Kelly, C. H. Barlow, T. M. Jinguji, J. B. Callis, *Anal. Chem.*, 61, (1989), 313.
- [16] P. Geladi, D. McDougall, H. Martens, *Appl. Spectrosc.*, 39, (1985), 491.
- [17] F. C. Sanchez, S. C. Rutan, M. D. G. Garcia, D. L. Massart, *Chemom. Intell. Lab. Syst.*, 36, (1997), 153.
- [18] Y. M. Jung, H. S. Shin, S. B. Kim, I. Noda, *Appl. Spectrosc.*, 56, (2002), 1562.
- [19] P. C. Gillette, J. L. Koenig, *Appl. Spectrosc.*, 36, (1982), 535.

- [20] Noda, Appl. Spectrosc., 54, (2000), 994.
- [21] Noda and Y. Ozaki, Two-Dimensional Correlation Spectroscopy, John Wiley & Sons, Chitester, West Sussex, 2004, ch. 2, pp. 20-25.
- [22] Noda, A. E. Dowrey, C. Marcoli, G. M. Story and Y. Ozaki, Appl. Spectrosc., 54, (2000), 236A.
- [23] S. Šašić, A. Muszynski, Y. Ozaki, Appl. Spectrosc., 55, (2001), 343.
- [24] 2Dshige© Shigeaki Morita, Kwansei-Gakuin University, 2004-2006. All rights reserved.
- [25] G. H. Golub and F. van Loan, Matrix Computations; Johns Hopkins University Press: Baltimore, 2nd edn., 1983, p. 50.
- [26] A. De Juan, E. Casassas, R. Tauler, Soft modeling of analytical data: Encyclopedia of Analytical Chemistry: Applications Theory and Instrumentation, ed. R. A. Meyers, Wiley, New York, 2000, 11, pp. 9800.
- [27] R. Tauler, B. Kowalski, S. Fleming, Anal. Chem., 65, (1993), 2040.
- [28] <http://www.ub.edu/mcr/nttheory.htm>. Group of Solution Equilibria and Chemometrics, Analytical Chemistry Department, University of Barcelona.
- [29] P. Chabanne, L. Tighzert, J. P. Pascault, J. Polym. Sci. Part A: Polym. Chem., 53, (1994), 787.
- [30] M. Amrhein, B. Srinivasan, D. Bonvin, M. M. Schumacher, Chemom. Intell. Lab. Syst., 33, (1996), 17.

UNIVERSITAT ROVIRA I VIRGILI

TWO-DIMENSIONAL INFRARED CORRELATION SPECTROSCOPY AND MULTIVARIATE CURVE RESOLUTION

METHODS: APPLICATION TO QUANTITATIVE MONITORING OF CURING PROCESS

Nicolas Spegazzini

ISBN:978-84-693-4049-3/DL:T.998-2010

3.2 Study of a curing reaction using wavenumber-wavenumber two-dimensional FTIR correlation spectroscopy and evolving factor analysis (EFA)

A curing epoxy monitored by FTIR-ATR was considered. The reaction corresponds to the polymerization between DGEBA and γ -valerolactone. The possible reactions involved in this process have already been reported in the literature, but their sequential order has not been reported. The reaction pathway was corroborated by 2DCOS and the sequential order in which the reaction takes place is proposed by combining evolving factor analysis and 2DCOS.

UNIVERSITAT ROVIRA I VIRGILI

TWO-DIMENSIONAL INFRARED CORRELATION SPECTROSCOPY AND MULTIVARIATE CURVE RESOLUTION

METHODS: APPLICATION TO QUANTITATIVE MONITORING OF CURING PROCESS

Nicolas Spegazzini

ISBN:978-84-693-4049-3/DL:T.998-2010

Two-Dimensional Fourier Transform Infrared Correlation Spectroscopy and Evolving Factor Analysis in the Study of Cationic Curing of DGEBA and γ -Valerolactone Mixtures

Journal of Polymer Science Part A: Polymer Chemistry
46, (2008), 3886

Nicolás Spegazzini,¹ Itziar Ruisánchez,¹ M. Soledad Larrechi¹
Angels Serra,² Ana Mantecón²

¹Chemometrics, Qualimetrics and Nanosensors Group, ²Polymer's
Research Group, Department of Analytical and Organic Chemistry,
Rovira i Virgili University. Marcel·lí Domingo s/n, 43007, Tarragona,
Spain

Abstract

Generalized two dimensional (2D) correlation spectroscopy and evolving factor analysis (EFA) have been applied to the study of cationic curing reaction of mixtures of diglycidyl ether of bisphenol A (DGEBA) and γ -valerolactone (γ -VL). The reaction has been monitored by Fourier Transform Infrared (FTIR) Spectroscopy. The reaction periods in which a chemical change takes place are identified using EFA and then the sequence of changes are established by means of the interpretation of the synchronous and asynchronous spectra obtained with 2D correlation spectroscopy. By combining this information, in the curing process, four reactions have been detected: 1) DGEBA and γ -valerolactone reaction to obtain a spiroorthoester intermediate; 2) homopolymerization of DGEBA;

3) copolymerization of DGEBA with the spiroorthoester intermediate (SOE) 4) homopolymerization of the spiroorthoester.

Keywords: two-dimensional correlation spectroscopy; evolving factor analysis; curing reaction; fourier transform infrared; epoxy resin

1 Introduction

Glycidyl type epoxy resins, prepared mainly from bisphenol A and other phenolic compounds have long been used as starting products to prepare epoxy thermosets. Several curing agents, such as aromatic amines, have been used to achieve good results in reinforced materials, molding powders, coatings, adhesives, insulation materials, and foams [1]. However, diglycidyl ether of bisphenol A (DGEBA) epoxy resins present some drawbacks as a consequence of the shrinkage produced during the curing process, which worsens the mechanical properties due to the formation of microvoids and microcracks and the adhesion is reduced [2]. Of the different methods of polymerization, ring-opening mechanism leads to the lowest shrinkage, because when a Van der Waals distance is converted to a covalent bond, another covalent bond is converted to a Van der Waals distance. Bailey [3,4] introduced the term expanding monomers, which refers to monomers that lead to zero shrinkage or even positive expansion during polymerization. These monomers are generally bicyclic that open with the conversion of covalent bonds to van der Waals distances. Of these bicyclic compounds, spiroorthoesters (SOEs) are some of the most commonly used [2]. SOEs can readily be synthesized from lactones and epoxides in the presence of a Lewis acid as a catalyst [5,6]. The high cost of synthesizing these SOEs means that their technological applications are limited. Thus, we proposed that three-dimensional networks prepared by copolymerization of epoxy resins and lactones can form an intermediate SOE, reducing the volume shrinkage during curing. In the firsts stages of curing SOE is formed with shrinkage, when the curing mixture is still liquid, and then polymerize or copolymerize with epoxides with expansion until the end of the curing process. In this way, the shrinkage after gelation is strongly reduced [7,8]. In addition to the aforementioned reactions, the homopolymerization of epoxide

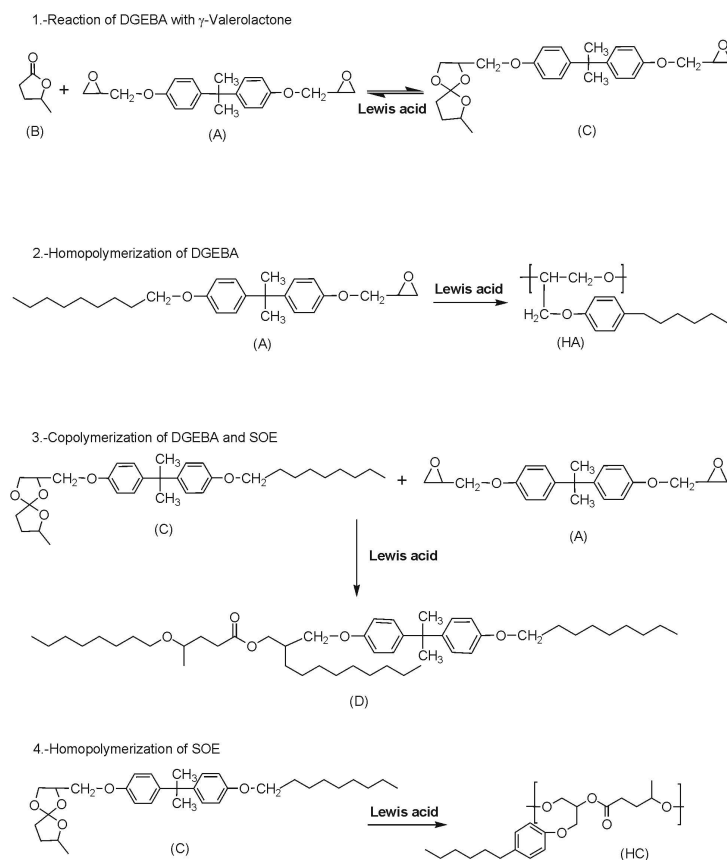
can also occur (Scheme 1). It should be mentioned that -VL does not homopolymerize in these conditions by thermodynamical reasons [9]. To get low shrinkage during curing and materials with good properties the knowledge of the individual reactive processes that occur during curing is of great importance. Fourier Transform infrared spectroscopy (FTIR) has been widely used to study the structural changes that take place during polymerization such as the curing of epoxy resins [9-12]. The spectral analysis is usually based on changes observed in the characteristics of the spectroscopic frequencies of each functional group; it is therefore a univariate analysis. Applying chemometric methods to data obtained during spectral monitoring of a reaction provides information about correlated and uncorrelated spectral changes and describes the overall changes between different spectra of the data sets. The best chemometric methods for this purpose are based on factor analysis techniques or two-dimensional (2D) correlation spectroscopy. Since they rely on different mathematical approaches, they differ fundamentally both in usability and in how the results of the data analysis are obtained. One method for analyzing evolving data sets is based on evolving factor analysis (EFA) [13]. This method determines the significant number of chemical/physical components that contribute to the experimental data measured during the reaction. The number of significant EFA factors is an indication of the sources of variability in the data and can be correlated with the number of species that take part in the reaction. Further information can be obtained about the time at which the significant changes take place. This information is useful for determining the number of stages (subreactions) and their sequential order [14]. A second chemometric method is generalized 2D correlation spectroscopy. This method, proposed by Noda [15-18], has become a powerful and versatile tool for elucidating spectral changes (e.g., reaction time) induced by external perturbation. It has several advantages. First, it has powerful deconvolution ability for highly overlapped bands. Second, it provides information about the interintramolecular interaction by correlating absorption band intensities of different functional groups. And third, the changes in intensity of a specific sequence that occurs during the measurement can be derived. Several research groups have reported applications of generalized 2D correlation spectroscopy. Some applications have focused on temperature-dependent spectral variations of self-associated molecules [19] and composition-dependent spectral variations in ethy-

lene/vinyl acetate copolymers [20] revealing the system dynamics decomposition of the perturbation domain [21]. No studies combining these techniques have been found in the literature for curing reactions. In this study, we present the use of EFA analysis in conjunction with 2D FTIR correlation spectroscopy for studying the cationic curing reaction of a mixture of DGEBA and γ -valerolactone (γ -VL) in the presence of a Lewis acid, ytterbium triflate. In a previous work, this curing process was reported using several rare earth triflates as initiators [22]. However, the investigation of the mechanism can be done in a more accurate way by the use of chemometrics methods. Since there is a competitive reaction of the epoxy homopolymerization in the curing reaction, we also used these techniques to study DGEBA homopolymerization. We focus on the use of EFA analysis to identify the reaction periods in which a chemical change takes place. These chemical changes can be related to several chemical reactions that take place during the curing process. Once we have identified these periods, we focus on the cross correlation peaks in the synchronous and asynchronous 2D spectra to establish the sequence of these changes. Finally, we combine all of this information first to identify the chemical reactions that cause the chemical or spectral variations and second to identify the sequential order of these reactions. This study shows the great potential of combining these techniques to accurately interpret the spectral changes that take place during curing reactions monitored by FTIR.

2 Experimental

2.1 Studied reaction

The curing reaction of the DGEBA/ γ -VL mixture involves several reactions (Scheme 1). The first indicated is the DGEBA homopolymerization, which should be considered because we work in an equivalent excess of epoxide/lactone (four epoxide groups for each lactone). The second corresponds to the formation of an intermediate SOE. The third reaction is the copolymerization of the SOE with epoxide. Finally, the fourth reaction corresponds to the homopolymerization of SOE, which is the least favored process and is only important when there is no epoxide in the reaction medium [11]. Note that, as γ -VL does not homopolymerize for thermodynamic reasons, this reaction



Scheme 1: Chemical reaction of DGEBA with γ -VL (2:1) at $T = 160^{\circ}\text{C}$. (A) DGEBA; (HA) homopolymer of DGEBA; (B) γ -VL; (C) spiroorthoester (SOE); (D) Copolymer, and (HC) homopolymer of SOE.

does not appear in Scheme 1. To facilitate the study, we also carried out the curing of DGEBA with 1 phr of ytterbium triflate. In this process, the only reaction that takes place is reaction 1 in Scheme 1.

2.2 Materials

DGEBA Epikote 827 was supplied by Shell (EEW 182.08 g/mol), γ -VL and ytterbium (III) triflate were supplied by Aldrich. They were used without previous purification.

2.3 Sample preparation procedures and FTIR spectroscopy

Two experimental curing processes were carried out. One of these was the curing of DGEBA/ γ -VL (2:1 mol/mol) mixture in the presence of 1 phr (parts of initiator per 100 part of mixture, w/w) of ytterbium triflate. The reaction was carried out at 160°C. The second process was the homopolymerization of DGEBA with 1 phr of initiator in the same experimental conditions as the first reaction. In both processes, the sample was placed on a small diamond crystal in the spectrophotometer ATR cell (FTIR-680PLUS JASCO), which has a 3000 SeriesTM High Stability Temperature Controller with a RS232 Control to take the measurements. For each experiment we automatically acquired data at intervals of 30 s at 4 cm⁻¹ resolution between 700 and 1850 cm⁻¹ until no changes over time were observed in the spectra. The curing reaction ended after 23 min. For each experiment, 47 spectra were obtained. The spectra were exported and converted into MATLAB binary files [23]. The experimental data were arranged in matrices of (47 x 1247) whose rows were the recorded spectra and whose columns were the absorbance values at different wavenumbers. All spectra were pretreated with a multiplicative scattering correction for eliminating the additive scatter factor (offset deviation) and de multiplicative scatter factor [24].

2.4 Evolving Factor Analysis

The core of algorithms based on EFA is the determination of the chemical rank of submatrices of the total matrix of measurements. In EFA, windows of linearly increasing size are subjected to rank analysis. In our study we started with the first two spectra and then calculated the rank by adding one spectrum at a time until we reached the total matrix (47 x 1247). The matrix rank was evaluated using the singular value decomposition algorithm [25]. The singular values were calculated in both directions (forwards and backwards) [23].

2.5 Two-Dimensional Correlation Analysis

Several spectra, at equal time intervals over a certain wavenumber range, were selected for 2D correlation analysis using “2D shige” of Shigeaki Morita (Kwansei-Gakuin University) [26]. For the purposes

of comparison, a time-averaged 1D reference spectrum is shown at the side and top of the 2D correlation maps. In these maps, the red regions indicate positive correlation intensities and the blue regions indicate negative correlation intensities. In the contours maps (ampliation of specific regions), the white regions indicate positive correlation intensities and the gray regions indicate negative correlation intensities. In 2D correlation analysis, two types of correlation spectra are obtained and depicted in two different maps: these synchronous and asynchronous maps provide complementary information about the spectral bands. In the synchronous spectra correlation $\Phi(\nu_1, \nu_2)$, the cross peaks indicate the correlation between spectroscopic variables (wavenumber). Under the same perturbation, the increase or decrease is simultaneous. More information can be obtained from the corresponding asynchronous correlation spectra $\Psi(\nu_1, \nu_2)$, where the cross peaks develop only if the intensities of two dynamic bands change asynchronously. Also, the sign of an asynchronous correlation peak, $\Psi(\nu_1, \nu_2)$, provides information about the sequential order of intensity variations between band ν_1 and ν_2 . According to the Noda and Ozaki [18] publications, when $\Phi(\nu_1, \nu_2) > 0$, if $\Psi(\nu_1, \nu_2)$ is positive, band ν_1 varies before to band ν_2 , and, if $\Psi(\nu_1, \nu_2)$ is negative, band ν_1 varies after ν_2 . If $\Phi(\nu_1, \nu_2) < 0$, the rules are the other way round [16].

3 Results and discussion

3.1 One-Dimensional Analysis

Figures 1 and 2 show the most relevant spectra of the spectroscopic changes that take place during the curing of DGEBA and γ -VL mixture and those that take place during the DGEBA homopolymerization, respectively. The spectroscopic band assignments of the two processes are shown in Table 1. Spectral analysis of the curing process (Fig. 1) shows that the 1776 cm^{-1} stretching band characteristic of the carbonyl group of the γ -VL, decreases during the first 23 spectra and then increases until the end of the crosslinking. The 1736 cm^{-1} band, characteristic of an aliphatic lineal ester, increases during the curing process. This band can be assigned (Table 1) to the copolymer (D) and to the SOE homopolymer (HC) (Scheme 1). The 910 cm^{-1} band characteristic of the oxirane ring decreases until it disappears.

If we make the difference between the last (47) and the first spec-

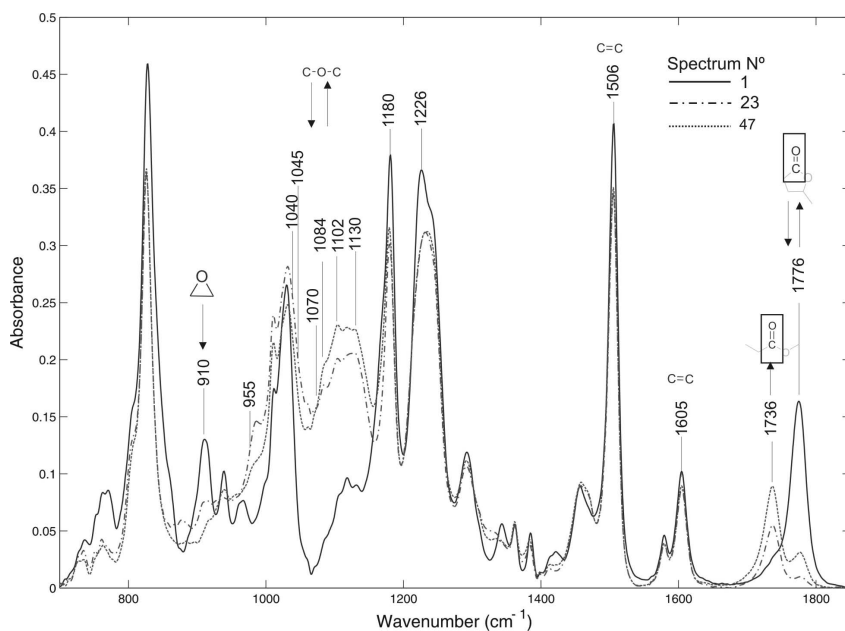


Figure 1: Spectra N° 1, 47 and the spectrum N° 23 (where the band increases again of 1776 cm^{-1}) in the polymerization process.

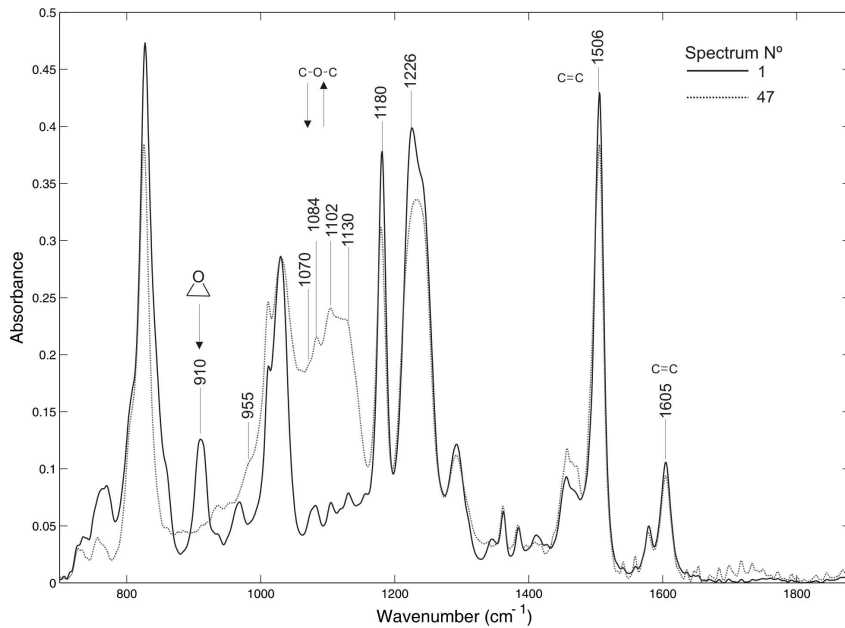


Figure 2: Spectra N° 1 and 47 of the homopolymerization of DGEBA.

Table 1. Assignment of the bands in the FT-IR spectrum reactions compounds. Characteristics of DGEBA (A), γ -Val (B), Homopolymer DGEBA (HA), SOE (C), γ Copolymer (D). ^a(See Refs. ²⁷⁻⁴²)

Frequency wavenumber (cm ⁻¹)	Intensity	Assignment	Functional group	Compounds
735	w	=C-Hoop def vib		All
760	w	=C-Hoop def vib	Sust. Sist. Aromatic =C-H	All
770	w	=C-Hoop def vib	Sust. Sist. Aromatic =C-H	All
840	s	=C-Hoop def vib	Sust. Sist. Aromatic =C-H	All
910	m	C-O str vib (asym)	Epoxy C-O-C oxirane ring	A
940	w	C-O	γ -Lactone C-O	B
950	sh	C-O str vib	Ether C-O-C	A, HA, C, D, HC
955	sh	C-O str vib	Ether C-O-C	A, HA, C, D, HC
984	w	C-O str vib	Epoxy C-O-C	A
1010	s	C-O str vib	Cyclic C-O-C ether	C
1030	s	C-O str vib	Cyclic C-O-C ether	C
1040	w	C-O str vib	Cyclic C-O-C ether	C
1045	w	C-O str vib	Cyclic C-O-C ether	C
1070	m-s	C-O str vib (asym)	Cyclic C-O-C ether	HA
1084	m-s	C-O str vib (asym)	Cyclic C-O-C ether	HA
1102	m-s	C-O str vib (asym)	Cyclic C-O-C ether	HA
1130	m-s	C-O str vib (asym)	Cyclic C-O-C ether	HA
1180	s	C-O str vib (asym)	Cyclic C-O-C ether	HA
1226	s	C-O str vib (asym)	Aryl-O-CH ₂	A, HA, C, D, HC
1234	s	C-O str vib (asym)	Aryl-O-CH ₂	A, HA, C, D, HC
1292	m	C-O str vib (asym)	Aryl-O-CH ₂	A, HA, C, D, HC
1362	w	C-H def vib sym	-CH ₃	A, C,
1384	w	C-H def vib sym	-CH o C-CH ₃	A, HA, C,
1455	m	C-H def vib asym	-CH ₃	A, C, D, HC
1480		C-H def vib asym	-CH ₃	A, C, D, HC, HA
1506	s	C=C str vib	Ring -C=C-	A, HA, C, HC, D
1580	w	C=C str vib	Ring -C=C-	A, HA, C, HC, D
1605	m	C=C str vib	Ring -C=C-	A, HA, C, HC, D
1736	m	C=O str vib	Linear ester	D, HC

^a Symbols used: w (weak), m (medium), s (strong), m-s (me strong), v (variable), sh (sharp), oop (out-of-plane), asym (asymetric), sym (symetric), str (stretching), def (deformation), vib (vibration).

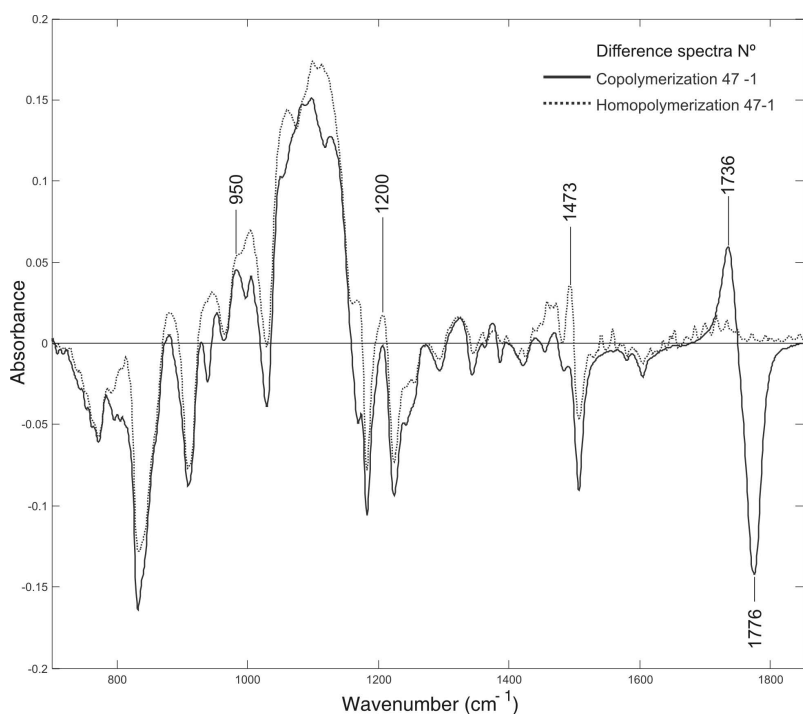


Figure 3: Difference spectrum obtained by the subtraction of the initial spectrum N°1 in the spectrum N° 47 of copolymerization and homopolymerization process.

trum (1) for both processes and we compare them (Fig. 3), without looking at the bands at 1736 and 1776 cm^{-1} , we can observe a different behavior in the 950-1200 cm^{-1} spectral range, which corresponds mainly to C-O-C stretching [27-33]. In addition, we can see a difference at 1473 cm^{-1} associated with the asymmetric stretching of CH_3 groups [33-35]. Both moieties are present in practically all the structures involved in the studied processes, although they are in a different chemical environment. This leads to the conclusion that in this spectral range, 950-1200 cm^{-1} , they are some C-O-C characteristic bands associated to SOE structures, different from those attributed to the ether stretching bonds, present in the final material. In his context, the studies by Wellingshof et al. [34] on mixtures of aromatic polystyrene and polyether show that phenyl ring interaction may affect chain mobility and some changes therefore occur in the tension band of the C-O-C group.

For the curing reaction of the mixture of DGEBA and γ -VL, the EFA results (Fig. 4) show that, in both directions (forwards and backwards), four factors are significantly different from noise. Note that, in the forward direction, there are two significant factors at the beginning of the reaction, one after spectrum 5 and one after spectrum 20. However, if the analysis is made in the opposite direction, one factor is significant between spectrum 47 and spectrum 40, two are significant between spectrum 40 and spectrum 25 and the fourth significant factor is observed at spectrum 10. Figure 5 shows the most relevant spectra for the above time reaction intervals (spectra 1, 5, 20, 37, and 47). A detailed analysis of these spectra shows that, between spectra 1 and 5, there are decreases in intensity of 910 and 1776 cm^{-1} band, which are characteristic of the oxirane group and γ -VL, respectively. These changes indicate that the intermediate SOE is formed. There are also significant changes around 955, 1030, 1180, and 1226 cm^{-1} and between 1030 and 1180 cm^{-1} . According to the spectroscopic assignation of Table 1, intensities at 955 and 1180 cm^{-1} can be assigned to aliphatic C-O-C stretching, whereas the band at 1226 cm^{-1} corresponds to the tension vibrations of Aryl-O-CH₂. All of the above changes can also, therefore, be explained by epoxy homopolymerization.

At spectrum 20 the band at 1736 cm^{-1} clearly appears. As this band is characteristic of an aliphatic ester, it indicates that copolymer D (reaction 3, Scheme 1) is present. The increase in intensity may also be related to SOE homopolymerization (reaction 4, Scheme 1), though this reaction is not favored in the presence of oxirane groups [7], since although the intensity of the band at 910 cm^{-1} decreases. These reactions may be responsible for a new chemical situation and, therefore, for the new significant factor (Fig. 4). At spectrum 37, the intensity of the band at 1776 cm^{-1} , characteristic of the carbonyl group present of the γ -VL and which disappeared at spectrum 20, newly increases. This increase may indicate the reversibility of reaction 2 (Scheme 1). Booth [2] demonstrated the breakdown of SOE on addition of boron trifluoride etherate catalyst to the compounds from which it was prepared (epoxide and lactone). Spectral variations may be the cause of the fourth and last significant factor (Fig. 4). From here until the end of the reaction (spectrum 47), there are no more significant spectral variations so all the chemical variation due to the copolymerization reactions is explained in these four factors.

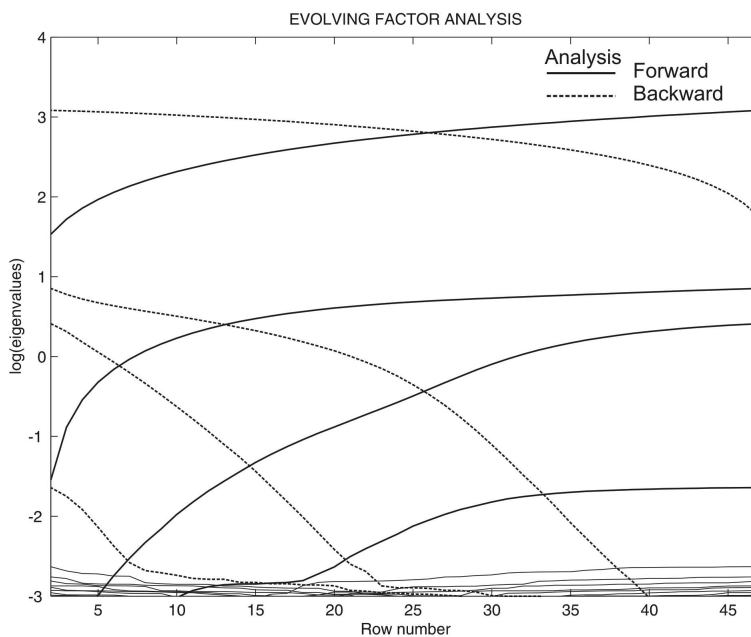


Figure 4: EFA of the obtained results of the experimental matrix D_1 for chemical reaction of DGEBA with γ -VL.

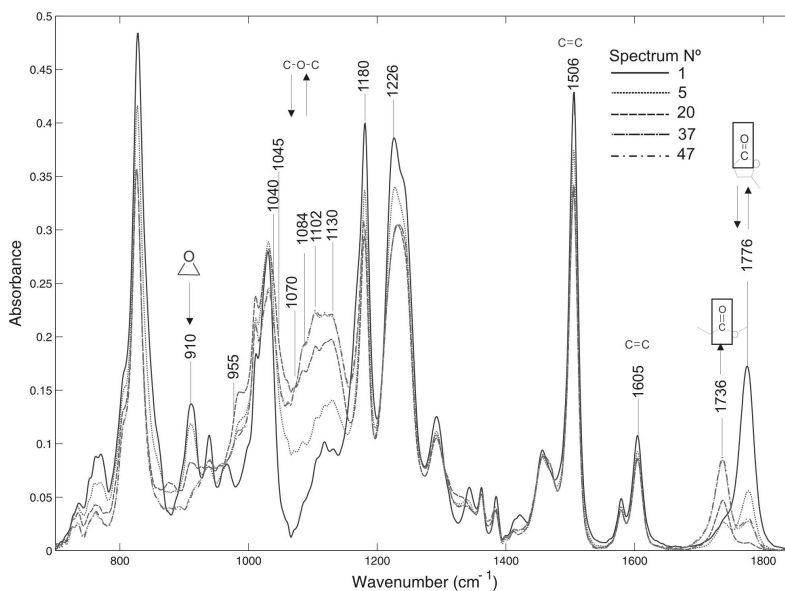


Figure 5: Spectra N° 1, 5, 20, 37 and 47 the copolymerization of DGEBA with γ -VL.

We should stress that, when the EFA study is done in the backward direction, between spectrum 47 and spectrum 40, the chemical variation is explained by only one factor. During this reaction period, there are no changes in the band intensity characteristics of the oxirane group (910 cm^{-1}) and we can therefore conclude that no reactions in which DGEBA is involved take place. If this is true, chemical process other than reversibility must take place to explain the increase in intensity of the 1776 cm^{-1} band.

Similarly, when the EFA is applied to the DGEBA homopolymerization process (Fig. 6), there are also four significant factors during the reaction time. As in the copolymerization process, forward analysis shows two significant factors at the beginning of the reaction. These two factors may be related to the fact that we were working with DGEBA, which has several hydroxyl groups. The hydroxyl groups could be responsible for the competition between the activated monomer (AM) mechanism and the active chain end mechanism (ACE) [36]. These two mechanisms are illustrated in Scheme 2. We should stress that the mechanism competition is not as great in the presence of lactone since the coordination of the lactone takes place with the initiator [7,11]. Also, in our case, the proportion of hydroxyl groups in the mixture is much lower.

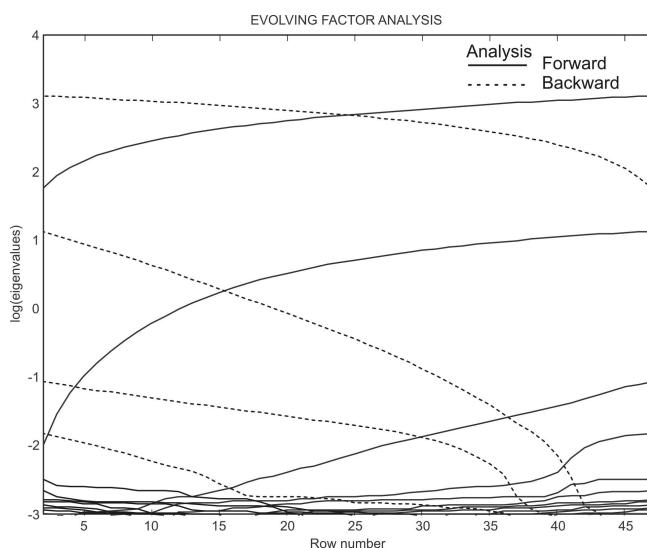
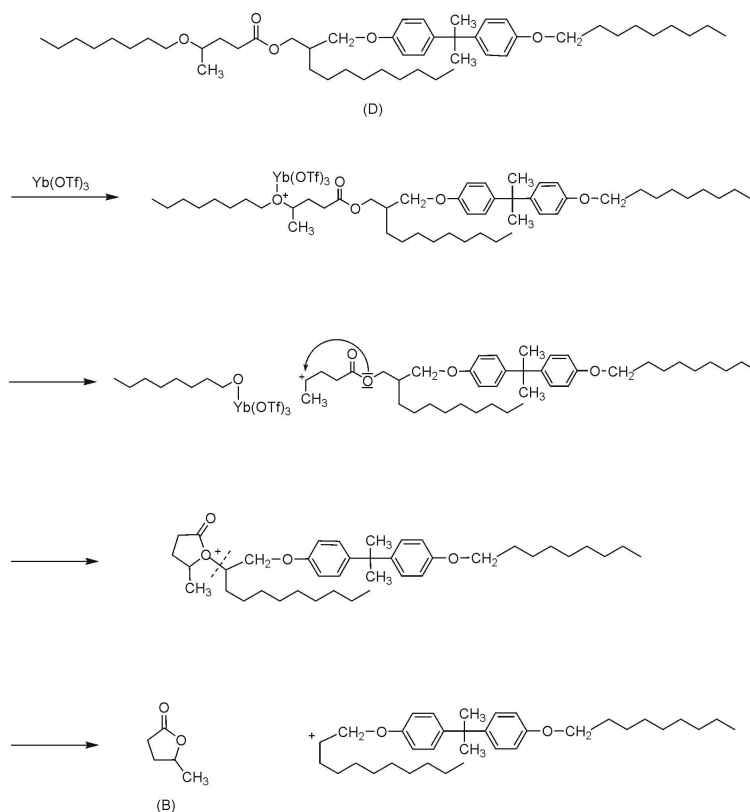


Figure 6: EFA of the obtained results of the experimental matrix \mathbf{D}_2 for chemical reaction (1) of the homopolymerization of DGEBA.



Scheme 2: Mechanism of despolymerization of the copolymer begun for $\text{Yb}(\text{OTf})_3$. (D) Copolymer and (B) γ -VL.

The other two significant factors in the EFA plot (Fig. 6) can be explained by the formation of different polyether structures such as 1,4-dioxanes, whose presence has been described in the cationic polymerization of epoxides with Lewis acids [37-39]. Another possible explanation is the formation of big cycles or chain transference due to a “back-biting” processes [3]. As well as these explanations, we must also consider variations in the mobility chain due to the gelification process.

3.2 Two-dimensional analysis

We take into account the information from the EFA study of the DGEBA/ γ -VL curing, (a) to study the 2D spectra correlation for the most important reaction time intervals. Synchronous correlation of the first four spectra, [Fig. 7(a), 1] shows, that the 1776 cm^{-1} band characteristic of the γ -VL has a negative correlation with the 910 cm^{-1} band characteristic of the oxirane group. Because both bands are characteristic of the reagents, and that their intensities diminish, Figure 5, it is expected a positive correlation between both bands. The negative sign of the synchronous peak can be understand taking into account that the reaction of the DGEBA homopolymerization, which leads to intensity variations at 910 cm^{-1} , occurs no simultaneously with the process in which DGEBA reacts with the γ -VL. [Fig. 7(a), 2] Moreover, such as expected, both bands have a negative correlation with bands at 955 , 1040 , 1045 , 1070 , 1084 , 1102 , and 1130 cm^{-1} , some of which, according to Table 1, are characteristic of the C-O-C stretching vibrations present in the chemical structures formed in both processes: the epoxy homopolymerization (reaction 1,

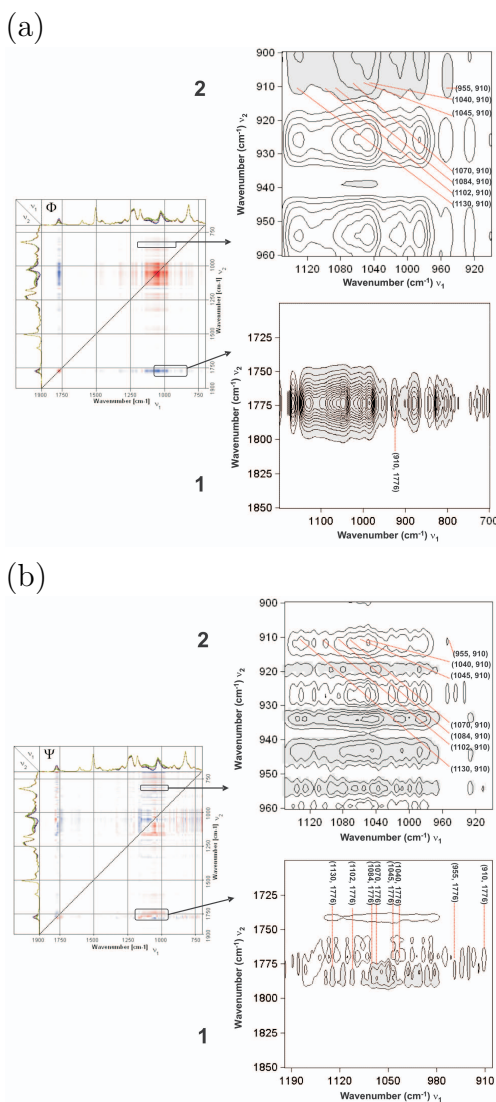


Figure 7: Set (1-4). Spectra a) synchronous and b) asynchronous of the chemical reaction of the DGEBA with γ -VL

Scheme 1) and in the intermediate SOE formation (reaction 2, Scheme 1).

More information can be obtained from the asynchronous spectra [Fig. 7(b)] in which cross peaks appear only if the band intensity changes asynchronously. Asynchronous peaks can be observed between the same bands mentioned in the synchronous spectra. If we consider the correlation sign and apply the Noda rules (Table 2), we can draw the following conclusions. The sign of asynchronous peak between 910 and 1776 cm^{-1} [Fig. 7(b), 1] is positive and for this reason, the variation in the intensity of the band at 910 cm^{-1} is retarded in reference to that at 1776 cm^{-1} . This means that the reaction of γ -VL with DGEBA is more favored than the DGEBA homopolymerization. The variations in intensity (Table 2) of the 955, 1070, 1084, 1102, and 1130 cm^{-1} bands occur before the variations in the 1776 cm^{-1} band that are characteristic of γ -VL and after the variation in the 910 cm^{-1} band that is characteristic of DGEBA. This sequence means that they may be considered as characteristic of the C-O-C stretching of the molecular structures produced in the epoxy homopolymerization. Moreover, the variations in the intensity of the 1045 and 1040 cm^{-1} bands occur after the variations in 1776 cm^{-1} band [Fig. 7(b), 1], so they may be associated with SOE stretching. This is in agreement with the Nishida assignation [40,41], which describes these bands as characteristic of the SOEs.

Table 2. Synchronous, Asynchronous 2D correlation intensities and order of intensities variations between bands for set (1-4) in the characterization of DGEBA (A), γ -VL (B), homopolymer of DGEBA (HA), and SOE (C).

no.	Φ	Ψ	Assignment	Order
1	$\Phi(910, 1776) < 0$	$\Psi(910, 1776) > 0$	(A, B)	910 after 1776 cm^{-1}
2	$\Phi(955, 1776) < 0$	$\Psi(955, 1776) < 0$	(HA, B)	955 before 1776 cm^{-1}
3	$\Phi(1040, 1776) < 0$	$\Psi(1040, 1776) > 0$	(C, B)	1040 after 1776 cm^{-1}
4	$\Phi(1045, 1776) < 0$	$\Psi(1045, 1776) > 0$	(C, B)	1045 after 1776 cm^{-1}
5	$\Phi(1070, 1776) < 0$	$\Psi(1070, 1776) < 0$	(HA, B)	1070 before 1776 cm^{-1}
6	$\Phi(1084, 1776) < 0$	$\Psi(1084, 1776) < 0$	(HA, B)	1084 before 1776 cm^{-1}
7	$\Phi(1102, 1776) < 0$	$\Psi(1102, 1776) < 0$	(HA, B)	1102 before 1776 cm^{-1}
8	$\Phi(1130, 1776) < 0$	$\Psi(1130, 1776) < 0$	(HA, B)	1130 before 1776 cm^{-1}
9	$\Phi(955, 910) < 0$	$\Psi(955, 910) > 0$	(HA, A)	955 after 910 cm^{-1}
10	$\Phi(1040, 910) < 0$	$\Psi(1040, 910) > 0$	(C, A)	1040 after 910 cm^{-1}
11	$\Phi(1045, 910) < 0$	$\Psi(1045, 910) > 0$	(C, A)	1045 after 910 cm^{-1}
12	$\Phi(1070, 910) < 0$	$\Psi(1070, 910) > 0$	(HA, A)	1070 after 910 cm^{-1}
13	$\Phi(1084, 910) < 0$	$\Psi(1084, 910) > 0$	(HA, A)	1084 after 910 cm^{-1}
14	$\Phi(1102, 910) < 0$	$\Psi(1102, 910) > 0$	(HA, A)	1102 after 910 cm^{-1}
15	$\Phi(1130, 910) < 0$	$\Psi(1130, 910) > 0$	(HA, A)	1130 after 910 cm^{-1}

We can therefore conclude that during this reaction time (120 s), which corresponds to the first four spectra, the two mentioned reactions take place but in the following order: firstly SOE formation and then epoxy homopolymerization. Figures 8(a,b) show the synchronous and asynchronous spectra obtained between spectra 5 and 15, where applying EFA to this time, we observe three significant factors (Fig. 4). This extra information refers to the 1736 cm^{-1} band, which is characteristic of the ester of the copolymer. Again, applying Noda rules allows us to estimate the sequential intensity band variations shown in Table 3. The 1736 cm^{-1} band can be related to the SOE homopolymerization (scheme 1, reaction 4) and to the epoxy and SOE copolymerization (Scheme 1, reaction 3). If SOE homopolymerization takes place, the synchronous spectra must have negative cross peaks of the 1736 cm^{-1} band with the 1040 and 1045 cm^{-1} band. This does not happen [Fig. 8(a), 2]. We therefore conclude that, up to this reaction time, there is no SOE homopolymerization. On the other hand, if the increase in intensity in the 1736 cm^{-1} band is due to the formation of the copolymer, we should have a synchronous cross negative peak between that band and the 910 cm^{-1} band, which does happen [Fig. 8(a), 2]. Moreover, if we consider the sign of the asynchronous peaks for these two bands, we can con-

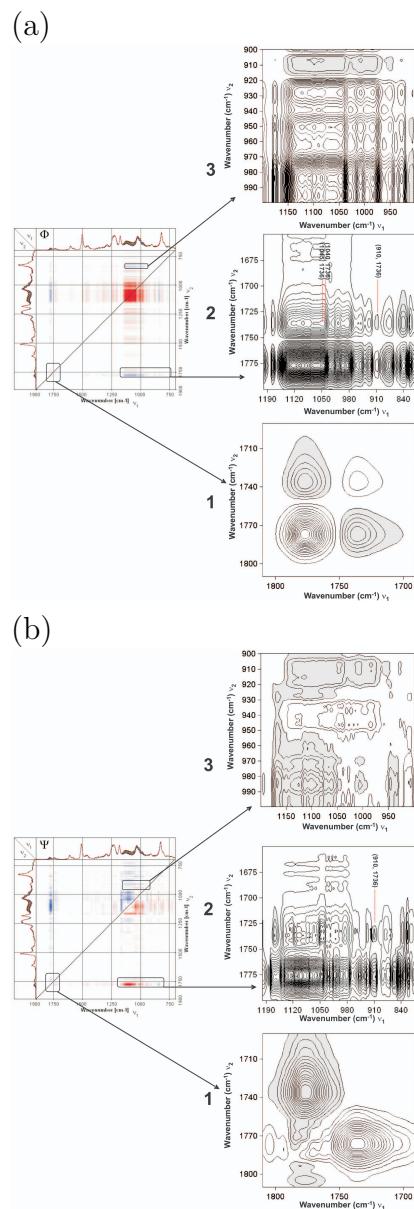


Figure 8: Set (5-15). Spectra a) synchronous and b) asynchronous of the chemical reaction of the DGEBA with γ -VL

clude that the intensity of the 1736 cm^{-1} band varies after the intensity of the 910 cm^{-1} band. We can therefore assign the variation in intensity of the 1736 cm^{-1} band to the formation of the copolymer. This conclusion agrees with the work of Mas et al. [11] who showed that SOE homopolymerization is not favored when there is an excess of epoxy in the curing of mixtures of DGEBA and γ -lactone. Until spectrum 15, that is, in the first 420 s of the reaction, three reactions took place in the following order: (1) intermediate SOE formation, (2) epoxy homopolymerization, and (3) epoxy and SOE copolymerization.

Table 3. Synchronous, Asynchronous 2D correlation intensities and order of intensities variations between bands for set (5-15) in the characterization of DGEBA (A), γ -VL (B), homopolymer of DGEBA (HA), SOE (C), and copolymer (D).

no.	Φ	Ψ	Assignment	Order
1	$\Phi(910, 1736) < 0$	$\Psi(910, 1736) < 0$	(A, D)	910 before 1736 cm^{-1}
2	$\Phi(950, 1736) > 0$	$\Psi(950, 1736) > 0$	(C, D)	950 before 1736 cm^{-1}
3	$\Phi(955, 1736) > 0$	$\Psi(955, 1736) > 0$	(HA, D)	955 before 1736 cm^{-1}
4	$\Phi(1040, 1736) > 0$	$\Psi(1040, 1736) > 0$	(C, D)	1040 before 1736 cm^{-1}
5	$\Phi(1045, 1736) > 0$	$\Psi(1045, 1736) > 0$	(C, D)	1045 before 1736 cm^{-1}
6	$\Phi(1070, 1736) > 0$	$\Psi(1070, 1736) > 0$	(HA, D)	1070 before 1736 cm^{-1}
7	$\Phi(1084, 1736) > 0$	$\Psi(1084, 1736) > 0$	(HA, D)	1084 before 1736 cm^{-1}
8	$\Phi(1102, 1736) > 0$	$\Psi(1102, 1736) > 0$	(HA, D)	1102 before 1736 cm^{-1}
9	$\Phi(1130, 1736) > 0$	$\Psi(1130, 1736) > 0$	(HA, D)	1130 before 1736 cm^{-1}
10	$\Phi(1776, 1736) < 0$	$\Psi(1776, 1736) < 0$	(B, D)	1776 before 1736 cm^{-1}
11	$\Phi(955, 910) < 0$	$\Psi(955, 910) < 0$	(HA, A)	955 before 910 cm^{-1}
12	$\Phi(1070, 910) < 0$	$\Psi(1070, 910) < 0$	(HA, A)	1070 before 910 cm^{-1}
13	$\Phi(1084, 910) < 0$	$\Psi(1084, 910) < 0$	(HA, A)	1084 before 910 cm^{-1}
14	$\Phi(1102, 910) < 0$	$\Psi(1102, 910) < 0$	(HA, A)	1102 before 910 cm^{-1}
15	$\Phi(1130, 910) < 0$	$\Psi(1130, 910) < 0$	(HA, A)	1130 before 910 cm^{-1}

As we stated for the one-dimensional analysis, the intensity of the 1776 cm^{-1} band, which is characteristic of γ -VL, decreased until spectrum 22 was reached and then increased. Although only one new factor is significant from spectrum 15 until the end of the reaction, we therefore split this time period into three. First we studied the 2D correlation from spectrum 15 to 20. The synchronous spectra (Fig. 9, 1) show no cross peaks related to the 1776 cm^{-1} band which is characteristic of the γ -VL. We can therefore conclude, since there is no more γ -VL, that no more SOE is generated during this reaction period (at 570 s) (Scheme 1, reaction 2). In Figure 9 (2) we do have cross negative peaks between the 1736 band and the 910 cm^{-1} band, which indicates that there is still some copolymer (Scheme 1, reaction 3). The asynchronous spectra (not shown) do not provide further information. The second reaction period corresponds to spectrum 20 to 40. We end at spectrum 40 because the EFA analysis in the backward direction (Fig. 3) shows that from this point a new factor is significant.

Figure 10(a) shows the synchronous and Figure 10(b) shows the asynchronous correlation spectra and Table 4 shows the Noda signs. The 1070 , 1084 , 1102 , and 1130 cm^{-1} bands, characteristic of the C-O-C groups related to the structures generated during the epoxy homopolymerization process (Table 1), have positive synchronous cross peaks with the 1776 cm^{-1} band, characteristic of γ -VL, and with the 1736 cm^{-1} band, characteristic of a linear ester [Fig. 10(a),1]. The 1045 and 1040 cm^{-1} bands, characteristic of the SOE, and the 910 cm^{-1} band, from the oxirane group, have negative synchronous cross peaks with the 1736 and 1776 cm^{-1} bands.

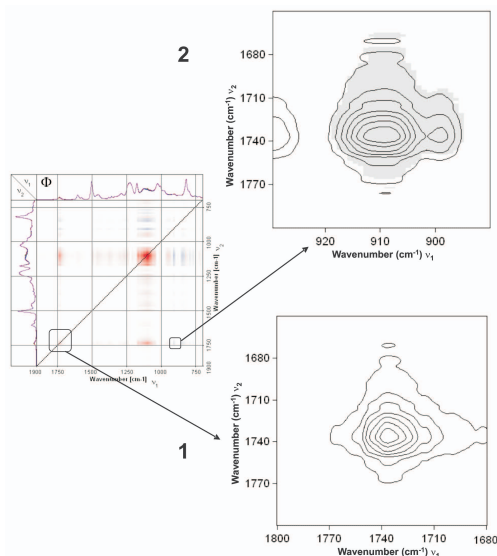


Figure 9: Set (15-20). Spectra synchronous of the chemical reaction of the DGEBA with γ -VL

This analysis is similar to that for the one-dimensional study (Fig. 5). Therefore, the intensity bands of carbonyl (1776 and 1736 cm^{-1}), [Fig. 10(a), 1] and those associated with the epoxy homopolymerization (1070 , 1084 , 1102 , and 1130 cm^{-1}) increase, whereas the intensity bands of the SOE (1040 and 1045 cm^{-1}) decrease and that of the oxirane group (910 cm^{-1}) disappears [Fig. 10(a), 2].

At this point, a chemical interpretation is not simple. The increase in intensity of the 1776 cm^{-1} band may suggest the reversibility of the SOE formation reaction (Scheme 1, reaction 2), [Fig. 10(a), 1 and (b)]. However, if that is the case, the SOE characteristic bands (1045 and 1040 cm^{-1}) should decrease, which indeed happens, and the band characteristic of oxirane (the one at 910 cm^{-1}) should also increase, but this does not happen. The fact that the 910 cm^{-1} band does not increase may be explained by the SOE copolymerization reaction, since the 1736 cm^{-1} band also increases. Another reaction that may be present during this period is SOE homopolymerization, since it would explain the increase in intensity of the 1736 cm^{-1} band even without the presence of oxirane groups and the negative synchronous peak with the SOE bands (1045 and 1040 cm^{-1}). To sum up, the possible reactions during this period are: copolymer formation, SOE reversibility, and SOE homopolymerization. All of these hypotheses are supported by the synchronous and asynchronous peaks shown in Table 4. Finally,

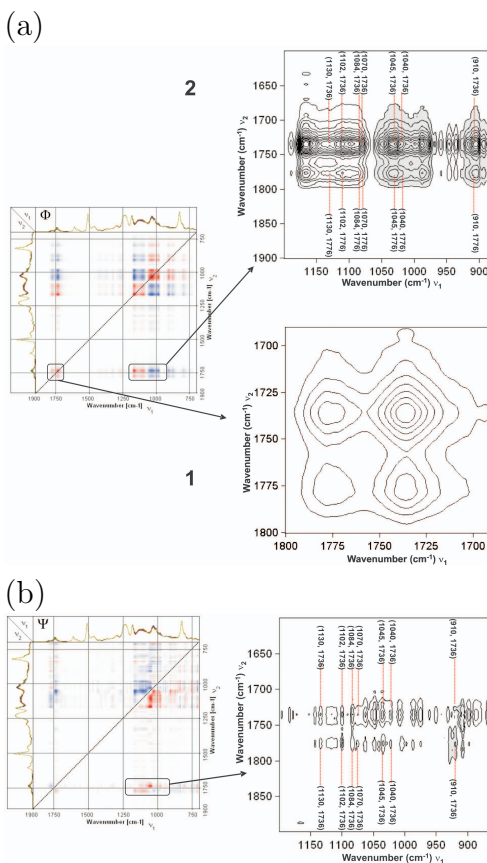


Figure 10: Set (20-40). Spectra a) synchronous and b) Asynchronous of the chemical reaction of the DGEBA with γ -VL

although the 2D correlation spectra for the reaction time between spectrum 40 (1170 s) and the last spectrum are not shown, we can conclude from them that, as no cross peaks are observed with the 910 cm^{-1} band, no epoxy group is present. At that moment, therefore, the only possible reaction is SOE homopolymerization. This could be the reason why there is only one significant factor in the backward EFA analysis (Fig. 3) in the last reaction period.

Table 4. Synchronous, Asynchronous 2D correlation intensities and order of intensities variations between bands for set (20-40) in the characterization of DGEBA (A), γ -VL (B), homopolymer of DGEBA (HA), SOE (C), and copolymer (D).

no.	Φ	Ψ	Assignment	Order
1	$\Phi(910, 1736) < 0$	$\Psi(910, 1736) < 0$	(A,D)	910 before 1736 cm^{-1}
2	$\Phi(1040, 1736) < 0$	$\Psi(1040, 1736) > 0$	(C, D)	1040 after 1736 cm^{-1}
3	$\Phi(1045, 1736) < 0$	$\Psi(1045, 1736) > 0$	(C, D)	1045 after 1736 cm^{-1}
4	$\Phi(1070, 1736) > 0$	$\Psi(1070, 1736) > 0$	(HA, D)	1070 before 1736 cm^{-1}
5	$\Phi(1084, 1736) > 0$	$\Psi(1084, 1736) > 0$	(HA, D)	1084 before 1736 cm^{-1}
6	$\Phi(1102, 1736) > 0$	$\Psi(1102, 1736) > 0$	(HA, D)	1102 before 1736 cm^{-1}
7	$\Phi(1130, 1736) > 0$	$\Psi(1130, 1736) > 0$	(HA, D)	1130 before 1736 cm^{-1}
8	$\Phi(910, 1776) < 0$	$\Psi(910, 1776) < 0$	(A,B)	910 before 1776 cm^{-1}
9	$\Phi(1040, 1776) < 0$	$\Psi(1040, 1776) > 0$	(C, D)	1040 after 1776 cm^{-1}
10	$\Phi(1045, 1776) < 0$	$\Psi(1045, 1776) > 0$	(C, D)	1045 after 1776 cm^{-1}
11	$\Phi(1070, 1776) > 0$	$\Psi(1070, 1776) > 0$	(HA, B)	1070 before 1776 cm^{-1}
12	$\Phi(1084, 1776) > 0$	$\Psi(1084, 1776) > 0$	(HA, B)	1084 before 1776 cm^{-1}
13	$\Phi(1102, 1776) > 0$	$\Psi(1102, 1776) > 0$	(HA, B)	1102 before 1776 cm^{-1}
14	$\Phi(1130, 1776) > 0$	$\Psi(1130, 1776) > 0$	(HA, B)	1130 before 1776 cm^{-1}

4 Conclusions

In this study, we have shown that generalized 2D IR correlation spectroscopy with EFA is a powerful strategy for identifying the sequential order to chemical reactions. By EFA analysis, we could detect the concurrence between AM and ACE polymerization mechanisms in the cationic curing of pure DGEBA, which cannot be detected directly from the direct observation of FTIR spectra. The AM mechanism could not be detected in the curing of DGEBA/ γ -VL mixtures. During the curing, four reactions were detected: (1) epoxide and γ -VL reaction to obtain an intermediate SOEs; (2) homopolymerization of the epoxide; (3) epoxide and SOE copolymerization; and (4) homopolymerization of SOEs. We also observed a phenomenon that suggests the reversibility of the SOE formation reaction.

Acknowledgements

The authors would like to acknowledge the economic support provided by the MCyT (Project No. CTQ2007-6147/BQU), the CICYT (Comisión Interministerial de Ciencia y Tecnología), and FEDER (Fondo Europeo de Desarrollo Regional) (MAT2005-01,806).

References

- [1] Handbook of Epoxy resins, H. Lee, K. Neville, Eds., MacGraw-Hill: New York, 1982.
- [2] H. J. Booth, In Expanding Monomers. Synthesis, Characterization and Application, R. K. Sadhir, M. R. Luck, Eds., CRC Press: Boca Raton, FL, 1992, p. 208-209.
- [3] Ring-Opening Polymerization. Mechanism, Catalysis, Structure, Utility, D. J. Brunelle, Ed., Hanser: Munich, 1993, p. 12-13.
- [4] W. J. Bailey, J. Macromol. Sci. Chem., 9, (1975), 849.
- [5] K. Bodenbenner, Justus Liebig Ann. Chem., 625, (1959), 183-191.

- [6] M. Fedtke, J. Haufe, E. Kahlert, G. Müller, *Angew. Makromol. Chem.*, 255, (1998), 53.
- [7] C. Mas, A. Mantecón, A. Serra, X. Ramis, J. M. Salla, J. *Polym. Sci. Part. A: Polym. Chem.*, 42, (2004), 3782.
- [8] S. González, X. Fernández- Francos, J. M. Salla, A. Serra, A. Mantecón, X. Ramis, J. *Polym. Sci. Part. A: Polym. Chem.*, 45, (2007), 1968.
- [9] D. B. Johns, R. W. Lenz, A. Luecke, *Ring-Opening Polymerization*, K. J. Ivin, T. Saegusa, Eds., Elsevier Applied Science Publishers: London, 1984, 463-468.
- [10] L. Wang, C. P. Wong, *J. Appl. Polym. Sci.*, 81, (2001), 1868.
- [11] C. Mas, X. Ramis, J. M. Salla, A. Mantecón, A. Serra, J. *Polym. Sci. Part. A: Polym. Chem.*, 41, (2003), 2794.
- [12] M. Liu, P. Wu, Y. Ding, G. Chen, S. Li, *Macromolecules*, 35, (2002), 5500.
- [13] H. R. Keller, D. L. Massart, *Chemom. Intell. Lab. Syst.*, 12, (1992), 209.
- [14] M. S. Larrechi, F. X. Rius, *Appl. Spectrosc.*, 58, (2004), 47.
- [15] I. Noda, *Appl. Spectrosc.*, 47, (1993), 1329.
- [16] I. Noda, A. E. Dowrey, C. Marcott, G. M. Story, Y. Ozaki, *Appl. Spectrosc.*, 54, (2000), 236A-248A.
- [17] I. Noda, *Appl. Spectrosc.*, 54, (2000), 994.
- [18] I. Noda, Y. Ozaki, *Two-Dimensional Correlation Spectroscopy*, John Wiley & Sons: Chitester, West Sussex, 2004, p 86-94.
- [19] Y. Ozaki, Y. Liu, I. Noda, *Macromolecules*, 30, (1997), 2391.
- [20] Y. Ren, M. Shimoyama, T. Ninomiya, K. Matsukawa, H. Inoue, I. Noda, Y. Ozaki, *Appl. Spectrosc.*, 53, (1999), 919-926.
- [21] A. Jirasek, G. Schulze, M. W. Blades, R. F. B. Turner, *Appl. Spectrosc.*, 57, (2003), 1551.

- [22] M. Arasa, X. Ramis, J. M. Salla, A. Mantecón, A. Serra, J. Polym. Sci. Part. A: Polym. Chem., 45, (2007), 2129.
- [23] The Mathwork, MATLAB Version 6.5. 2002, Natick, MA.
- [24] P. Geladi, D. McDougall, H. Martens, Appl. Spectrosc., 39, (1985), 491.
- [25] G.H. Golub, F. van Loan, Matrix Computations, Johns Hopkins University Press: Baltimore, MD, 1983, p. 50.
- [26] 2Dshige© Shigeaki Morita, Kwansei-Gakuin University, 2004-2006. All rights reserved.
- [27] M. Fanliang, Z. Weian, Z. Sixun, J. Mater. Sci., 40, (2005), 6367.
- [28] S. V. Patel, D. K. Raval, J. R. Thakkar, High Perform. Polym., 11, (1999), 467.
- [29] I. E. Dell'Erba, R. J. J. Williams, J. Polym. Eng. Sci., 46, (2006), 351.
- [30] R. Gimenez, X. Fernandez-Francos, J. M. Salla, A. Serra, A. Mantecon, X. Ramis, Polymer, 46, (2005), 10637.
- [31] L. Monney, R. Belali, J. Vebrel, C. Dubois, A. Chambaudet, Polym. Degrad. Stab., 62, (1998), 353.
- [32] A. Mija, C. N. Cascaval, G. Stoica, D. Rosu, B. C. Simionescu, Eur. Polym. J., 32, (1996), 779.
- [33] V. Razafindrakoto, B. Bonnetot, C. Pautet, H. Mongeot, Polym. Bull., 40, (1998), 439.
- [34] S. T. Wellinghoff, J. L. Koenig, E. Baer, J. Polym. Sci.: Polym. Phys., 15, (1977), 1913.
- [35] K. El Gersifi, G. Durand, G. Tersac, Polym. Degrad. Stab., 91, (2006), 690.
- [36] P. Kubisa, S. Penczek, Prog. Polym. Sci., 24, (1999), 1409.
- [37] D. J. Worsfold, A. M. Eastham, J. Am. Chem. Soc., 79, (1957), 897.

- [38] R. O. Colclough, G. Gee, W. C. E. Higginson, J. B. Jackson, M. Litt, *J. Polym. Sci.*, 34, (1959), 171.
- [39] W. Tänzer, J. Wintzer, H. Müller, M. Fedtke, *Polym. Bull.*, 17, (1987), 31.
- [40] H. Nishida, F. Sanda, T. Endo, T. Nakahara, T. Ogata, K. Kusumoto, *J. Polym. Sci. Part. A: Polym. Chem.*, 37, (1999), 4502.
- [41] H. Nishida, F. Sanda, T. Endo, T. Nakahara, T. Ogata, K. Kusumoto, *J. Polym. Sci. Part. A: Polym. Chem.*, 38, (2000), 68.

3.3 Quantitative resolution of a curing reaction using global phase angle spectroscopy and MCR-ALS

Once the pathway of the curing process between DGEBA and γ -valerolactone had been established, the spectral and concentration profiles of the chemical species involved in the reaction were obtained by MCR-ALS. We propose using the information from the 2DCOS as the convergence criterion in the optimization step of the solutions found by MCR-ALS. Following this strategy, the final estimated solution is the optimal solution that reproduces the original information.

UNIVERSITAT ROVIRA I VIRGILI

TWO-DIMENSIONAL INFRARED CORRELATION SPECTROSCOPY AND MULTIVARIATE CURVE RESOLUTION

METHODS: APPLICATION TO QUANTITATIVE MONITORING OF CURING PROCESS

Nicolas Spegazzini

ISBN:978-84-693-4049-3/DL:T.998-2010

MCR-ALS for Sequential Estimation of FTIR-ATR Spectra to Resolve a Curing Process Using Global Phase Angle Convergence Criterion

Analytica Chimica Acta 642, (2009), 155

Nicolás Spegazzini, Itziar Ruisánchez, M. Soledad Larrechi

Chemometrics, Qualimetrics and Nanosensors Group, Department of Analytical and Organic Chemistry, Rovira i Virgili University.
Marcel·lí Domingo s/n, 43007, Tarragona, Spain

Abstract

Curing reactions include side and consecutive reactions while the polymer is growing. In this paper, we used multivariate curve resolution - alternating least squares (MCR-ALS) to obtain quantitative information about the concentration of the chemical species involved in these reactions. The cationic curing reaction between diglycidyl ether of bisphenol A (DGEBA) and γ -valerolactone (γ -VL) was monitored by infrared spectroscopy (FTIR-ATR). If the MCR-ALS method is to be used with recorded spectral data, the rank deficiency usually present in the data matrix needs to be overcome and the goodness of the results depends on the initial estimates of the chemical species involved in the reaction. Our strategy was to sequentially apply MCR-ALS in the time intervals where there is selectivity for some reactions and to use the error criterion based on the global phase angle to identify the optimal number of iterations in ALS. The estimated spectra were sequentially incorporated into the data matrix to overcome the rank deficiency.

The MCR-ALS results are evaluated by the residuals and parameters such as lack of fit, the percentage of explained variance and the coefficient of dissimilarity between the recovered spectra and the spectra of the pure species, when it is possible. For intermediate species, the correspondence between the ALS spectra solution and the chemical knowledge of this species was also qualitatively evaluated. The goodness of the estimated concentration profile of the two reagents γ -VL and DGEBA, was evaluated by the correlation coefficient value between the estimated profile and the profile obtained when the specific absorption bands were monitored at 1776 cm^{-1} and 910 cm^{-1} , respectively for each reagent. The correlation coefficient values were: 0.9954 and 0.9885, respectively.

Keywords: FTIR-ATR; MCR-ALS; Global phase angle; Curing reaction

1 Introduction

The final properties of the crosslinked resins significantly depend on the extent of the curing, the curing conditions and the mechanism involved in the reaction [1,2]. Therefore, the study of curing kinetics contributes not only to a better knowledge of process development but also to an improvement in the quality of final products. The availability of reliable methods for monitoring curing also plays a crucial role in process control and the optimization of polymer network processing [3-5]. This paper deals with the cationic curing of DGEBA and γ -valerolactone, a very complex process because many reactive processes occur simultaneously [6]. Several techniques can be used to examine the kinetics of curing reactions [7-9]. The most common is non-isothermal differential scanning calorimetry (DSC), which is used at different rates to determine kinetic parameters and kinetic models. This technique gives information about the overall kinetic constant but not about the evolution of each species involved in the reaction. Fourier transform infrared spectroscopy (FTIR) and multivariate curve resolution-alternating-least squares (MCR-ALS) are powerful tools for obtaining information about how the concentration of the species involved in the reactions evolve [10,11]. In conjunction with

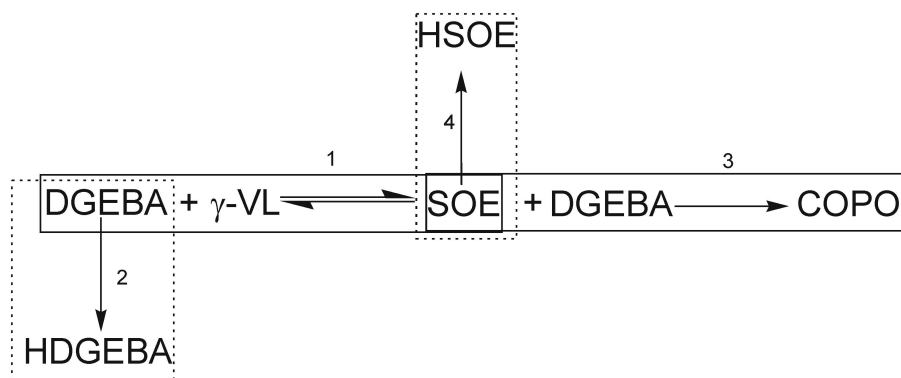
hard modelling methods, they also provide kinetic information about the reaction [12-15]. These methods assume a linear relation between the spectral changes observed during the reaction and the chemical concentration of the species involved in the reaction [16,17]. In the papers referenced, the reactions are relatively simple, and some of the polymerization reactions are mono-functional compound model reactions [11]. These attractive methodologies will be challenged when physical changes produce spectral changes in the absorption bands that are unrelated to concentration, as is the case of copolymerization reactions in which polymers are growing. The MCR-ALS method is based on factor analysis. Ideally, the number of significant factors should be the same as the number of chemical species involved in the reaction. The physical changes associated with the polymer growth might also be reflected in the number of factors, thus increasing the number of significant factors. If this is the case, as happens in the studied reaction, confusion arises. On the basis of our experience, this can be overcome by determining the number of chemical species and the number of reactions involved by spectroscopic analysis of the data recorded during the reaction. So MCR-ALS is a powerful tool for approximating how the concentration of the chemical species evolves when rank deficiency is overcome. In addition, to have a good initial estimate when working with MCR-ALS is a challenge. These are the main objects of the strategy presented in this paper, which studies the copolymerization reaction between diglycidyl ether bisphenol A (DGEBA) and γ -valerolactone (γ -VL). Strategies based on matrix augmentation can be used [18,19] to overcome rank deficiency. This information can be obtained by simultaneously analyzing different mixtures of the same compound in different chemical or physical conditions or appending a matrix of standards to the unknown rank-deficient data set that describes the chemical system being studied. Initial estimates of the intermediate species can be made by using such algorithms as SIMPLISMA [20], OPA [21], HELP [22] and IT-TFA [23]. These algorithms present some difficulties in the case of curing reactions in which side reactions occur [6] and polymers are growing. In this reaction, pure variables are difficult to find because of the severe overlapping between bands and it is difficult to know what the final product is. This paper proposes a strategy based on the sequential application of MCR-ALS to FTIR spectra recorded during the reaction to obtain representative spectra of the compounds that

participate in the different reactions involved in the curing reaction: competing side reactions and consecutive reactions. The number of reactions involved in the curing process and their time intervals with regions of selectivity for some species were determined by evolving factor analysis (EFA) and two-dimensional correlation spectroscopy (2D-COS) analysis of the FTIR/ATR spectra recorded in a previous study [6]. In the present study, this information is considered so that MCR-ALS can be sequentially applied to sub data sets of the FTIR spectra in which the spectrum of only one chemical species was unknown. In the sequential process, two approaches have been considered to determine the number of iterations for the ALS optimization step. One approach is based on minimizing the global phase angle calculated between the original spectra and the recovered MCR-ALS spectra [24,25]. The other is based in minimizing the residual between the original spectra and the recovered MCR-ALS spectra [17]. The goodness of the estimate spectrum corresponding to the intermediate compounds was evaluated by analyzing the typical absorption bands of similar compounds referenced in the literature. The rank deficiency was overcome by appending the estimate spectrum to the previous matrix. The spectra estimated as the representatives of each species during this sequential process were used as the initial estimates in the final step of optimization using ALS with the whole data set. The results were evaluated by studying the residuals and such parameters as lack of fit, the percentage of explained variance and the coefficient of dissimilarity between the recovered spectra and the spectra of the reagent species. The goodness of the estimated concentration profile of the two reagents γ -VL and DGEBA, was evaluated by the correlation coefficient values between the estimated profile and the profile obtained when the specific absorption bands were monitored at 1776 cm^{-1} and 910 cm^{-1} , respectively for each reagent.

2 Experimental and data treatment

2.1 Reaction conditions and procedure

Scheme 1 is a diagram of the reactions involved in the cationic curing process between the diglycidyl ether of bisphenol A (DGEBA) and γ -valerolactone (γ -VL) to obtain the copolymer (COPO). In this process, it takes place through the intermediate compound spiroorthoester



Scheme 1: Reaction of DGEBA with γ -Valerolactone (2:1) at $T=160$ °C. (DGEBA) Diglycidyl ether of bisphenol A; (HDGEBA) homopolymer of diglycidyl ether of bisphenol A; (γ -VL) γ -Valerolactone; (SOE) spiroorthoester; (COPO) copolymer, and (HSOE) homopolymer of spiroorthoester.

(SOE), which is a reversible reaction. In addition, there are side reactions corresponding to the homopolymerization of DGEBA and SOE obtaining HDGEBA and HSOE, respectively. Details of this curing process can be found in reference [6].

The curing of the DGEBA/ γ -VL (2:1 mol/mol) mixture in the presence of 1 phr (parts of initiator per 100 parts of mixture, w/w) of ytterbium triflate was carried out at 160°C . The sample was placed on a small diamond crystal in the spectrophotometer ATR cell (FTIR-680PLUS JASCO), which was equipped with a 3000 SeriesTM High Stability Temperature Controller and a RS232 Control to take the measurements.

2.2 Data acquisition and pre-treatment of FTIR spectra

The data correspond to the FTIR spectra recorded every 30 second between 700 and 1850 cm^{-1} until no changes over time were observed in the spectra. The curing reaction ended after 23 minutes so 47 spectra were recorded. Then, the spectra were exported and converted into MATLAB binary files [26]. The experimental data were arranged in matrices of (47×1247) . The rows were the recorded spectra and the columns were the absorbance values at different wavenumbers. Second derivatives of the spectra are used to clarify some figures and

have been calculated according the Savitztky-Golay [27].

2.3 Strategy to estimate representative spectra of the chemical species involved in the curing reaction. Sequential application of multivariate curve resolution - alternating least squares (MCR-ALS)

The aim of the MCR-ALS method is to transform the theoretical solution obtained by factor analysis of the experimental data matrix \mathbf{D} into matrices \mathbf{C} and \mathbf{S}^T which have a real chemical significance, according to eqn (1):

$$\mathbf{D} = \mathbf{C}\mathbf{S}^T + \mathbf{E} \quad (1)$$

in which matrix \mathbf{C} ($n \times c$) has column vectors corresponding to the profiles of the c pure components that are present in matrix \mathbf{D} . The row vectors of matrix \mathbf{S}^T ($c \times m$) correspond to the spectra of the c pure components and \mathbf{E} is the matrix of the residuals. First, the number of compounds present in \mathbf{D} that have chemical information is estimated from the “chemical rank” associated with the data matrix \mathbf{D} . This determination is performed by Singular Value Decomposition (SVD) [28] because singular values associated with chemical compounds are known to be larger than singular values associated with noise and experimental error. Ideally the number of singular values is the same as the number of compounds involved in the reaction, but in chemical reactions rank deficiency usually appears in matrix \mathbf{D} [29, 30].

Fig. 1 shows the strategy used to overcome the rank deficiency and to estimate the representative spectra of the intermediates involved in the curing reaction. New FTIR/ATR spectra are appended as new row vectors to sub-matrices \mathbf{D}_1 and \mathbf{D}_2 of experimental data matrix \mathbf{D} and, in the final step, to \mathbf{D} to provide new augmented matrices \mathbf{M}_1 , \mathbf{M}_2 and \mathbf{M} , respectively. The new sequentially appended row vectors correspond to the spectra of the reagents (diglycidyl ether bisphenol A (DGEBA) and γ -valerolactone (γ -VL)), the spectra of the homopolymer of DGEBA (HDGEBA) that was obtained experimentally [6] and the spectra of the products (spiroorthoester (SOE), copolymer (COPO) and spiroorthoester homopolymer (HSOE)). The spectra of the products are appended to the experimental sub-matrices \mathbf{D}_1 , \mathbf{D}_2 and matrix \mathbf{D} while they are estimated by MCR-ALS. The spectrum

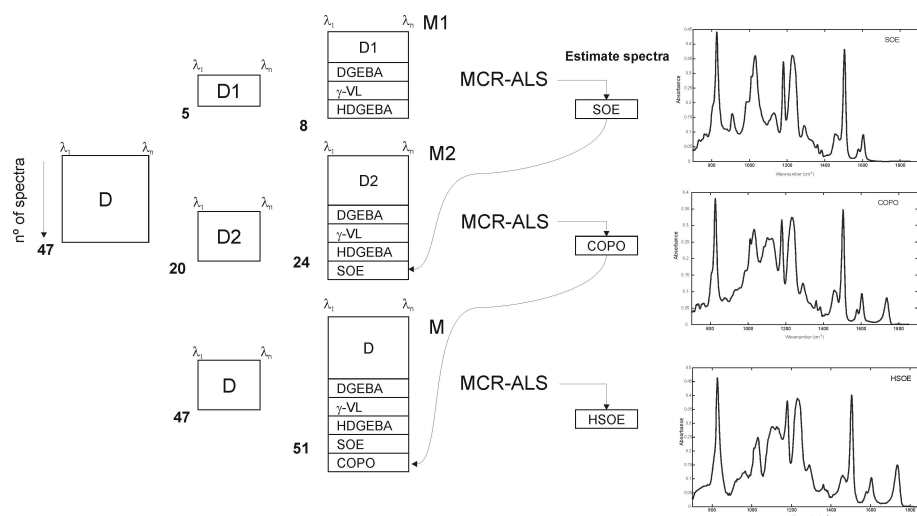


Figure 1: Strategy to overcome rank-deficient: sequential estimation of intermediate compounds by appending the estimated spectra to the submatrices.

of the intermediate SOE is estimated by applying MCR-ALS to the augmented matrix \mathbf{M}_1 , obtained with the first five FTIR spectra (matrix \mathbf{D}_1) monitored in matrix \mathbf{D} plus the experimental spectrum of HDGEBA. In this time interval, spectral information was attributed to the presence of compounds involved in reactions 1 and 2 (Scheme 1) [6]. Likewise, the spectrum of the copolymer COPO is estimated from the augmented matrix \mathbf{M}_2 with the twenty first spectra of matrix \mathbf{D} (matrix \mathbf{D}_2) plus the experimental spectrum of HDGEBA and the previously estimated spectra of SOE. In this time interval Spectral information was attributed to the presence of compounds involved in the reactions 1, 2 and 3 of Scheme 1 were postulated [6]. Finally, the HSOE spectrum (reaction 4, Scheme 1) is estimated by applying MCR-ALS to the complete augmented matrix \mathbf{M} that includes all previous information. In all the steps, the number of iterations used in ALS was determined by the global phase angle criterion. [24,25]. In the optimization process, in which ALS is applied to the matrices \mathbf{M}_1 , \mathbf{M}_2 and \mathbf{M} , several constraints were imposed: non-negativity for the concentration profiles to be resolved in matrix \mathbf{C} and for the spectral profiles in matrix \mathbf{S}^T , and closure for the concentration profiles. Likewise, a local rank constraint of selectivity was imposed at the

starting point of the reaction so that the concentration of the product associated with spiroorthoester (SOE) was zero. This constraint is an approximation of reality because the first spectrum was recorded immediately after the two reagents had been mixed. Also, the arbitrary units were constrained to being equal at the starting point of the concentration values associated with the reagents DGEBA and γ -VL. The theory and application of MCR-ALS have been described in detail [19,31] and freely available subroutines for MATLAB by R. Tauler were used for MCR-ALS analysis [32].

2.4 Error criterion based on global phase angle

The global phase angle represent information related to the coherence of signals and can be served as a kind of index to estimate similarity between two signal [33,34]. It is derived from synchronous and asynchronous correlation intensities. The synchronous give information about the in-phase variation caused by the perturbation considered, in our case the reaction. The variation that occur out-of-phase are in the asynchronous correlation [24,25].

The global phase angle is described as

$$\Phi = \frac{1}{n-1} \tilde{\mathbf{D}}^T \tilde{\mathbf{D}} \quad (2)$$

$$\Psi = \frac{1}{n-1} \tilde{\mathbf{D}}^T \mathbf{N} \tilde{\mathbf{D}} \quad (3)$$

where $\tilde{\mathbf{D}}$ denotes the mean-centered matrix of \mathbf{D} and \mathbf{N} is the Hilbert-Noda transformation matrix defined as

$$\mathbf{N} = \frac{1}{\pi} \begin{bmatrix} 0 & 1 & 1/2 & 1/3 & \dots \\ -1 & 0 & 1 & 1/2 & \dots \\ -1/2 & -1 & 0 & 1 & \dots \\ -1/3 & -1/2 & -1 & 0 & \dots \\ \vdots & \vdots & \vdots & \vdots & \ddots \end{bmatrix} \quad (4)$$

Global phase angle [33,34] can be directly obtained from synchronous and asynchronous correlation intensities as

$$\Theta = \arctan \left(\frac{\Psi}{\Phi} \right) \quad (5)$$

The global phase angle error criterion is defined as the sum of the squared residuals between the global phase angle with original spectra \mathbf{D} and the global phase angle with reconstructed spectra $\hat{\mathbf{D}} = \mathbf{C}\mathbf{S}^T$

$$\text{SSR}_{\Theta} = \|\Theta - \hat{\Theta}\| \quad (6)$$

where $\hat{\Theta}$ is the global phase of the reconstructed spectra $\hat{\mathbf{D}}$.

If this criterion is to be used, the global optima of must be identified during the iteration process in ALS. ALS minimizes SSR ($\text{SSR} = \mathbf{D} - \mathbf{C}\mathbf{S}^T$) by a sequential matrix rotation process while the global phase angle error criterion is a reflection of the underlying physical model [25]. Fig. 2 shows the procedure for determining the optimal number of iterations in ALS. The information associated to the synchronous and asynchronous experimental matrices \mathbf{D}_1 , \mathbf{D}_2 and \mathbf{D} has been discussed in a previous study [6]. All calculations of error criterion based on global phase angle, were performed by in-house programs coded in MATLAB [26].

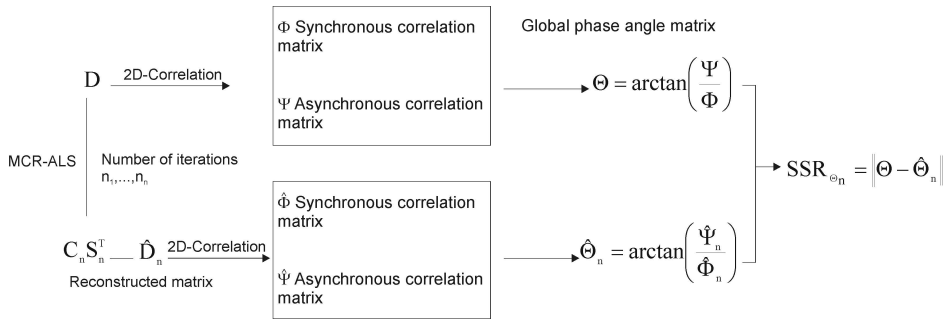


Figure 2: Procedure to determine the optimal number of iterations in ALS

3 Results and discussion

3.1 Data

Fig. 3 shows the 47 FTIR spectra recorded throughout the 1380 seconds of reaction. According to a previous study [6] using evolving factor analysis (EFA) three time intervals were identified. By two-dimensional correlation spectroscopy (2D-COS) analysis, in each interval the recorded spectra were attributed to the presence of different chemical compounds involved in the curing process, Scheme 1, a) from the beginning until 120 seconds: to DGEBA, γ -VL, SOE and HDGEBA, b) from the beginning until 570 seconds: the previous mentioned compounds and COPO and c) when all spectra were considered: HSOE was additionally identify.

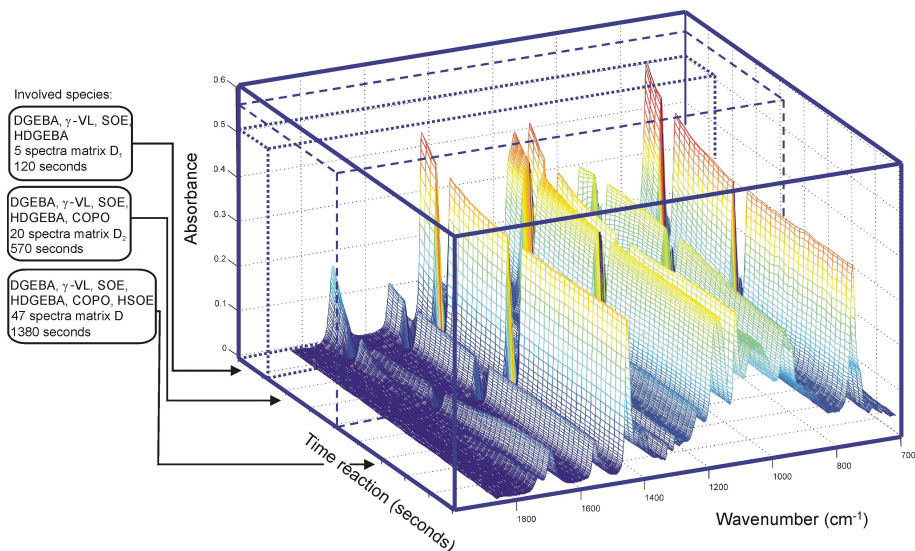


Figure 3: FT-IR spectra recorded along the reaction and the time intervals where the different species involved in the curing of DGEBA and γ -VL takes place.

3.2 Rank estimation using SVD

Table 1 shows the singular values of the data set corresponding to the experimental matrices D_1 (spectra recorder during 120 seconds),

\mathbf{D}_2 (spectra recorder during 570 seconds and \mathbf{D} (all spectra recorder during 1380 seconds). The singular values associated with noise are marked in bold, and has been calculated using the value from 70 spectral channels between 1780 and 1850 cm^{-1} where no signal contribution is observed and which can be considered as a threshold. Rank deficiency is detected in all matrices since the number of significant eigenvalues is lower than the number of species postulated by 2D-COS [6] in the corresponding data matrix. Rank deficiency can be caused

Table 1. Singular values of the matrices \mathbf{D}_1 , \mathbf{D}_2 and \mathbf{D} and the column-wise augmented matrices \mathbf{M}_1 , \mathbf{M}_2 and \mathbf{M} and factor indicator function (IND) for augmented matrices.

Number of factors	Singular value of the \mathbf{D} matrix	Singular value of the \mathbf{M} matrix	IND ($\times 10^{-3}$)
	\mathbf{D}_1	\mathbf{M}_1	\mathbf{M}_1
1	10.8797	12.7365	5.25
2	0.8482	2.5437	2.72
3	0.0399	1.6410	2.23
4	0.0313	0.5897	2.12
5	0.0250	0.2971	2.29
6		0.0383	2.32
	\mathbf{D}_2	\mathbf{M}_2	\mathbf{M}_2
1	20.8773	22.4031	7.124
2	2.3659	2.7198	6.547
3	0.3868	2.5973	6.034
4	0.0490	0.8159	5.852
5	0.0472	0.4558	5.235
6	0.0339	0.3111	5.456
7		0.0485	5.335
	\mathbf{D}	\mathbf{M}	\mathbf{M}
1	29.4560	32.9337	8.070
2	2.9426	3.5204	7.325
3	1.4771	1.8717	6.734
4	0.1583	1.0850	6.035
5	0.0529	0.4800	5.843
6	0.0411	0.3009	5.449
7		0.1992	5.608
8		0.0585	6.012

for several situations [18] like closure and linear dependencies between the concentrations of the chemical compounds, both present in the case study. Therefore, the expected rank of the data matrix is the number of the species whose concentrations are linearly independent. The rank estimated for \mathbf{D}_1 matrix is two and corresponds with the number of independent concentrations. \mathbf{D}_1 contains spectral information that was associated with the initial reagents DGEBA, γ -VL and their product (SOE), and HDGEBA obtained from the DGEBA homopolymerization. The concentration of the products SOE and HDGEBA

are linearly dependent with DGEBA concentration and so only two significant values has been found. These results confirm the hypothesis postulated [6] that in this period of time, both the formation of SOE and of HDGEBA takes place and are side reactions.

The rank estimation for \mathbf{D}_2 matrix indicates three significant contributions. Newly in this case two sources of rank-deficiency are present in the data matrix, one associated with the closed system and other related with the side reactions. The additional eigenvalue, indicates that a new chemical situation is done. Regarding the scheme 1, this new chemical situation could be attributed only to the COPO formation (reaction 3, Scheme 1) or in addition to the COPO formation also to the presence of the SOE homopolymerization (reaction 4, Scheme 1) and so to the HSOE formation. In both cases, only one additional factor is expected, as is the case. So, based in the previous work [6], in the strategy followed (Fig. 1) only the first option has been considered. Finally, the chemical rank estimated for \mathbf{D} matrix is four which again can be associated to a new chemical situation. At the end of the reaction, important spectroscopic changes appear at 1085, 1110, 1130 and 1144 cm^{-1} related to HSOE, and also an increase of the 1776 cm^{-1} band characteristic of the γ -VL is observed, this situation is due to the reversibility of the reaction 1, postulated in scheme 1. In our opinion, this explains the new contribution in the rank analysis of the matrix \mathbf{D} . Therefore, in the followed strategy (Fig. 1) the spectrum of HSOE was estimate in the last step indicated.

3.3 Rank estimation in augmented matrices

Rank deficiency problem is overcome when the singular values are calculated for the augmented matrices, \mathbf{M}_1 , \mathbf{M}_2 and \mathbf{M} (Table 1). There are several criteria to determine the number of significant values. Considering the noise as a criterion, in the three matrices the number of significant values is higher than the number of chemical compounds postulated. But it is possible to observe that the last singular values considered have similar magnitude. To define it more accurately, the Malinowski criterion is introduced (Table 1) [35]. Considering the IND value, in the three matrices \mathbf{M}_1 , \mathbf{M}_2 and \mathbf{M} the significant values, marked in bold, are the same than the chemical compound postulated.

3.4 Sequential resolution using MCR-ALS and the global phase angle convergence criterion

Fig. 4 shows the spectra obtained by sequentially applying MCR-ALS to the augmented matrices. These spectra were obtained in the optimization step of MCR-ALS using the number of iteration determined according to the criterion based on global phase angle. For the sake of clarity, this decision will be argument in detail later in Table 2 and Fig. 5 and 6. As a consequence of the complexity of these copolymer-

Table 2. Dissimilarities coefficients between experimental spectrum profiles and the recovered by MCR-ALS using global phase angle criteria SSR_0 and ALS minimum residual criteria SSR : for DGEBA, γ -VL and HDGEBA.

Dissimilarity coefficient	Criteria SSR_0	Criteria SSR
DGEBA	0.0027	0.0080
γ -VL	0.0015	0.0025
HDGEBA	0.0028	0.0060

ization reactions and the considerable overlapping of the FTIR absorption bands, it is not easy to obtain a pure spectrum of the compounds that can be used to fit the estimate. For this reason, goodness is evaluated by considering the characteristic IR absorption band of each compound referenced in the literature. The first estimate corresponds to the SOE spectrum (Fig. 4a), which has referenced absorption bands at 1040, 1065, 1110 and 1120 cm^{-1} associated to stretching vibrations of the bicyclic (C-O-C) [36-40]. These bands are not present at the beginning of the reaction, as can be concluded from the comparison of the second derivative of the estimated SOE spectrum and of the first spectrum in matrix \mathbf{D}_1 (see also Fig. 4a).

Fig. 4b shows the COPO spectrum estimated by MCR-ALS. The C=O functional group is associated to the linear ester (Scheme 1) and the literature [39,40] has shown that absorption bands are associated to stretching molecular vibrations of this group at 1736 cm^{-1} . Also referenced bands of the C-O-C stretching of the molecular structures produced in the epoxy copolymerisation have been reported at 1070, 1080, 1105 and 1135 cm^{-1} . As expected for a representative spectrum of a COPO product, comparing the second derivative of the estimated COPO spectrum and of the first spectrum in matrix \mathbf{D}_2 shows an increase in the intensity of the absorption bands of the es-

timated spectrum at the wavenumber indicated. Fig. 4c shows the

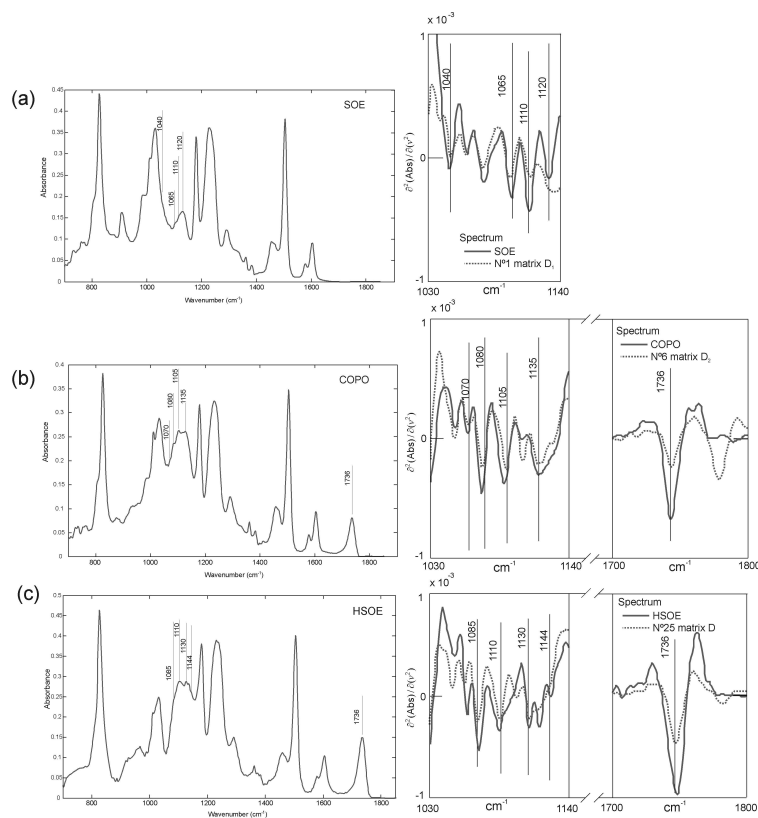


Figure 4: Spectra obtained in the sequential application of ALS to the augmented matrices (left side) and its second derivative joint with of the second derivative of the reference spectrum (right side). (a) SOE spectrum and the second derivative of the SOE spectrum and of the first spectrum in the matrix \mathbf{D}_1 , (b) the COPO spectrum and the second derivative of the COPO spectrum and of the first spectrum in the matrix \mathbf{D}_2 and (c) the HSOE spectrum and the second derivative of HSOE spectrum and the spectrum number 25 of the matrix \mathbf{D} .

HSOE spectrum estimated by MCR-ALS, the second derivate of this spectrum and spectrum number 25 of matrix \mathbf{D} . This spectrum corresponds to the time at which the beginning of reaction 4 was detected [6]. HSOE corresponds to the product of SOE homopolymerization (Scheme 1). In its structure, the C=O functional group characteristic of a linear ester is also present so an absorption band is expected

at 1736 cm^{-1} . In a previous study of the spiroorthoester homopolymerization reaction, in which the opening of the bicyclic structure is made, bands were reported at 1085, 1115, 1130 and 1144 cm^{-1} associated with the stretching vibration of the structure (-C-O-C-) [39,40]. All of these bands can be observed in the estimated spectrum of HSOE when MCR-ALS is applied to the \mathbf{M} matrix, which contains all of the recorded spectra and the five appended spectra. A comparison of the second-derivative spectra clearly shows that they have increased. It should be pointed out that the reaction studied is complex since all chemical species have similar functional groups and are strongly overlapped.

Fig. 5 plots the sum of squared residuals (SSR) vs the number of iterations for the \mathbf{D}_1 , \mathbf{D}_2 , and \mathbf{D} matrices according to: Fig. 5a, the criterion based on global phase angle which represent information related to the coherence of signals [24] and Fig. 5b, the criterion included in ALS method which satisfies the mathematical constraints of minimizing the error criterion of the sum of squared residuals (SSR). The arrow indicates the optimal number of iterations. In all cases, the number of iterations necessary to obtain a minimum is higher for ALS. The results of MCR-ALS previously discussed in Fig. 4 were obtained with 3, 8 and 11 iterations, for \mathbf{M}_1 , \mathbf{M}_2 and \mathbf{M} matrices, respectively.

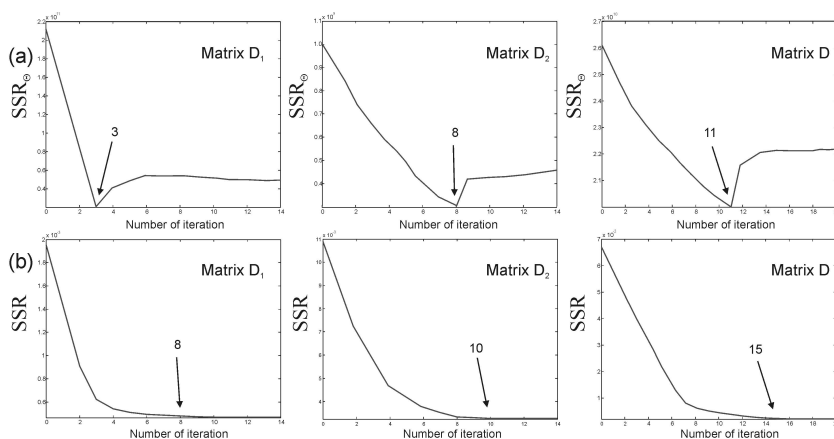


Figure 5: Plots of the number of iterations in ALS for \mathbf{D}_1 , \mathbf{D}_2 and \mathbf{D} matrices according to the criterion based on global phase angle SSR_{Θ} (a), and according the error criterion based of the sum of squared residuals SSR (b).

To compare the two approaches, the results obtained for matrix **M** are shown. Table 2 contains the dissimilarity coefficients calculated between the spectra recovered by MCR-ALS and the pure spectra of the reagents (DGEBA and γ -VL) and the experimental spectra obtained for HDGEBA [6]. It is possible to observe that although the values are not very different, the dissimilarity coefficient is always lower using the iteration number obtained by SSR_{θ} criterion. Also, Fig. 6 plots the spectra recovered by MCR-ALS using the two approaches, for: SOE (Fig. 6a), COPO (Fig. 6b) and HSOE (Fig. 6c). Only, the more characteristic bands, previously discussed in Fig. 4, are indicated. Both solutions are quite similar but the referenced spectroscopic absorption bands associated with the compounds SOE, HSOE and COPO, are better defined when the SSR_{θ} criterion is consider. This is important in such kind of reactions, as the case studied, where is not easy to isolate the intermediate compounds and the final copolymer, so

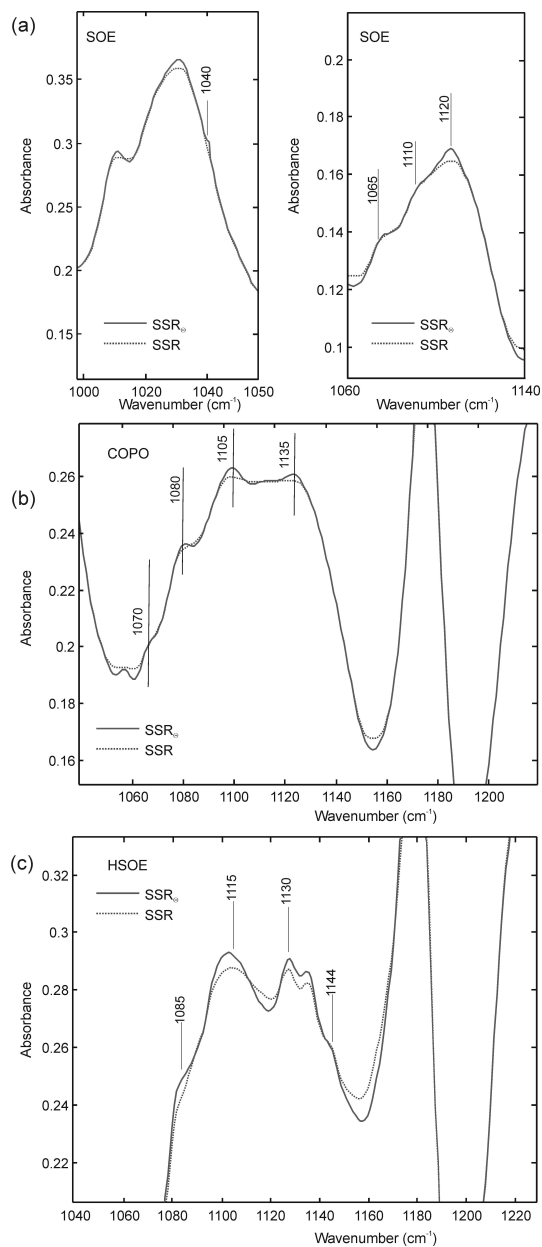


Figure 6: Spectra recovered by MCR-ALS according to the SSR_{θ} criterion (-), and the SSR criterion (...) for: (a) SOE, (b) COPO, and (c) HSOE.

no pure spectra can be obtained.

3.5 Concentration profiles obtained by MCR-ALS

The results found during the optimization process gave rise to matrix \mathbf{C} (47 x 6), which contains the concentration profiles for the three compounds, and to matrix \mathbf{S}^T (6 x 1247), which contains the corresponding spectra profiles. The product of both matrices, in accordance with eqn (1), accounts for 99.99% of the variance associated with the augmented experimental \mathbf{M} matrix. The percentage of lack of fit was 0.97%, which in quantitative terms means that it explains practically all the variability of the experimental data as a product of the found spectra and concentration profiles. However, this fit parameter provides an overall measure of the residual.

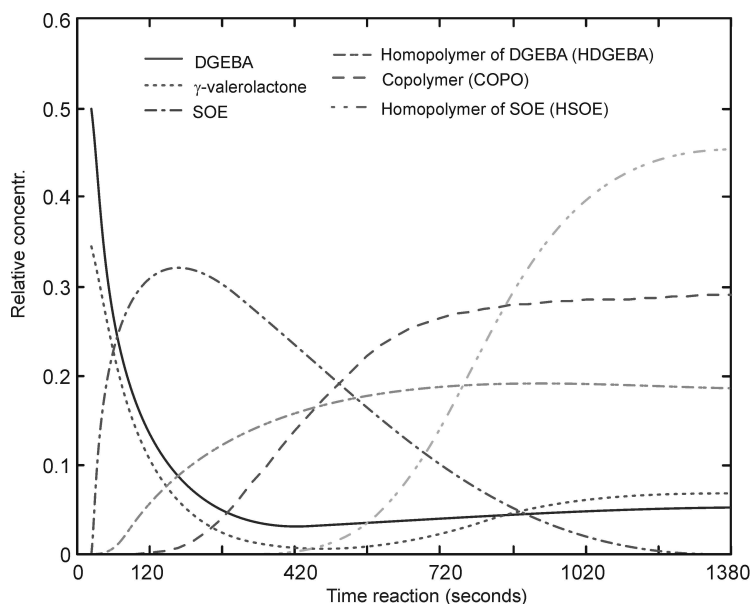


Figure 7: Concentration profiles of the chemical species recovered by MCR-ALS. DGEBA (-), γ -valerolactone (- - -), SOE (- · -), HDGEBA (- -), and HSOE (· · -).

Fig. 7 shows the concentration profiles of the chemical species in arbitrary units. It can be stated that the profiles of the reagents DGEBA and γ -VL are according to the reaction 1 postulated in Scheme 1,

which is known their reversibility at some point of the reaction but not from the beginning of it [6]. Therefore, the concentration profile of γ -VL increases from 420 seconds and this effect is not so strong for DGEBA since other reactions, in which it is involved, are taking place. In addition, these compounds have specific absorption bands (1776 cm^{-1} for γ -VL and 910 cm^{-1} for DGEBA) that can be monitored to obtain a representative profile of their evolution which can be used to calculate the correlation coefficient. Those values are 0.9954 and 0.9885, respectively for γ -VL and DGEBA. Again, it is not possible to calculate this value for compounds that do not have specific absorptions bands as the intermediate and final compounds.

4 Conclusions

Sequential application of MCR-ALS makes possible to estimate the spectra of the compounds involved in a curing process, in which there are several side and consecutive reactions, while polymers are growing. The strategy applied overcomes the rank deficiency of the data matrix by appending these estimates to the original data matrix. The global phase angle convergence criterion is a good strategy for calculating the optimal number of iterations in ALS and for balancing the purely mathematical and physical model underlying the system. It has to be emphasized that the MCR-ALS solutions are always affected by ambiguity and in our opinion the SSR solution is included in the possible solutions of MCR-ALS. A deep study of the point will be analyzed in other work. The overall results of applying MCR-ALS to the augmented data matrix give a first solution to the evolution of the concentration profile of the compounds that participate in the reaction studied. This solution can be a first approach that might be used for interacting with hard-modeling methods and obtain kinetic constants.

Acknowledgements

The authors would like to acknowledge the economic support provided by the MCyT projects CTQ2007-61474/BQU.

References

- [1] H. Ishida, Y. Rodriguez, *Polymer*, 36, (1995), 3151.
- [2] H. Ishida, Y. Rodriguez, *J. Appl. Polym. Sci.*, 58, (1995), 1751.
- [3] D. Rosu, A. Mititelu, C.N. Cascaval, F. Mustata, C. Ciobanu, *Thermochim. Acta*, 383, (2002), 119.
- [4] D. Rosu, A. Mititelu, C.N. Cascaval, *Polym. Test.*, 23, (2004), 209.
- [5] Y. He, *Thermochim. Acta*, 367-368, (2001), 101.
- [6] N. Spegazzini, I. Ruisánchez, M. S. Larrechi, A. Serra, A. Mantecón, *J. Polym. Sci. Part A: Polym. Chem.*, 46, (2008), 3886.
- [7] Y. C. Su, D. R. Yei, F. C. Chang, *J. Appl. Polym. Sci.*, 95, (2005), 730.
- [8] S. Vyazovkin, N. Sbirrazzuoli, *Macromolecules*, 29, (1996), 1867.
- [9] N. Sbirrazzuoli, S. Vyazovkin, *Thermochim. Acta*, 388, (2002), 289.
- [10] M. Garrido, I. Lázaro, M. S. Larrechi, F. X. Rius, *Anal. Chim. Acta*, 515, (2004), 65.
- [11] N. Spegazzini, I. Ruisánchez, M.S. Larrechi, V. Cádiz, J. Canadell, *Analyst*, 133, (2008), 1028.
- [12] M. Maeder, A.D. Zuberbülher, *Anal. Chem.*, 62, (1990), 2220.
- [13] A. de Juan, M. Maeder, M. Martínez, R. Tauler, *Chemom. Intell. Lab. Syst.*, 54, (2000), 123.
- [14] A. de Juan, M. Maeder, M. Martínez, R. Tauler, *Anal. Chim. Acta*, 442, (2001), 337.
- [15] E. Bezemer, S. C. Rutan, *Chemom. Intell. Lab. Syst.*, 59, (2001), 19.
- [16] R. Tauler, *Chemom. Intell. Lab. Syst.*, 30, (1995), 133.

- [17] R. Tauler, A. Smilde, B. R. Kowalski, *J. Chemom.*, 9, (1995), 31.
- [18] M. Amrhein, B. Srinivasan, D. Bonvin, M. M. Shumacher, *Chemom. Intell. Lab. Syst.*, 33, (1996), 17.
- [19] A. De Juan, E. Casassas, R. Tauler in: R.A. Meyers (Ed.), *Encyclopedia of Analytical Chemistry*, John Wiley & Sons, Ltd., Chichester, 2000, pp 9800-9837.
- [20] W. Windig, J. Guilmont, *Anal. Chem.*, 63, (1991), 1425.
- [21] F. C. Sánchez, J. Toft, B. Van den Bogaert, D. L. Massart, *Anal. Chem.* 68, (1996), 79.
- [22] Y. Z. Liang, O. M. Kvalheim, *Chemom. Intell. Lab. Syst.*, 20, (1993), 115.
- [23] P. J. Gemperline, *Anal. Chem.*, 58, (1986), 2656.
- [24] H. Shinzawa, J.H. Jiang, M. Iwahashi, I. Noda, Y. Ozaki, *Anal. Chim. Acta*, 595, (2007), 275.
- [25] H. Shinzawa, M. Iwahashi, I. Noda, Y. Ozaki *J. Mol. Struct.*, 883-884, (2008), 73.
- [26] The Mathworks, MATLAB Version 6.5, Natick, MA, 2002.
- [27] A. Savitzky, M. J. E. Golay, *Anal. Chem.*, 36, (1964), 1627.
- [28] G. H. Golub, Ch. F. Van Loan, *Matrix Computations*, The John Hopkins university Press, Baltimore, 1989; p50.
- [29] A. Izquierdo-Ridorsa, J. Saurina, S. Hernandez-Cassou and R. Tauler, *Chemom. Intell. Lab. Syst.*, 38, (1997), 183.
- [30] J. Saurina, S. Hernandez-Cassou, R. Tauler and A. Izquierdo-Ridorsa, *J. Chemom.*, 12, (1998), 183.
- [31] R. Tauler, B. Kowalski, S. Fleming, *Anal. Chem.*, 65, (1993), 2040.
- [32] <http://www.ub.edu/mcr/ntheory.htm>, Group of Solution Equilibria and Chemometrics, Analytical Chemistry Department, University of Barcelona.

- [33] S. Morita, Y. Ozaki, I. Noda, *Appl. Spectrosc.*, 55, (2001), 1618.
- [34] S. Morita, Y. Ozaki, I. Noda, *Appl. Spectrosc.*, 55, (2001), 1622.
- [35] E. R. Malinowski, *Anal. Chem.*, 49, (1977), 612.
- [36] H. Nishida, F. Sanda, T. Endo, T. Nakahara, T. Ogata, K. Kusumoto, *J. Polym. Sci. Part A: Polym. Chem.*, 37, (1999), 4502.
- [37] H. Nishida, F. Sanda, T. Endo, T. Nakahara, T. Ogata, K. Kusumoto, *J. Polym. Sci. Part. A: Polym. Chem.*, 38, (2000), 68.
- [38] M. Kume, A. Hirano, B. Ochiai, T. Endo, *J. Polym. Sci. Part. A: Polym. Chem.*, 44, (2006), 3666.
- [39] M. Hitomi, F. Sanda, T. Endo, *Macromol. Chem. Phys.*, 200, (1999), 1268.
- [40] K. Inomata, S. Kawasaki, A. Kameyama, T. Nishikubo, *React. Funct. Polym.*, 45, (2000), 1.

UNIVERSITAT ROVIRA I VIRGILI

TWO-DIMENSIONAL INFRARED CORRELATION SPECTROSCOPY AND MULTIVARIATE CURVE RESOLUTION

METHODS: APPLICATION TO QUANTITATIVE MONITORING OF CURING PROCESS

Nicolas Spegazzini

ISBN:978-84-693-4049-3/DL:T.998-2010

3.4 Methodology to estimate concentration profiles from sample-sample two-dimensional covariance spectroscopy

We propose using sample-sample 2DCOS to find the concentration profiles of the reactive species involved in the reaction. A new analytical methodology for detecting the most representatives species, based on the correlation coefficient value, was applied for this purpose. This methodology was applied in the curing reaction described above (DGEBA with γ -valerolactone) and the estimated concentration profile was used in MCR-ALS

UNIVERSITAT ROVIRA I VIRGILI

TWO-DIMENSIONAL INFRARED CORRELATION SPECTROSCOPY AND MULTIVARIATE CURVE RESOLUTION

METHODS: APPLICATION TO QUANTITATIVE MONITORING OF CURING PROCESS

Nicolas Spegazzini

ISBN:978-84-693-4049-3/DL:T.998-2010

A Methodology to Estimate Concentration Profiles from 2D Covariance Spectroscopy Applied to Kinetic Data

Applied Spectroscopy 64, (2010), 177

Nicolás Spegazzini, Itziar Ruisánchez, Angels Serra,
Ana Mantecón, M. Soledad Larrechi

Department of Analytical and Organic Chemistry, Rovira i Virgili
University. Marcel·lí Domingo s/n, 43007, Tarragona, Spain

Abstract

Two dimensional (2D) covariance analyses applied to spectroscopy data obtained monitoring chemical process allow exploring the chemical reactions involved. Some slices of the sample-sample covariance map are an approach to the concentration profiles of the reactive species and we present a novel methodology to identify them. The method overcome problems habitually referenced in the application of this technique and it is based in the selection of spectral zones with similar standard deviation of the variables and row centering the spectra data in each zone. The slices are identified according to the correlation coefficient value. The method is illustrated using simulated spectra data set representatives of two model reactions $A \rightarrow B$ and $A \rightarrow I \rightarrow B$. It has been applied to analyze the effect of rare earth metal triflate initiators in the cationic curing process of diglycidyl ether of bisphenol A with γ -valerolactone. The number of significant slices found is equal to the number of reactive species. This is interesting information that can be used as initial estimation to find profiles concentration using other methods as Multivariate Curve Resolution- Alternating Least Squares (MCR-ALS).

Index Headings: Sample-Sample correlation analysis; Two-dimensional correlation spectroscopy; FT-IR spectroscopy; Curing reaction.

1 Introduction

Two dimensional (2D) correlation techniques, based on monitoring covariance's among variations at the variables [1,2] has been employed in the last years as a useful analytical tool to explore chemical reactions. The first work was reported by Nakano et al. [3] to analyze IR spectra monitored in a photochemical reaction. The use of other spectroscopic techniques as near infrared (NIR) [4] and Raman [5], has also been referenced. Some examples of different chemical reactions that have been studied are: $\text{Mo}(\text{CO})_6$ photochemical reaction [6], study of transients radicals of cyanooxomethyl radical [7], identification of the nature of sulfur species formed on an industrial SO_x sorbent material [8,9], synthesis of the spiroorthoester [4], polycondensation reactions during self-assembly of mesostructured films [10], curing process of bis-maleimide and dicyanate ester [11], reaction of malonitrile with KOH carried out in ionic liquids [5]. Recently, the 2D correlation analysis has been extended to the covariance analysis among the sample variations (SS). This approach was introduced by Zimba [12] and later refined by Šašić and Ozaki [13-15]. In successive works Isaksson [16] and Šašić [17,18] revised the terminology and considered the term 2D covariance spectroscopy as the most adequate. Although in essence SS correlation is very simple and intuitively understandable, there are few reports applied to study chemical reactions with SS correlation in comparison with variable-variable correlation analysis [19]. 2D covariance map or synchronous spectrum is obtained from this technique. The slice of the SS correlation values for each sample in the map [20,21] is a useful representation to evaluate the concentration profiles of the reactive species involved in the reaction.

In the referenced applications of SS technique, two topics are usually considered. One is related to the data pretreatment and the other to the selection of the most representative slice of the reactive species involved in the reaction [20,22]. The data pretreatment was considered

by Šašić et al. [13,15] where mean normalization and mean centering along the concentration profiles or sample axis was introduced. However, the efficacy of this pretreatment was questioned by the same author in their applications to IR data of polycondensation reactions [20] as a consequence of the strong amplification of noise and distortions introduced in the experimental data. In subsequent works [22,23] the pre-treatment usually employed is the mean centering of the spectra or columns centering.

Regarding the more representative slice, usually the first and the last one among all the slices calculated [20,22,23] are considered because there are the most representative of the reagents and of the final products. This simple rule it is not very useful when in the process several reactions and intermediate compounds are involved. Some information about the possible intermediates is obtained by the referenced authors [20,22,23] analyzing the disvariance or asynchronous spectra, which chemical interpretation it is not easy.

In this work a new methodology is proposed to estimate the concentration profiles from 2D covariance spectroscopy applied to kinetic data in such a way to overcome some of the problems above mentioned. It is based in: a) a previous fragmentation of the data in order to select a zone where the standard deviation between samples is similar for each variable considered in the zone. This avoids the need for mean-normalization and avoids amplification of noise in the experimental data, b) in each selected zone, 2D covariance analysis is done with the pre-treated data using mean-centering along the sample axis and c) the value of the coefficient correlation calculated between the slice derivate of the 2D covariance analysis is used to select the more representative slice of the evolution of the reactive species.

This methodology has been studied using two simulated data set of spectra, one correspond to a first order kinetic reaction $A \rightarrow B$ and the other correspond to a consecutive reaction $A \rightarrow I \rightarrow B$. Afterwards, it has been applied to analyze the effect of rare earth metal triflate initiators in the cationic curing process of diglycidyl ether of bisphenol A (DGEBA) with γ -valerolactone (γ -VL). This process, used to prepare modified epoxy thermosets, is a complex system in which parallel and successive reactions are involved [4,24]. An optimal quantitative resolution of this system, when the process is carried out in presence of ytterbium triflate, was obtained by multivariate curve resolution-alternating-least squares (MCR-ALS) using global phase angle con-

verge criterion [25]. As it was shown, the application of this methodology gives valuable information but it needs to overcome the rank deficiency problem present in the data matrix by sequential estimation [25]. In the present work, the strategy proposed can be used to estimate concentration profiles of the reactive species involved in the reaction, which are very useful to comparatively analyze the effect of the different rare earth metal triflates used as initiators in the curing process. In our opinion, this technique is an easy way that can be employed to found good initial estimation to find the quantitative resolution of complex systems using MCR-ALS, if it is necessary.

2 Background and applied strategy

In this section the basis of the data analysis and the strategy proposed are introduced. In all expressions the data matrix \mathbf{D} of dimensions ($n \times m$) correspond to the n spectra recorded in each experiment at the wavenumber m .

Sample-Sample 2D Covariance Analysis. The SS-2D covariance (cov) matrix of the experimental data \mathbf{D} that has been previously centered along the rows $\tilde{\mathbf{D}}$ is calculated according to equation 1:

$$\Phi = \frac{1}{m-1} \tilde{\mathbf{D}} \tilde{\mathbf{D}}^T \quad (1)$$

Each point in the sample-sample covariance matrix represents the covariance between a given pair of sample traces, such as those measured at different reaction times. Each vector or slice spectrum in this matrix gives information about the evolution of each sample in the matrix \mathbf{D} , thus if we correlated these slices we can detect point of the maxima dissimilarity or maxima variability.

Correlation-coefficient analysis. criteria to estimate the more representative slice spectra. The correlation coefficient ρ between two vectors or slices (\mathbf{i} and \mathbf{j}) from matrix is defined as it is expressed in equation 2. It is a measure of their similarity and range between +1 and -1.

$$\rho_{ij} = \frac{cov(\mathbf{i}, \mathbf{j})}{SD_{\mathbf{i}} \cdot SD_{\mathbf{j}}} \quad (2)$$

The evolution of the reactive species of a reaction as $A \rightarrow B$ can be represented by a conjunct of symmetric profiles, ones corresponding

to the evolution of A and the other to the evolution of B. The values of correlation coefficient between two profiles are always +1 or -1 depending on whether the shape of the two profiles (slices) considered will be representative of the evolution of the specie A or the specie B. However, if intermediate compounds take part in the reaction, as an example $A \rightarrow I \rightarrow B$, several and different concentration profiles can be found to represent the dynamic evolution of the system depending on the reaction kinetics involved in the system and values different from +1 or -1 can be found. The correlation coefficient is zero when the angle between the two slice spectrums (vectors) correlated is 90° . Obviously, this point is related to a point of maxima dissimilarity between the vectors. Figure A-1 (see Appendix) shows the geometrical representation of the angle formed among vectors.

Selecting spectral zone with similar standard deviation.

Why selecting variables zone with similar standard deviation? When 2D covariance analysis is applied to a data set that has been row centered, only if the magnitude of each variable in the vector of each sample in the data set is similar, it is possible to obtain good information of the variations between the samples. This is the usual situation when working with spectroscopic data. An easy way to select variables zone is to determine the zones that have similar standard deviation values. In addition, this procedure allows detecting zones which variability can be associated with noise.

The methodology developed to apply SS covariance spectroscopy to a data set is:

1. Define wavenumber zones where the intensity variations could be observed in the application of the methodology. The information is hidden when the methodology is applied when there are intensity bands with different standard deviation. This step has to be optimized. An easy strategy could be: a) use the spectral bands characteristics of the functional groups representatives of the chemical species involved in the reaction; b) calculate the maximum and minimum standard deviation values of them; c) calculate the increment and use it as criteria in the optimization process.
2. Calculate the SS covariance map in each zone. Previously the spectral data are mean centering along the concentration profiles or sample axis in each zone. From this map the slice spectra for each sample is obtained.
3. Calculate the correlation coefficient value between all slices to

determine the most representative, through the points of maxima similarity (1), dissimilarity (0) or inverse similarity (-1).

3 Experimental

Simulated data set spectra. Two data sets of spectra were simulated in order to assess the performance of the methodology presented in this work. Each trace of the spectra, as a function of spectral variable (ν), consists of two or three peaks (Figure 1A and 1B). The spectral intensity of each peak changes as a function of the perturbation variable t . The simulated spectra are given as a sum of two or three Lorentzian peaks.

$$I(\nu, t) = \frac{I_0(t)}{1 + 4(\nu - \nu_0)^2/\Gamma^2} \quad (3)$$

Where I_0 , ν_0 , and Γ are: the peak intensity, peak position and band width measured at the half height of the peak, respectively. The parameters for the simulated spectra were, $I_0 = 0.1563$, $\nu_0 = 65$ and 125 in Figure 1A and $I_0 = 0.1563$ or 0.086 , $\nu_0 = 65, 90$ and 125 in Figure 1B, in both figures $\Gamma = 40$. In both cases 100 spectra with 191 variables were simulated. The two data sets can be fit to a first order kinetic as it is indicated in the Figures 1A and 1B, where the profiles of the reactive species A, B or I are shown.

Curing process. Just a brief description of the experiments is given here because the details can be found in ref [24]. The three independent experimental curing processes were carried out with DGEBA/ γ -VL (2:1 mol/mol) mixture in the presence of 1 phr (parts of initiator per 100 part of mixture, w/w) of scandium, ytterbium or lanthanum triflate. The reaction was carried out at 160°C. In the processes, the sample was placed on a small diamond crystal in the spectrophotometer ATR cell (FTIR-680PLUS JASCO), which has a 3000 SeriesTM High Stability Temperature Controller with a RS232 Control to take the measurements. For each experiment we automatically acquired data at intervals of 30 seconds between 700 and 1850 cm^{-1} until no changes over time were observed in the spectra. The spectra recorded were exported and converted into Matlab binary files, in each experiment were aligned in three independently matrices which dimensions were (40 x 1247) for scandium, (47 x 1247) for ytterbium and (150 x 1247) for lanthanum triflates.

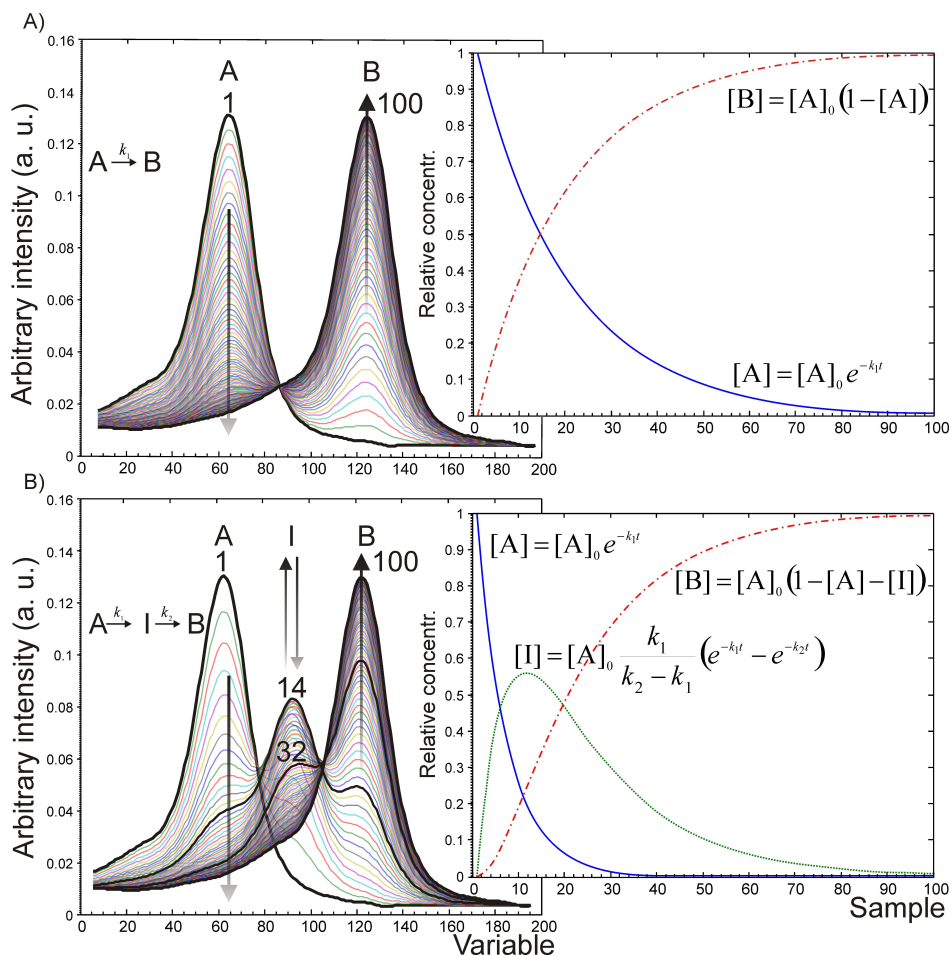


Figure 1: Simulated data set of spectra and their corresponding concentration profiles in a model reaction $A \rightarrow B$ (A), and a model reaction $A \rightarrow I \rightarrow B$ (B).

4 Computer programs

All calculations of ordinary differential equations are solved by ODE45, Runge-Kutta integrated numerically and sample-sample 2D covariance. Coefficient-correlation and all plots were performed with Matlab subroutines, (version 6.5 The mathWorks, INC., Nattick. MA).

5 Results and discussion

Figure 2 (A and B) contains the slice spectra obtained when 2D covariance analysis is carried out with the simulated data shown in Figure 1 (A and B), respectively, after centering the data by rows. Regarding the Figure 2 (A and B) it is easy to conclude that the first and the last slices are the most representative of the concentration profiles of the reagent A and the final product B, since the coefficient correlation between them and the known concentration of the reagents are 0.998 and 0.995, respectively. However, determine which slices are the most representative of the concentration profile of the intermediate I is not so simple. Figure 2 (C and D) shows the correlation coefficient between the first slice and the following of Figure 2 (A and B). The values are always +1 or -1, in Figure 2C, because the slice spectra data, Figure 2A, are representative of a reaction in which there is no intermediates, whereas when intermediates are present, the coefficients can take any value between +1 and -1 as can be observed in Figure 2D.

The zero value corresponds to the sample 14, which has the highest peak of the intermediate (Figure 1B) and therefore it is the optimal to represent the intermediate. It should be said, that this information could not be obtained if during the pretreatment of the data they were not centered by columns. The corresponding figures can be seen in Figures A-2 (Appendix). For the case $A \rightarrow I \rightarrow B$, it is not possible to found the zero value and the best approach is the 0.19 which corresponds to the correlation coefficient between the slice 1 and the slice 32. Obviously, the slice 32 is not the optimum to represent the profile of the intermediate compounds (Figure 1B). Considering that the proposed methodology is an easy way to select the most representative slices obtained by 2D covariance analysis of a data set, it has been employed to found the slices spectrum representatives of the curing process of DGEBA/ γ -VL mixtures in order to evaluate the effect of the initiator selected. As an example of the experimental data, Figure 3 shows the 150 FTIR spectra measured in situ during the curing reaction in presence of lanthanum triflate. Its profile is similar to that obtained when the reaction was carried out in the presence of ytterbium triflate [24]. In this work, all reactive species involved in the different reactions shown in the general Scheme 1, were postulated and discussed using two-dimensional correlation analyses.

In the experimental data, the standard deviation at each wavenumber between the samples was evaluated before performing the analysis.

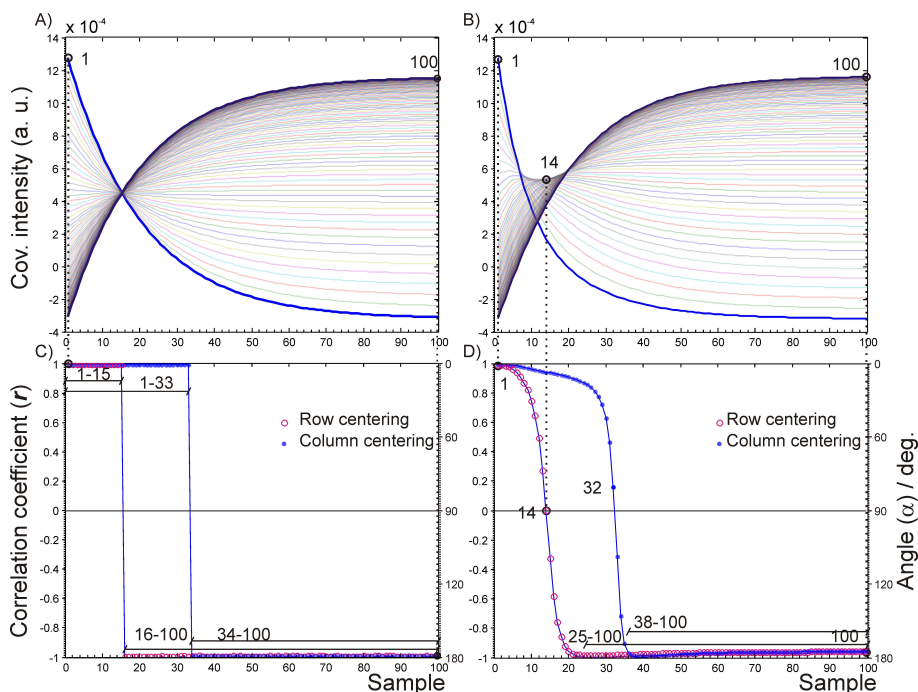
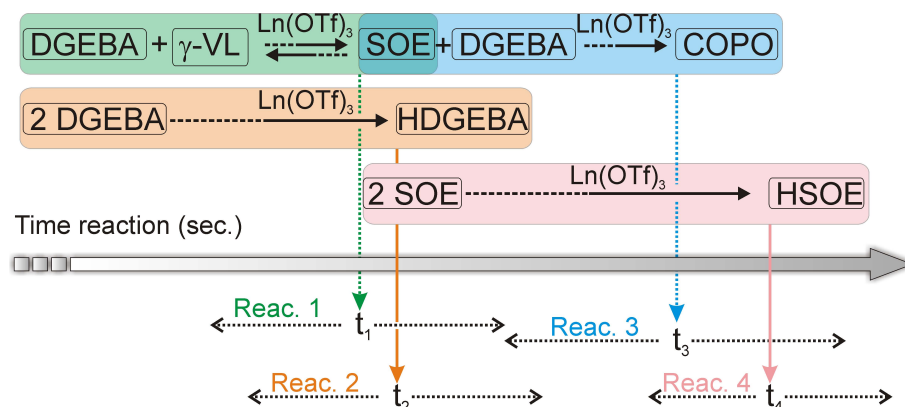


Figure 2: Slices spectra taken from SS covariance map using simulated data set of spectra (A and B) and correlation coefficient values between the slices (C and D) respectively. (○) values when the data were row centering and (●) when the data were column centering.



Scheme 1: Cationic curing process of diglycidyl ether of bisphenol A (DGEBA) with γ -valerolactone (γ -VL) (2:1) at $T=160^{\circ}\text{C}$. Time (t_i) is an indicator of the period of time in which each reaction of the process can occur depending of the lanthanide triflate used as initiator.

Figure 4 shows the results obtained. Three zones can be distinguished: the first between 800 and 1020 cm^{-1} , the second between 1020 and 1200 cm^{-1} and the third between 1650 and 1800 cm^{-1} and 2D covariance analysis was carried after a previous fragmentation of the spectra in the three zones. Each zone of the spectra was rows centered.

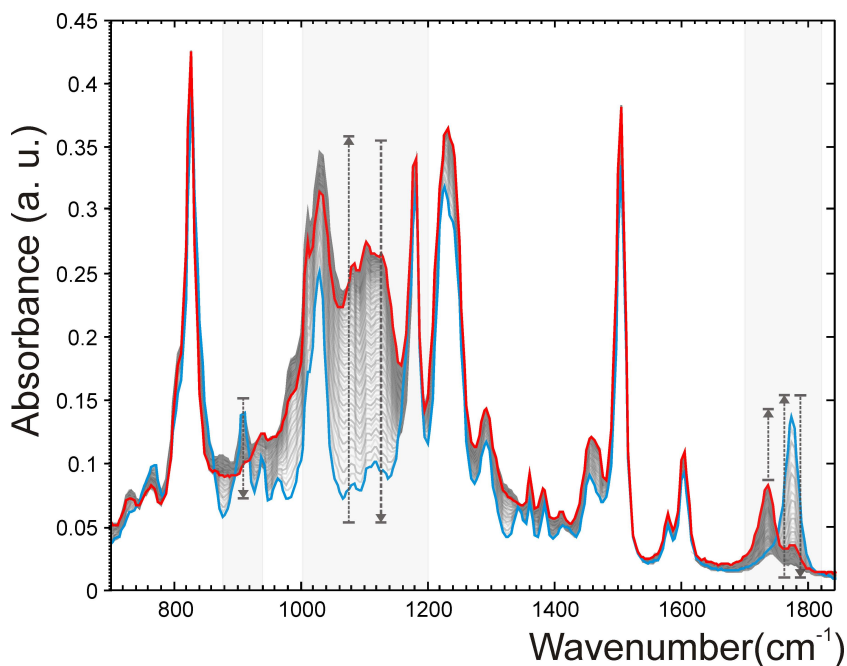


Figure 3: FTIR-ATR spectra recorder along the reaction between DGEBA and γ -VL, using $\text{La}(\text{OTf})_3$ as initiator.

In Figure 5(A-I) the spectra slices obtained in each spectral zone for the three experiments (scandium (A-C), ytterbium (D-F) and lanthanum (G-I) triflates) are shown. Always, in the first zone, Fig 5 (A, D and G between 800 and 1020 cm^{-1}), the profile of the first slice is characteristic of the evolution of a reagent, as might be expected if we consider that in this spectral zone the variations between the samples can be attributed to the intensity changes associated with the characteristic band (910 cm^{-1}) of oxirane group of DGEBA.

These first slices are the unique of all figures that have a profile characteristic of a reagent that is consumed along the reaction (similar to Figure 1, evolution of reactive specie A) and has been considered as a reference to calculate the correlation coefficients shown in Figure

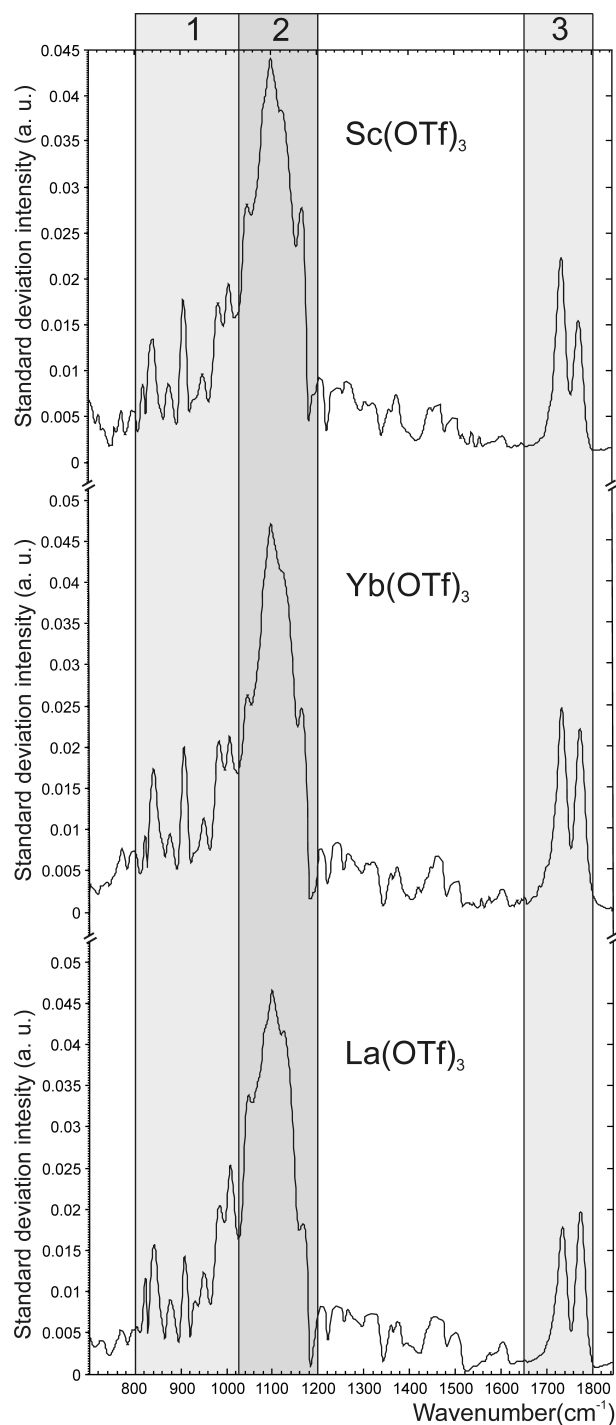


Figure 4: Spectral standard deviation along of wavenumber for the three curing process.

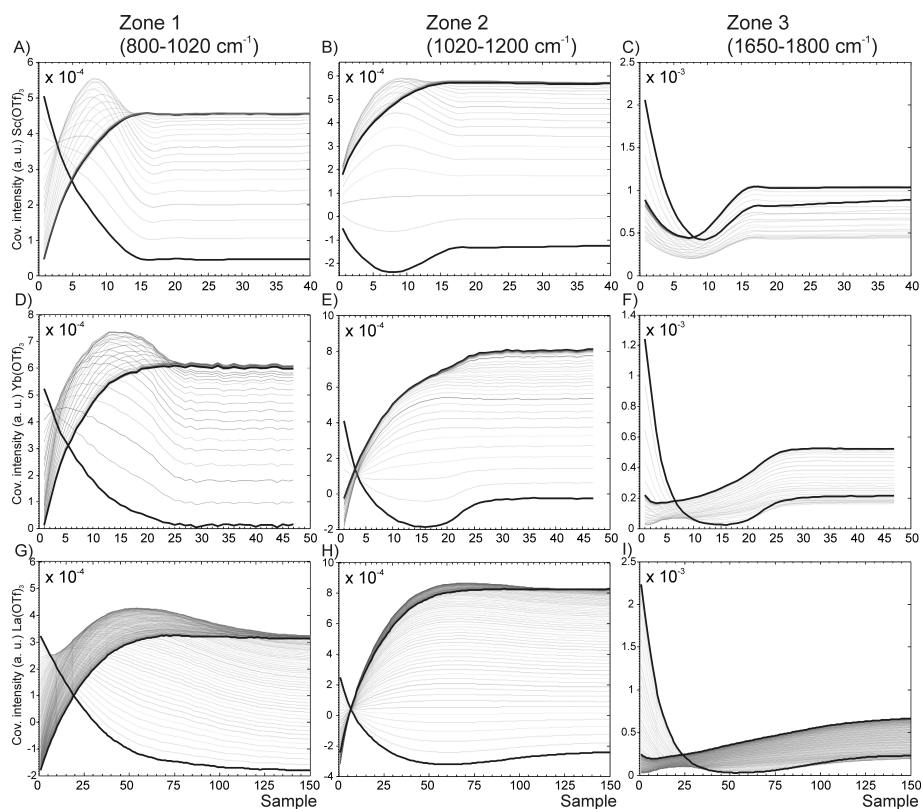


Figure 5: Slices spectra taken from a SS covariance map in the selected spectral zone with similar standard deviation for each initiator: $\text{Sc}(\text{OTf})_3$ (A-C), $\text{Yb}(\text{OTf})_3$ (D-F) and $\text{La}(\text{OTf})_3$ (G-I).

6. According to the background, the values nearly to (0 or -1) will be found when the most different slices are correlated and this occurs at different reaction times, depending on the initiator. When the reaction takes place in presence of scandium triflate, r values of -0.015 and -0.98 are obtained for the samples 10 and 21, respectively (Figure 6 A), $r = -0.92$ for sample 62 (Figure 6 B) and $r = 0.5$ and -0.75, for samples 81 and 95 respectively (Figure 6C). The spectrum slices of these samples and the sample 1 are shown in Figure 7A. The same procedure has been applied to detect the most representative slices when the reaction is taking place in presence of the ytterbium triflate (Figure 6, D-F) or the lanthanum triflate (Figure 6, G-I) and the corresponding slices spectrum are shown in Fig 7(B and C), respectively.

From the results shown until now an interesting point is that the

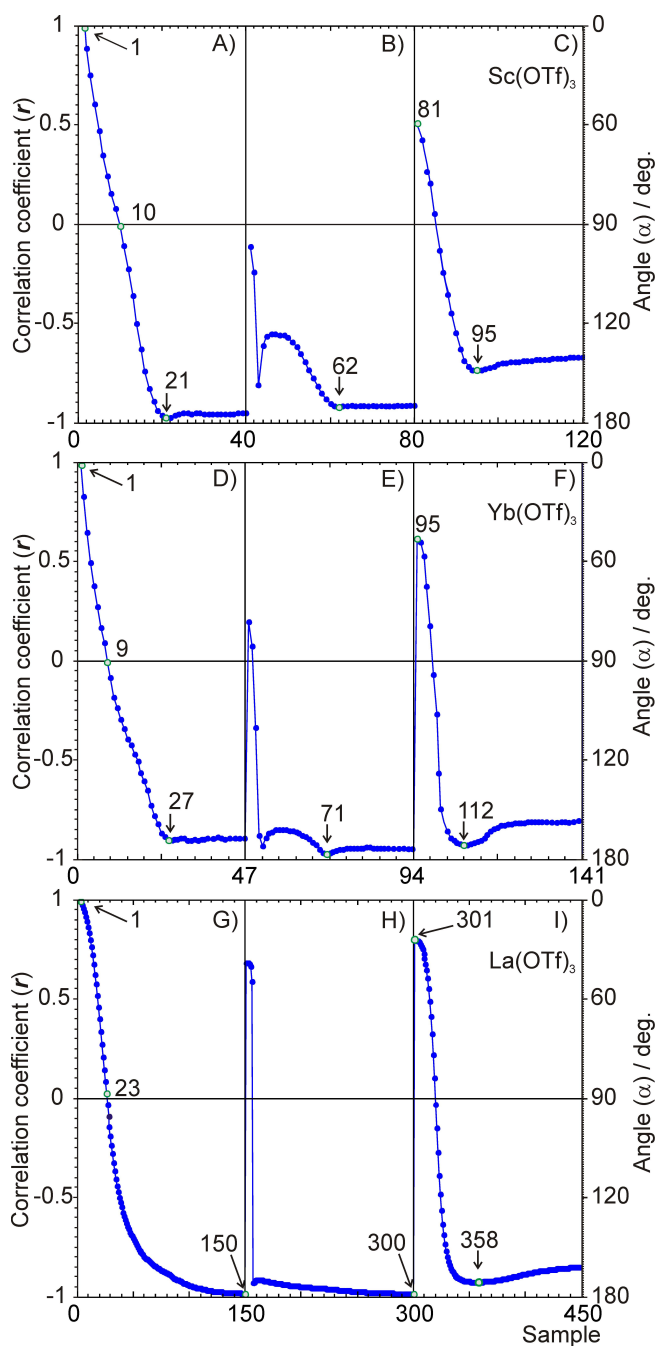


Figure 6: Correlation coefficient and angle between the first slice obtained in spectral zone of $800\text{-}1020\text{ cm}^{-1}$ and the slices obtained in each spectral zone, for each initiator: $\text{Sc}(\text{OTf})_3$ (A-C), $\text{Yb}(\text{OTf})_3$ (D-F) and $\text{La}(\text{OTf})_3$ (G-I).

number of slices considered as more representative is equal to the number of reactive species considered in the process. Also, it has to be said that the same number of slices and equally representative, will be found considering other band as a reference. Taking into account that in the FTIR there are no specific bands for each reactive species, to find a representative profile of their evolution is not a trivial task. To comparatively discuss the results, the covariance's values shown in Figure 7, have been normalized and if we focus the attention in this figure, it is possible to observe that the shape of the consecutive slices have similar trend in each one of the three experiments. More precisely, the first slices (sample 1) in figures 7A, B and C have similar shape; the second slice found, which correspond to a different sample (10 in Figure 7A, 9 in Figure 7D and 23 in Figure 7G) has also similar shape and so for all the slices (third until six). That is an indication that the reactions involved in the curing process, Scheme 1, are the same, independently of the initiator used. Therefore, considering the information obtained from the previous work, where WW 2D correlation spectroscopy was applied [24], a chemical discussion can be done associating each slice spectrum with the evolution of each reactive specie involved in the reaction. At this point, it is necessary to say that the profiles shown in Figure 7, are only one possible estimation of the real concentration profiles and, in order to check their goodness to analyze comparatively the effect of the three initiators in the curing reaction, the slice attributed to DGEBA and γ -VL are compared with the profiles experimentally obtained monitoring the absorbance values at 910 cm^{-1} and 1776 cm^{-1} , respectively, since these are characteristic bands of each compound. Table 1 shows the correlation coefficient between them, being in all cases higher than 0.97. So it can be conclude that the slides associated with DGEBA and γ -VL in Figure 7 can be considered as a useful concentration profiles to analyze the effect of the initiator in their evolution. This assumption has been extended to the other reactive species involved in the reaction.

Tables 1. Correlation coefficient for each initiator, between the experimental absorbance values profile at characteristic bands of DGEBA and γ -VL and the slices associated with them.

Profiles	Slice's $\text{Sc}(\text{OTf})_3$	Slice's $\text{Yb}(\text{OTf})_3$	Slice's $\text{La}(\text{OTf})_3$
A 910 cm^{-1} DGEBA	0.988	0.994	0.976
A 1776 cm^{-1} γ -VL	0.993	0.985	0.990

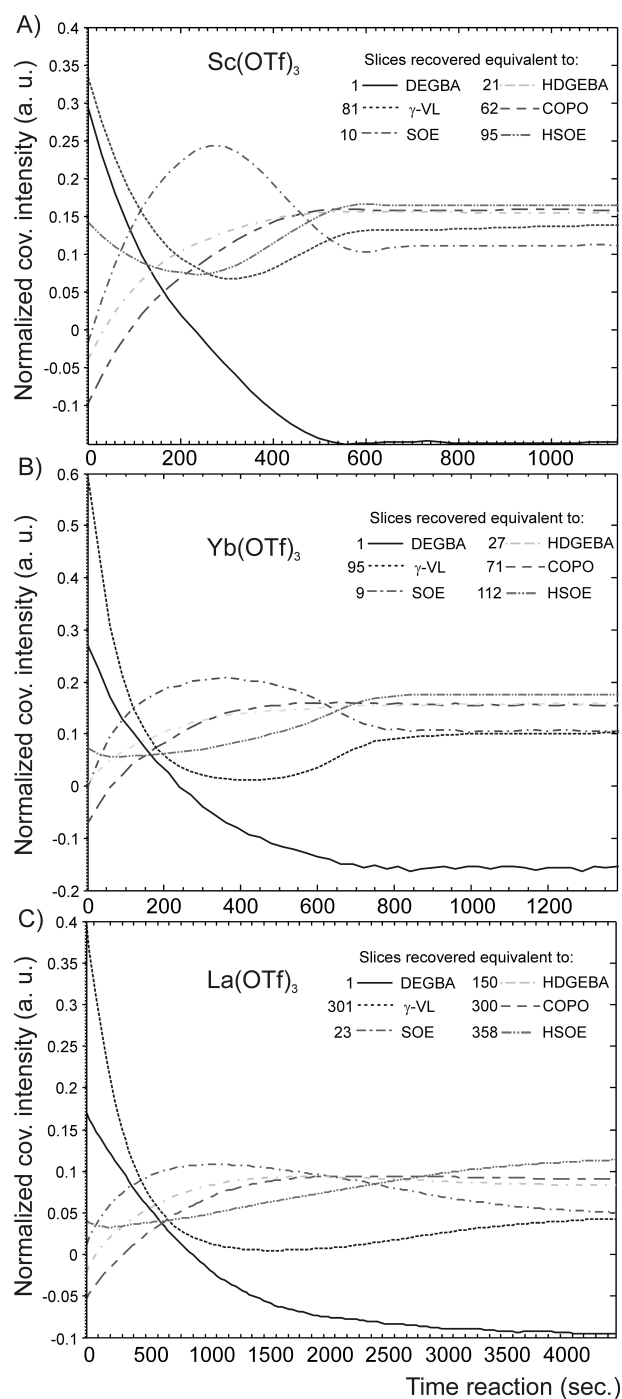


Figure 7: Estimate concentration profiles for the reactive species in the curing process for each initiator: $\text{Sc}(\text{OTf})_3$ (A) $\text{Yb}(\text{OTf})_3$ (B) and $\text{La}(\text{OTf})_3$ (C).

If we compare the curves of the different initiators (Figure 7), some differences arise. First refers to the time needed to complete the reactive process. With scandium triflate the reactive process is finished at about 600 seconds, with ytterbium salt it finishes at 800 seconds and with lanthanum reaction times longer than 4000 seconds are necessary to reach the complete disappearance of epoxide groups. This order of reactivity agrees with the Lewis acidity of the rare earth metal triflates, $\text{Sc} > \text{Yb} > \text{La}$. If we take into consideration the evolution of each reactive species for the three initiators, what it calls the attention is the evolution of the SOE and γ -VL groups. Scandium salt is the most active to produce SOEs from epoxide (DGEBA) and γ -VL whereas the lanthanum salt is the less active. However, after formation, some SOE disappears again. This disappearance is more pronounced for the scandium triflate initiated system, whereas for the lanthanum salt this disappearance is more smooth and slower and continue until 4400 seconds. Because SOE is an intermediate compound, produced during the cationic polymerization, it is expected that it polymerizes after formation. However, if we look at the γ -VL evolution an unexpected behavior can be observed. For all initiators, the lactone disappears from the very beginning of the curing, faster for the scandium salt and more slowly for the lanthanum, showing the ytterbium salt an intermediate behavior. However, a pronounced formation of the lactone, after exhaustion, can be observed in the scandium and ytterbium initiated systems, and only a smooth and slow appearance occurs for the lanthanum triflate. Thus, the disappearance of the SOE group can be explained not only by the expected polymerization but also for the reversion of SOE groups to the initial epoxide and lactone. Both processes, polymerization and reversion of SOE, seem to be faster and more pronounced in the following order: $\text{Sc} > \text{Yb} > \text{La}$. In the figure the curves corresponding to the homopolymerization of SOE and epoxide and to the copolymerization of SOE with epoxide are also represented. From these curves we can see that homopolymerization of epoxide and copolymerization of SOE and epoxide occurs from the beginning of the process, but epoxide homopolymerization seems to be more favorable than copolymerization. However, the homopolymerization of SOE takes only place when the proportion of epoxide is low and it does not begin until a considerable extent of polyetherification and copolymerization has occurred.

6 Conclusions

The proposed methodology allows estimating the concentration profiles of reactive species in a curing process from 2D covariance spectroscopy analysis applied to kinetic data. The developed strategy based in the selection of a spectral zone with similar standard deviation of the variables and the row centering of the data in each zone overcome problems habitually referenced in the literature in the application of SS 2D covariance as the amplification of noise of the experimental data. The value of the correlation coefficient calculated between the slices derivatives of the SS 2D covariance analysis is a useful tool to select the more representative of them. It is proved that when chemical information is available, correlation between the slices derivatives by 2D covariance analysis and the evolution of the reactive species involved in the process can be done. This information can be obtained using several methodologies as WW 2D correlation spectroscopy or MCR-ALS. In this latter case, the selected slices probably can be a useful initial estimation in the optimization step. In the application considered, the methodology allows to detect a number of significant slices equal to the number of species involved in the curing process. Considering that in the experimental spectra there are no specific bands for each reactive species, which is important information that is not easily obtained by other chemometrics methods. The results obtained in the considered case, allows concluding that in the present experimental conditions the involved reactions of the curing process are the same, independently of the initiator used. The initiator only affects the kinetic rate of the different reactions involved and their extension.

Acknowledgements

The authors would like to acknowledge the economic support provided by the MICINN projects CTQ2007-61474/BQU and MAT2008-06284-C03-01. Also N.S. acknowledges the Spanish Ministry of Education and Science (MEC) for the doctoral fellowship AP2006-04172.

References

- [1] I. Noda, *Appl. Spectrosc.*, 47, (1993), 1329.

- [2] I. Noda, *Appl. Spectrosc.*, 54, (2000), 994.
- [3] T. Nakano, S. Shimada, R. Saitoh, and I. Noda, *Appl. Spectrosc.*, 47, (1993), 1337
- [4] N. Spegazzini, I. Ruisánchez, M. S. Larrechi, V. Cádiz, and J. Canadell, *Analyst*, 133, (2008), 1028.
- [5] M. López-Pastor, A. Domínguez-Vidal, M. J. Ayora-Cañada, M. Valcárcel, and B. Lendl, *J. Mol. Struct.*, 799, (2006), 146.
- [6] P. J. Tandler, P. D. Harrington, and H. Richardson, *Anal. Chim. Acta*, 368, (1998), 45.
- [7] W. McNavage, and H.-L. Dai, *J. Chem. Phys.*, 123, (2005), 184104.
- [8] H. Dathe, P. Haider, A. Jentys, and J. A. Lercher, *J. Phys. Chem. B*, 110, (2006), 10729.
- [9] H. Dathe, P. Haider, A. Jentys, and J. A. Lercher, *J. Phys. Chem. B*, 110, (2006), 26024.
- [10] P. Innocenzi, L. Malfatti, T. Kidchob, P. Falcaro, M. C. Guidi, M. Piccinini, and A. Marcelli, *Chem. Commun.*, 18, (2005), 2384.
- [11] X. Liu, Y. Yu, and S. Li, *Polymer*, 47, (2006), 3767.
- [12] C. Zimba, Presented at the Second International Symposium on Advanced Infrared Spectroscopy (AIRS II), Durham, NC, 17 June (1996); and at the First International Symposium on Two-Dimensional Correlation Spectroscopy (2DCOS), Sanda, Japan, 30 August (1999).
- [13] S. Šašić, A. Muszynski, and Y. Ozaki, *J. Phys. Chem. A*, 104, (2000), 6380.
- [14] S. Šašić, A. Muszynski, and Y. Ozaki, *J. Phys. Chem. A*, 104, (2000), 6388.
- [15] S. Šašić, A. Muszynski, and Y. Ozaki, *Appl. Spectrosc.*, 55, (2001), 343.

- [16] T. Isaksson, Y. Katsumoto, Y. Ozaki, and I. Noda, *Appl. Spectrosc.*, 56, (2002), 1289.
- [17] S. Šašić, Y. Katsumoto, H. Sato, and Y. Ozaki, *Anal. Chem.*, 75, (2003), 4010.
- [18] S. Šašić, J.-H. Jiang, H. Sato, and Y. Ozaki, *Analyst*, 128, (2003), 1097.
- [19] I. Noda, *J. Mol. Struct.*, 883-884, (2008), 2.
- [20] S. Šašić, T. Amari, and Y. Ozaki, *Anal. Chem.*, 73, (2001), 5184.
- [21] S. Šašić, J. Zhang, and Y. Ozaki, *Vib. Spectrosc.*, 44, (2007), 50.
- [22] J. Diewok, M. J. Ayora-Cañada, and B. Lendl, *Anal. Chem.*, 74, (2002), 4944.
- [23] S. Šašić, J. -H. Jiang, and Y. Ozaki, *Chemom. Intell. Lab. Syst.*, 65, (2003), 1.
- [24] N. Spegazzini, I. Ruisánchez, M. S. Larrechi, A. Serra, and A. Mantecón, *J. Polym. Sci. Part. A: Polym. Chem.*, 46, (2008), 3886.
- [25] N. Spegazzini, I. Ruisánchez, and M. S. Larrechi, *Anal. Chim. Acta*, 642, (2009), 155.

Appendix

Theoretical figures

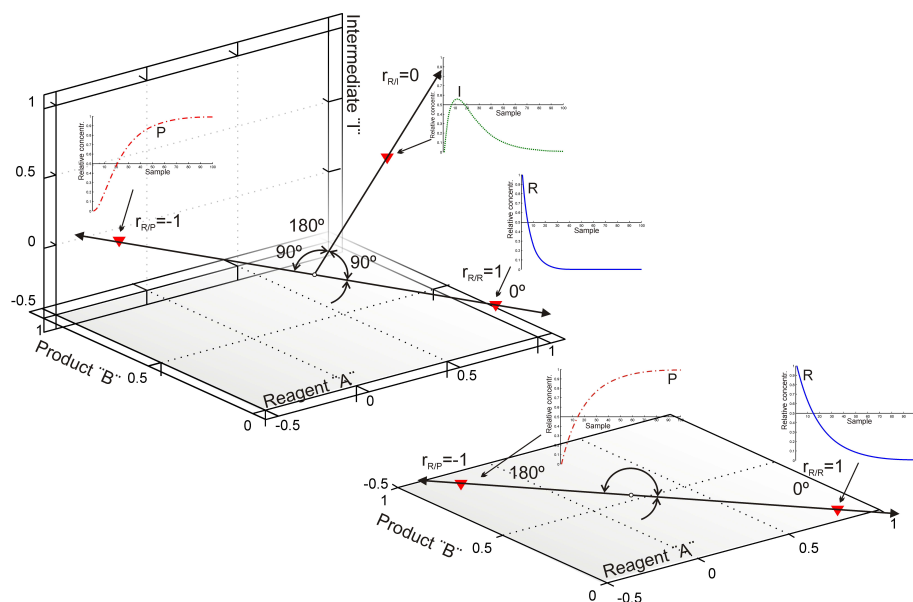


Figure A-1: Geometrical representation of the angle formed among vectors representative of the species involved, for the first kinetic order $A \rightarrow B$ and consecutive reaction $A \rightarrow I \rightarrow B$ respectively.

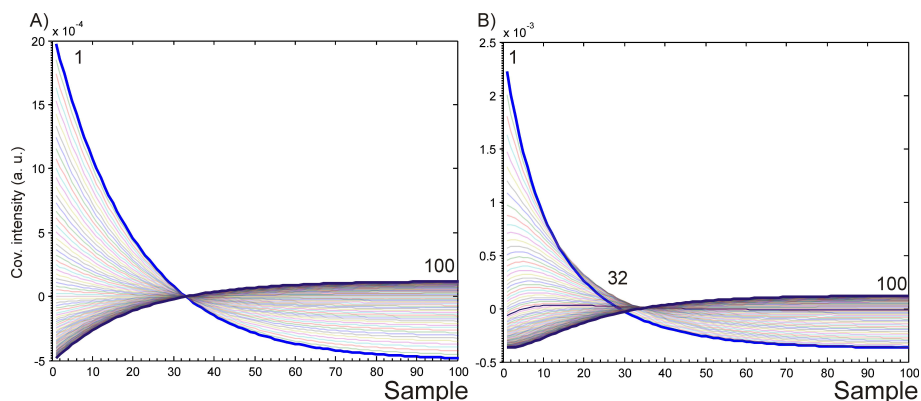


Figure A-2: Slice spectra taken from SS covariance map by column centering. (A) For the reaction $A \rightarrow B$ and (B) from the consecutive reaction $A \rightarrow I \rightarrow B$.

3.5 Study of mechanisms involved in the cationic curing process by perturbation-correlation analysis and a curve resolution method

This section describes a variation on 2D correlation analysis called PCMW2D that allows the analysis of complex spectral variations along a reaction. PCMW2D) was used to study the two mechanisms (ACE and AM) involved in the homopolymerization of DGEBA reaction in the presence of rare-earth metal triflates as initiators.

An individual spectrum of the transient species involved in the ACE mechanism was extracted by MCR-ALS using SS-2DCOS to find an initial estimate of the concentration profiles of the reactive species. The spectral profiles found suggest that the DGEBA polymerization mechanism has a living character.

UNIVERSITAT ROVIRA I VIRGILI

TWO-DIMENSIONAL INFRARED CORRELATION SPECTROSCOPY AND MULTIVARIATE CURVE RESOLUTION

METHODS: APPLICATION TO QUANTITATIVE MONITORING OF CURING PROCESS

Nicolas Spegazzini

ISBN:978-84-693-4049-3/DL:T.998-2010

Spectroscopic Evidence of the Mechanism Involved in the Cationic DGEBA Curing with Rare Earth Metal Triflates

Applied Spectroscopy 64, (2010), 104

Nicolás Spegazzini, Itziar Ruisánchez, M. Soledad Larrechi,
Angels Serra, Ana Mantecón,

Department of Analytical and Organic Chemistry, Rovira i Virgili
University. Marcel·lí Domingo s/n, 43007, Tarragona, Spain

Abstract

The crosslinking of DGEBA using three rare earth triflates as initiators (lanthanum, ytterbium and scandium) was studied by in situ FTIR spectroscopy. Cationic ring opening of epoxides can proceed through two different mechanisms: activated monomer (AM) and active chain end (ACE). Using advanced chemometric methods such as perturbation-correlation moving-windows two dimensional correlation spectroscopy (PCMW2D) and multivariate curve resolution - alternating least squares (MCR-ALS) it has been possible to obtain spectroscopic evidence of the two mechanisms. Traditionally, to evidence different mechanism pathways specific experiments requires being design. The novelty of the present study is to find, without a specific experimental design, spectroscopy evidence of the pathway of the polymerization process and analyze the effect of these initiators, and the evolution of the species that takes part in the curing process by structural techniques as FTIR/ATR.

Index Headings: Two dimensional correlation spectroscopy, PCMW2D correlation spectroscopy, ATR-FTIR spectroscopy, sample-sample correlation spectroscopy, multivariate curve resolution - alternating least squares method, crosslinking, cationic initiators, Lewis acids.

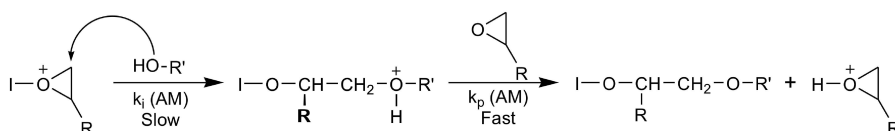
1 Introduction

The processability and the applicability of an epoxy resin critically depend on the pathway of the curing process. The used curing agents, which define the curing mechanism, have a large influence on the characteristics of the final thermoset. Curing agents can be stoichiometric, such as primary diamines or anhydrides, or catalytic, such as tertiary amines or Lewis acids. Rare earth triflates are Lewis acids stable in humid environments, commercially available, and their efficiency in the curing process of diglycidyl ether of bisphenol A (DGEBA) has been demonstrated [1]. These compounds are cationic initiators and are more active than boron trifluoride complexes in the crosslinking of epoxy resins and their copolymerization with lactones [2]. Cationic ring opening of epoxides has been extensively studied and it can proceed through two different mechanisms: activated monomer (AM) and active chain end (ACE) [3]. Both mechanisms, which can coexist, are represented in Scheme 1. It has been suggested that the AM mechanism is preferred in the presence of relatively high content of the initiator and hydroxylic groups [4,5]. In the cationic polymerization of heterocycles proceeding by ACE mechanism, propagation involves nucleophilic attack of the heteroatom of the monomer to the growing chain end, which is a cationic species. In the polymerization that proceeds by an AM mechanism there are no active species at the growing chain end, and the monomer is in this case activated by the initiator and undergoes the nucleophilic attack on the uncharged growing chain end. The ACE mechanism is characterized by back-biting processes that lead to oligomeric species. However, when ring-opening polymerization is applied to the formation of thermosetting materials, this mechanism produces inter- or intramolecular chain transfers, which do not lead to relevant changes in the network structure. On the contrary, AM mechanism produces chain transfer reactions, which shortens the chain length affecting the network morphology and the glass transition temperature of the thermoset. The present study is focused in the cationic curing of DGEBA, using three rare earth triflates as initiators: lanthanum, ytterbium and scandium. Since these metal triflates differ in their Lewis acidity and Pearson hardness, they can affect differently both mechanism and their kinetics. Traditionally [4-7], to evidence different mechanism pathways specific experiments requires being design. The novelty of the present study is to find, without a specific experimental design, spectroscopy evidence of the

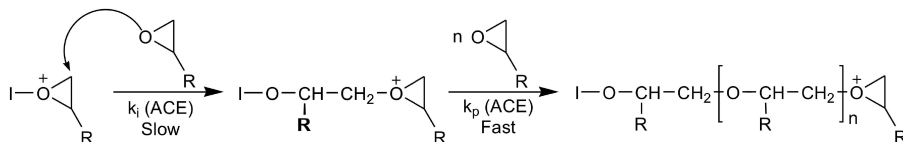
pathway of the polymerization process and analyze the effect of these initiators, and the evolution of the species that takes part in the curing process by structural techniques as FTIR/ATR. Infrared spectroscopy is sensitive to the conformation and local molecular environment and can provide structural information and therefore it can be used to monitor the curing process at real time.

In a first step, we use a powerful tool as perturbation-correlation moving-windows two dimensional correlation spectroscopy (PCMW2D) [8-10] for unraveling the reaction pathway. In a second step, multivariate curve resolution-alternating least squares (MCR-ALS) [11-13] has been employed to quantitative resolution of the reactive species involved in the curing process [14]. The initial estimates of the profile concentration of the chemical species required for MCR-ALS has been found by sample-sample covariance spectroscopy [15]. The study reveals that two mechanisms activate chain (ACE) and activate monomer (AM), are involved in the DGEBA homopolymerization being the later one more favorable with the scandium triflate. Also, a representative spectrum of the transient specie involved in the cross linking process of DGEBA according to the activated chain mechanism (ACE) has been found. These results are the first spectroscopic evidence of the mechanism involved in the cationic DGEBA curing.

Activated monomer mechanism (AM)



Activated chain end mechanism (ACE)



Schema 1: Cationic ring opening of epoxides by two different mechanisms: activated monomer (AM) and active chain end (ACE).

2 Background and procedure

Perturbation-correlation moving-windows two-dimensional correlation spectroscopy. The PCMW2D correlation spectroscopy [16] is derived from the generalized two-dimensional correlation spectroscopy [17,18] and moving-windows two dimensional correlation spectroscopy [19]. This method is characterized by a synchronous $\mathbf{\Pi}_{\Phi}$ and asynchronous $\mathbf{\Pi}_{\Psi}$ correlation spectra spread on a 2D plane defined by the spectral variable ν axis (here, wavenumber) and the perturbation variable t axis (here, reaction time). The correlation intensities are calculated in a sub-divided matrix named “moving-windows” along the perturbation directions. To do it, it is necessary to define the size window ($2m + 1 = \text{size}$). Correlation between the spectral variation and perturbation variation between the windows are calculated. According to the study of Morita et al. [16] the synchronous $\mathbf{\Pi}_{\Phi}$ and asynchronous $\mathbf{\Pi}_{\Psi}$ PCMW2D correlation spectra are proportional to the first derivative and the opposite sign of the perturbation second derivative, respectively eq 1:

$$\mathbf{\Pi}_{\Phi}(\nu, t) \sim \left[\frac{\partial A(\nu, t)}{\partial t} \right]_{\nu}; \mathbf{\Pi}_{\Psi}(\nu, t) \sim - \left[\frac{\partial^2 A(\nu, t)}{\partial t^2} \right]_{\nu} \quad (1)$$

Where A is the absorbance (spectral intensity) as function of wavenumber ν and time t . This method make possible to extract information about the variation of the spectral gradient along the reaction [8,9,16].

Sample-sample 2D covariance and correlation-coefficient analysis. The sample-sample covariance matrix $\mathbf{\Phi}$ of a data matrix $\tilde{\mathbf{D}}$ that contain the spectra recorded in a reaction is obtained according to eq. 2. Each point in the sample-sample covariance matrix represents the covariance between a given pair of sample traces, such as those measured at different reaction times. Each vector or slice spectrum in this matrix $\mathbf{\Phi}$ gives information about the evolution of each sample in the matrix \mathbf{D} :

$$\mathbf{\Phi} = \frac{1}{m-1} \tilde{\mathbf{D}} \tilde{\mathbf{D}}^T \quad (2)$$

In this work, previously to calculate the covariance matrix $\mathbf{\Phi}$, the experimental data \mathbf{D} has been previously centered along the rows to obtain matrix $\tilde{\mathbf{D}}$.

The more representative slices of the reactive species involved in the DGEBA homopolymerization process has been determined accord-

ing to the recently established methodology by our research group that use the value of the correlation coefficient ρ_{ij} between all slices:

$$\rho_{ij} = \frac{cov(\mathbf{i}, \mathbf{j})}{SD_{\mathbf{i}} \cdot SD_{\mathbf{j}}} \quad (3)$$

where \mathbf{i} and \mathbf{j} two vectors or slices from matrix Φ .

For the sake of clarity, some details of the mentioned methodology are explained. The concentration profiles of a reaction R (reactive) $\rightarrow P$ (product) can be represented by two symmetric profiles, corresponding to each of the species involved and the value of correlation coefficient between those two profiles is -1. When the in the reaction take part an intermediate compounds, i.e. R (reactive) $\rightarrow I$ (intermediate) $\rightarrow P$ (product), several and different concentration profiles can be found to represent the dynamic evolution of the system depending on the reaction kinetic. When the correlation coefficients are calculated between all the profiles, an interval between +1 and -1 is found. Corresponding the zero value to the point of maxima dissimilarity between the profiles [20].

Multivariate curve resolution-alternating least squares method (MCR-ALS). The aim of MCR-ALS [21] method is the bilinear decomposition of the experimental data set \mathbf{D} in order to obtain matrices \mathbf{C} and \mathbf{S}^T , which have a real chemical significance, according to eq. 4:

$$\mathbf{D} = \mathbf{C}\mathbf{S}^T + \mathbf{E} \quad (4)$$

Where the dimensions of the matrices are: \mathbf{D} ($n \times m$), \mathbf{C} ($n \times c$), \mathbf{S}^T ($c \times m$), \mathbf{E} ($n \times m$); and c is the number of components considered (chemical species contributing to the signal), n is the number of spectra and m is the number of wavelengths in data matrix \mathbf{D} . \mathbf{C} is the matrix that describes the changes in the concentration of the species in the system under study. \mathbf{S}^T is the matrix that contains the response profile of these species (spectra profiles) and \mathbf{E} is the residual matrix with the data variance unexplained by the product $\mathbf{C} \cdot \mathbf{S}^T$.

In this work the MCR-ALS analysis has been done with the first derivative of matrix \mathbf{D} called $\mathbf{D}' = der[\mathbf{D}]$, to cancel the baseline line fluctuations in the spectra [22]. The procedure has been carried out according to the following steps:

(1) First, the number of factors present in \mathbf{D}' that have chemical information is estimated from the chemical rank associated with

the data matrix \mathbf{D}' . This determination is performed according to information found by singular values decomposition (SVD) of the data matrix \mathbf{D}' .

(2) The initial estimate were the concentration profiles of the chemical species involved in the DGEBA homopolymerization process obtained by sample-sample 2D covariance and correlation-coefficient analysis of the data of the matrix \mathbf{D}' .

(3) In the optimization process, in which ALS is applied to the matrix \mathbf{D}' , constraint of non-negativity for the concentrations.

The percentage of variance explained by the product of $\mathbf{C} \cdot \text{int}[\mathbf{S}^T]$, the lack of fit and the coefficient of similarity between the recovered spectra and the spectra of the pure species were used as parameters to evaluate the goodness of the model.

3 Experimental

Materials. Diglycidylether of bisphenol A (DGEBA) (Epikote 827 resin from Shell Chemicals, epoxy equiv. = 182.08 g/eq), was used as received. Ytterbium (III), lanthanum (III) and scandium (III) triflates (Aldrich) were used without previous purification.

Preparation of the Curing Mixtures. The samples were prepared by the mixing the selected initiator in the corresponding amount of DGEBA with manual stirring. All the mixtures contained 1 phr of metal triflate (1 part per 100 parts of resin mixture, w/w). The prepared mixtures were kept at -18°C before use.

Experimental conditions and FTIR-ATR data recorded. Three independent experimental curing processes were carried out with DGEBA in the presence of 1 phr (parts of initiator per 100 part of mixture, w/w) of scandium, ytterbium or lanthanum triflate. The curing was carried out at 160°C . In each process, the sample was placed on a small diamond crystal in the spectrophotometer ATR cell (Specac Golden Gate) (FTIR-680PLUS JASCO), which has a 3000 SeriesTM High Stability Temperature Controller with a RS232 Control to take the measurements. For each experiment we automatically acquired data at intervals of 30 seconds between 700 and 3800 cm^{-1} until no changes over time were observed in the spectra. The spectra recorded were exported and converted into Matlab binary files, and aligned in three independently matrices \mathbf{D} which dimensions were (50 x 3528) for scandium, (80 x 3528) for ytterbium and (180 x 3528) for lanthanum

triflates respectively.

Two dimensional correlation spectroscopy and Multivariate Curve Resolution methods. All calculations PCMW2D correlation, sample-sample 2D covariance-coefficient correlation were performed by in-house program coded in Matlab. The first derivate spectra were calculated by Savitzky-Golay method [23] and MCR-ALS was performed using the Matlab subroutines developed by R. Tauler [24] (Matlab version 6.5 The MathWorks, INC., Nattick. MA).

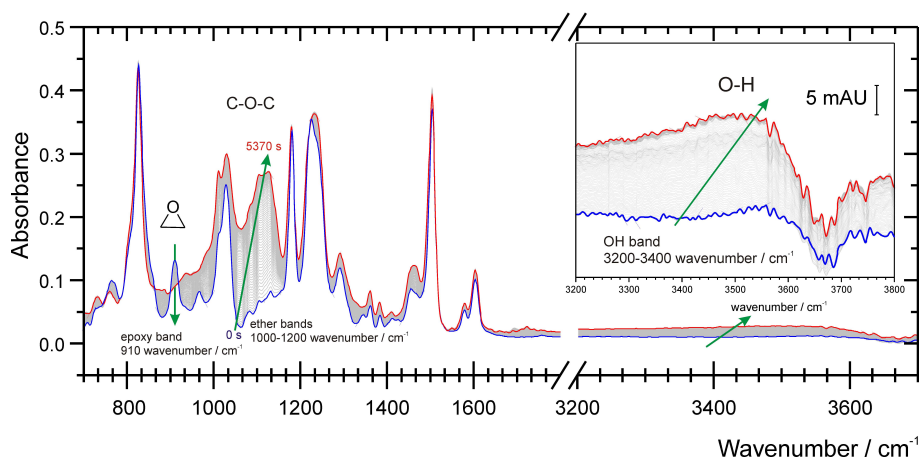


Figure 1: FTIR-ATR spectra recorder along the homopolymerization reaction of DGEBA at $T=160^{\circ}\text{C}$, using $\text{La}(\text{OTf})_3$ as cationic initiator.

4 Results and discussion

Spectral analysis. Spectroscopic analysis of spectra recorded for each experiment was done. Figure 1 displays the FTIR/ATR spectra obtained when the curing was carried out using $\text{La}(\text{OTf})_3$ as cationic initiator. We monitor the decrease of the intensities of the absorption band at 910 cm^{-1} along curing time. This band is assigned to the stretching modes of oxirane group present in DGEBA. Absorption bands in the region of $1000\text{-}1200\text{ cm}^{-1}$, which increase during the curing are attributable to the stretching of C-O-C of ether group present in the DGEBA or originated during curing. The weak and bad defined absorption bands in the region of $3200\text{-}3500\text{ cm}^{-1}$ are associated with

the stretching mode of OH group, present in the DGEBA. The spectral changes observed between 1600 and 1500 cm^{-1} , characteristic of the aromatic group, can be attributable to the variations produced as consequence of the increase of the viscosity during the curing process. Similar changes were observed when the curing was carried out using ytterbium or scandium triflates as initiators. With only this spectral analysis is not possible to extract information about the mechanism and to comparatively evaluate the effect of the initiators used. Therefore, PCMW2D correlation spectroscopy was utilized to analyze the changes produced in the IR spectra along the DGEBA homopolymerization reaction. The absorption in the hydroxylic zone (3500-3200 cm^{-1}) should not vary during the curing process even if AM mechanism participates. Therefore, the PCMW2D analysis was restricted to the 900 to 1150 cm^{-1} spectral region.

PCMW2D Correlation Analysis. Figure 2 shows the synchronous and asynchronous (PCMW2D) correlation spectrum obtained with a windows size equal to $(2m + 1 = 11)$ using lanthanum triflate as initiator. Positive and negative correlation areas are represented by red and blue hue colors, respectively. When a band shows a negative correlation value in a synchronous PCMW2D correlation spectrum, the intensity of the band decreases with the reaction time. An asynchronous PCMW2D correlation spectrum is proportional to the opposite sign of the second derivative of an intensity change with respect to the reaction time and their values can be correlated with the corresponding value in the synchronous spectrum using the rules of PCMW2D correlation analysis, shown in Table 1. This analysis allows to evaluate if the intensity variations for each absorption band, along of the reaction time, are constant or not and to compare their behavior with the other absorption bands, which allow studying the mechanism reaction. In Figure 2, the higher variations are centered around to 910 cm^{-1} characteristic of the oxirane group present in DGEBA and around of 1070 cm^{-1} and 1130 cm^{-1} characteristics of ether groups. Therefore, the information contained in the evolution of 910 cm^{-1} is the same but the opposite sign to the information contain in the evolution of band at 1070 or 1130 cm^{-1} and for this reasons to simplify the analysis, the slice spectrum extracted from the synchronous and asynchronous PCMW2D correlation spectrum at 910 cm^{-1} , was considered for all experiments. They will appear later in Figure 3. The information of synchronous and asynchronous

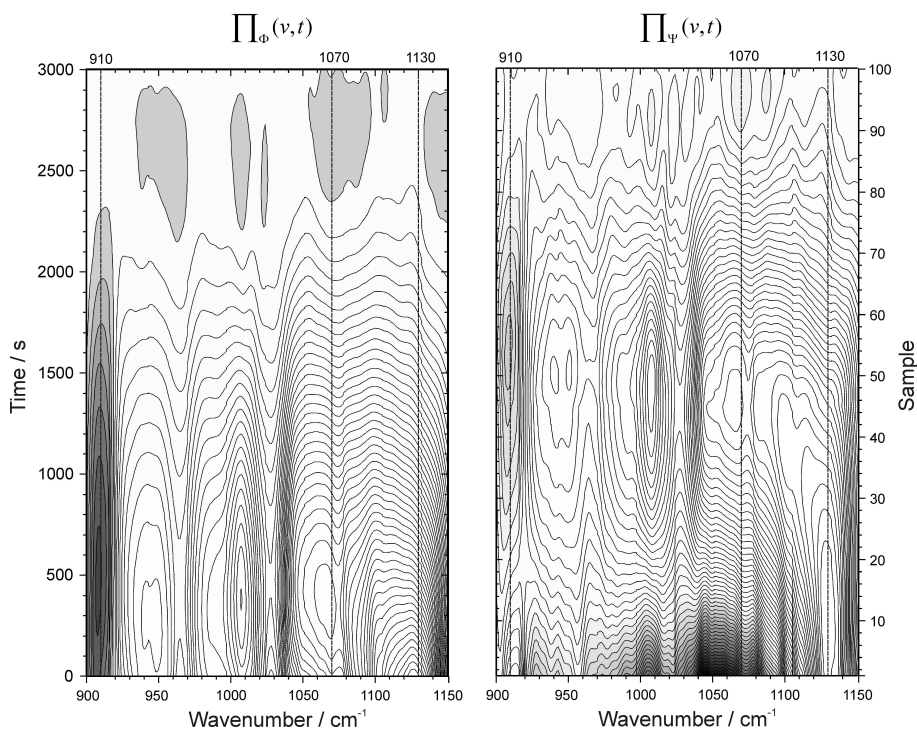


Figure 2: Synchronous and asynchronous PCMW2D correlation spectra in the 900-1150 cm^{-1} region calculated from the time-resolved IR spectra of the homopolymerization reaction of DGEBA, in presence of $\text{La}(\text{OTf})_3$ as initiator, measured over a time range 0-3000 s.

Table 1. Rules of PCMW2D Correlation spectroscopy in the case of linear increment of perturbation

Synchronous	Asynchronous	Spectral Changes
+	+	Convex increment
+	0	Linear increment
+	−	Concave increment
0	0	Constant
−	+	Convex decrement
−	0	Linear decrement
−	−	Concave decrement

PCMW2D spectra for 1070 and 1130 cm^{-1} , characteristic of ether group in transient species and product, is available in Figures A-1 and

A-2 of Appendix. Before detailing the results of the analysis, it is nec-

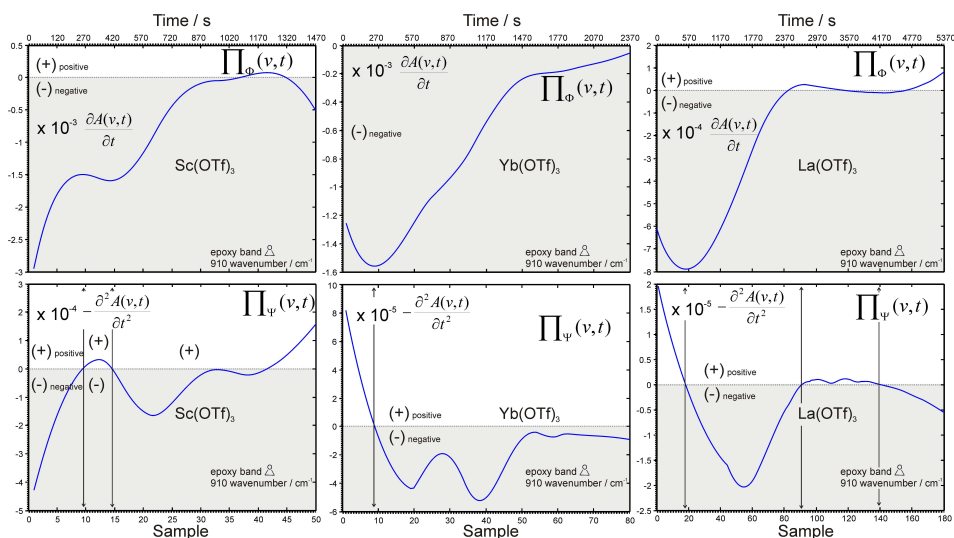


Figure 3: Slice spectra taken from the synchronous and asynchronous PCMW2D correlation spectra, for the epoxy band at 910 cm^{-1} , for each initiator: $\text{Sc}(\text{OTf})_3$, $\text{Yb}(\text{OTf})_3$, and $\text{La}(\text{OTf})_3$.

essary to indicate that the synchronous and asynchronous PCMW2D correlation spectrum obtained using ytterbium and scandium triflate as initiators were obtained using a windows size of $(2m + 1 = 11)$ respectively. Figure 3 shows the slices for the three initiators. It can be seen, that the values of the synchronous spectra (Π_Φ), are always negative, as was expected for a characteristic band of a reagent. However, their profile is different for each initiator. The similarity is higher between the profiles obtained when the initiator was ytterbium and lanthanum triflates. In the case of the scandium triflate, the more negative correlation is observed between sample 1 and 3. This is an indication that the variations of the absorption band at 910 cm^{-1} are more important between these samples. When using ytterbium triflate, the more negative correlation corresponds to sample 10 and when the initiator was the lanthanum, to sample 20. That is an indication that the opening of the oxirane group is quicker in presence of scandium versus ytterbium and this versus lanthanum which is in accordance with their Lewis acid trend. The different profiles obtained in each experiment can be an initial indication that the reaction mechanism is different for each initiator. This information can be obtained

combining, according to the rules of Table 1, the sign of the correlation values shown in the synchronous and the asynchronous slices spectrum (Π_{Ψ}) for each interval of samples. Numerical results of the sign combination can be obtained from equation 5 and the values corresponding to the diagonal slice $\xi(t, t)$, are show in Figure 4 for the epoxy band at 910 cm^{-1} :

$$\Xi(t_1, t_2) = \pi_{\Psi} \pi_{\Phi}^T \quad (5)$$

Now, it can clearly be seen that at the beginning of the reaction the variations of the band at 910 cm^{-1} , representative of the reagent, show a convex profile decrement (start at large negative value and goes to lower negative values), in the case of ytterbium and lanthanum. While the profile decrement is concave, (start at large positive value and goes to a lower positive value), for the scandium. The convex profile at 910 cm^{-1} at the beginning of the reaction is in agreement with the ACE mechanism postulated in Scheme 1, where the oxirane group is present in the transient species (HA^*) whereas in AM mechanism, the transient specie do not show the activated oxirane group at the end of the chain, as it is reflected in a concave decrement for scandium initiator. So, a possible interpretation is that at the beginning of the reaction the ACE mechanism is more favorable than the AM mechanism when the initiators used are ytterbium or lanthanum triflates. From this analysis it is clear that the curing process of DGEBA varies with the metal in the initiator. The AM mechanism requires the presence of OH in the medium, which is low accordingly to the weak spectral signal referenced between 3200 and 3500 cm^{-1} . In our opinion both mechanisms, shown in scheme 1, take place in the curing reaction independently of the initiators but the mechanism AM is more important in the case of scandium than for ytterbium and lanthanum. In order to evaluate the possibility to find the characteristic spectrum of the transient species involved in the curing process according to the ACE mechanism, multivariate curve resolution-alternating least squares (MCR-ALS) has been applied to the data matrix obtained with the lanthanum triflate as initiator as a consequence that it is in this experiment were the ACE mechanism is more evident during a longer period of time reaction, until sample 20.

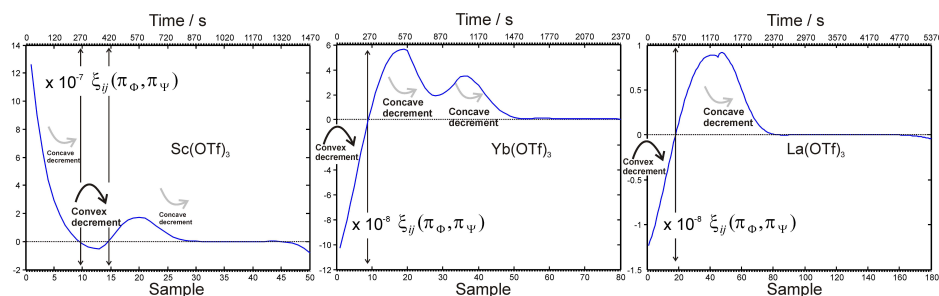


Figure 4: Graphics rules from PCMW2D Correlation analysis in time-dependent IR spectra, for the epoxy band at 910 cm^{-1} , for scandium, ytterbium and lanthanum triflates as initiators.

Multivariate Curve Resolution - Alternating Least Squares Analysis. First, the chemical rank of data matrix \mathbf{D}' that contains the first derivative of the spectra has been calculated by SVD [25]. According to Amrhein *et al.* [26], the chemical rank in a data matrix that contain the spectra recorded in a reaction is the minimum of $(r+1$ or $c)$ being r the number of independent reactions and c the number of the species involved in the process. In the spectral region considered in the data matrix it is possible to think that the present chemical species are the corresponding to the ACE mechanism in Scheme 1, therefore three. In this analysis three singular values ($\lambda_1 = 70.021$, $\lambda_2 = 5.700$, and $\lambda_3 = 0.545$) were considered significant, which is in agreement with the above mentioned. Initial estimation of concentration profiles of the chemical species associated with these factors, required by MCR-ALS, was obtained from sample-sample covariance spectroscopy.

Sample-sample covariance-correlation coefficient analyses. Figure 5 shows the 180 spectrum slice representatives of the evolution of the samples recorded in the DGEBA curing process in presence of lanthanum triflate. The more representative of them correspond to the samples 1, 29 and 180, which have a correlation coefficient of 1, 0.05 and -1 between the first spectrum slice.

Optimization step by alternating least-squares. Figure 6 shows the concentration profiles and the spectra profiles (figure A-3 Appendix) obtained in the optimization ALS step. In this process non-negativity constraints were imposed to matrix . The recovered variance according to Eq. (1) was 99.96%. The percentage of lack

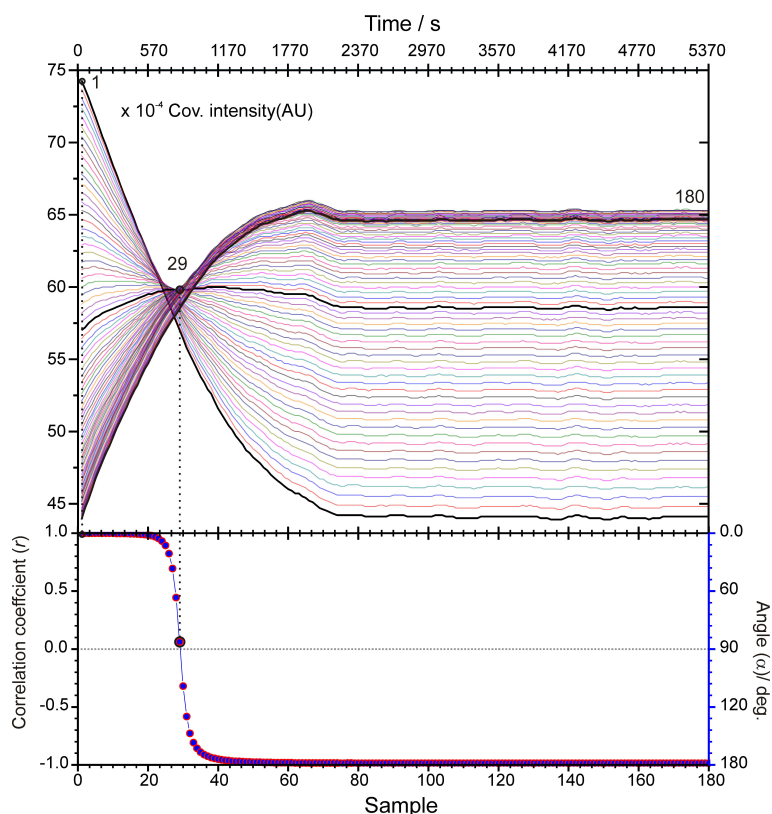


Figure 5: Estimate concentration profiles for the reactive species in the curing process for lanthanum as initiator from slices spectra taken of sample-sample covariance-correlation coefficient analyses.

of fit was 0.97%, which in quantitative terms means that it explains practically all the variability of the experimental data. Even more important than the concentration profiles is the fact that the recovered spectra associated to the transient species (HA^*) and product (PHA^*) are very similar. It is in agreement with two chemical species with the same chain end which could indicate that the polymerization mechanism has a living character. However, it should be said that the crosslinking of comonomers to form a thermoset implies that the reaction rate is reduced when the material gels and it loss its mobility. From this point the kinetics is diffusion controlled and some chain ends can not further react. The living character of rare earth metal triflates in the cationic polymerization of ϵ -caprolactone was demonstrated by

Nomura and co-workers [27].

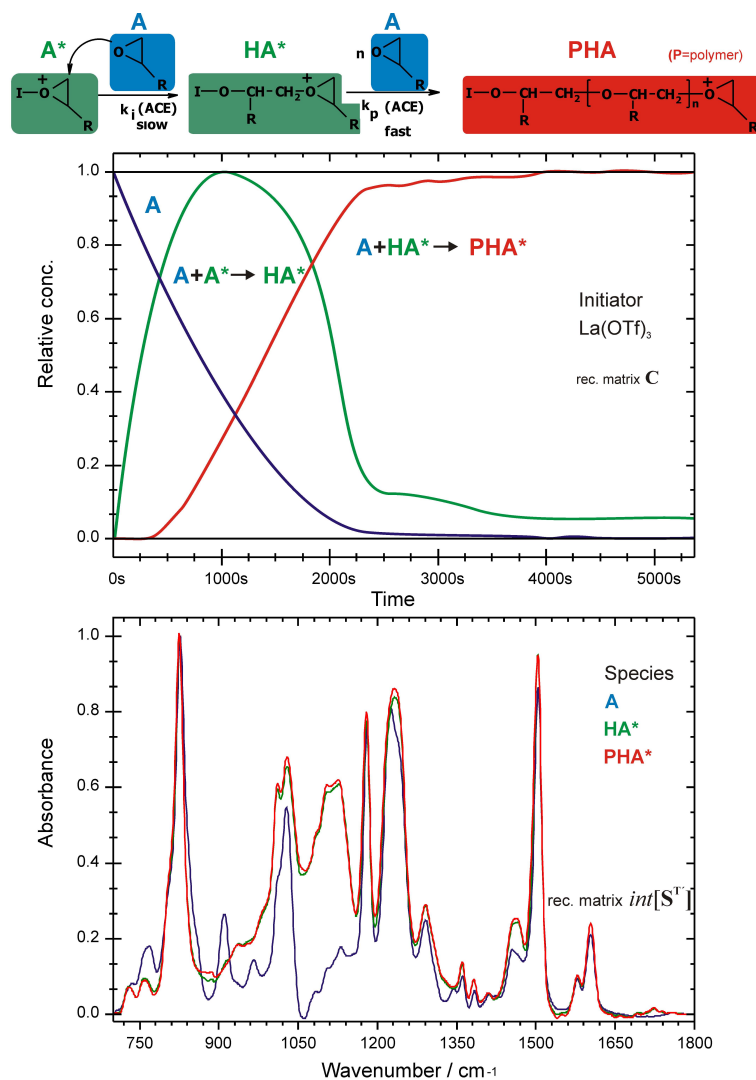


Figure 6: Concentration profiles and spectra recovered by MCR-ALS, for the reactive chemical species: A, HA* and PHA*.

5 Conclusions

The existence of the two mechanism ACE and AM in the homopolymerization process of DGEBA in presence of rare earth metal triflates, scandium, ytterbium and lanthanum, as initiators has been confirmed by PCMW2D correlation spectroscopy. AM mechanism is more favorable for scandium than for ytterbium or lanthanum triflates. The individual spectrum of the transient specie involved in the ACE mechanism has been extracted by MCR-ALS. Their spectra profile seems to suggest that the polymerization mechanism has a living character.

Acknowledgements

The authors would like to acknowledge the economic support provided by the MICINN projects CTQ2007-61474/BQU and MAT2008-06284-C03-01. Also N.S. acknowledges the Spanish Ministry of Education and Science (MEC) for the doctoral fellowship AP2006-04172.

References

- [1] P. Castell, M. Galià, A. Serra, J. M. Salla, and X. Ramis, *Polymer*, 41, (2000), 8465.
- [2] C. Mas, X. Ramis, J. M. Salla, A. Mantecón, and A. Serra, *J. Polym. Sci. Part. A: Polym. Chem.*, 41, (2003), 2794.
- [3] S. Penczek, P. Kubisa, and K. Matyjaszewski, *Adv. Polym. Sci.*, 37, (1980), 1.
- [4] E. J. Goethals, and S. Penczek, *Comprehensive Polymer Science*, Allen, G. and Bevington, J. C. Eds. Vol.3 Pergamon Press, Exeter, 1989, Chap. 45.
- [5] P. Kubisa, and S. Penczek, *Prog. Polym. Sci.*, 24, (1999), 1409.
- [6] S. Kobayashi, M. Sugiura, H. Kitagawa, and W. W.-L. Lam, *Chem. Rev.*, 102, (2002), 2227.
- [7] R. G. J. Pearson, *J. Am. Chem. Soc.*, 85, (1963), 3533.

- [8] A. Watanabe, S. Morita, and Y. Ozaki, *Appl. Spectrosc.*, 60, (2006), 611.
- [9] A. Watanabe, S. Morita, and Y. Ozaki, *Biomacromolecules*, 7, (2006), 3164.
- [10] M. A. do Nascimento, C. A. Paskocimas, A. J. N. Silva, and R. C. Ambrosio *J. Phys. Chem. C*, 111, (2007), 6813.
- [11] M. Lopez-Pastor, M. J. Ayora-Cañada, M Valcárcel, and B. Lendl, *J. Phys. Chem. B*, 110, (2006), 10896.
- [12] H. Dathe, P. Haider, A. Jentys, and J. A. Lercher, *J. Phys. Chem. B*, 110, (2006), 10729.
- [13] H. Dathe, P. Haider, A. Jentys, and J. A. Lercher, *J. Phys. Chem. B*, 110, (2006), 26024.
- [14] S. Šašić, A. Muszynski, and Y. Ozaki, *J. Phys. Chem. A*, 104, (2000), 6380.
- [15] N. Spegazzini, I. Ruisánchez, and M. S. Larrechi, *Anal. Chim. Acta*, 642, (2009), 155.
- [16] S. Morita, H. Shinzawa, I. Noda, and Y. Ozaki, *Appl. Spectrosc.*, 60, (2006), 398.
- [17] I. Noda, *Appl. Spectrosc.*, 47, (1993), 1329.
- [18] I. Noda, *Appl. Spectrosc.*, 54, (2000), 994.
- [19] M. Thomas, and H. Richardson, *Vib. Spectrosc.*, 24, (2000), 137.
- [20] N. Spegazzini, I. Ruisánchez, A. Serra, A. Mantecón, M. S. Larrechi, *Appl. Spectrosc.*, 64, (2010), 177.
- [21] R. Tauler, B. Kowalski, S. Fleming, *Anal. Chem.*, 65, (1993), 2040.
- [22] V. A. Lorenz-Fonfría, and H. J. Kandori, *J. Am. Chem. Soc.*, 131, (2009), 5891.
- [23] A. Savitzky, and M. J. E. Golay, *Anal. Chem.*, 36, (1964), 1627.

- [24] <http://www.ub.edu/mcr/ntheory.htm>, Group of Solution Equilibria and Chemometrics, Analytical Chemistry Department, University of Barcelona.
- [25] Golub, G. H.; Van Loan, Ch. F. *Matrix Computations*, The John Hopkins university Press, Baltimore, 1989; p50.
- [26] M. Amrhein, B. Srinivasan, D. Bonvin, and M. M. Schumacher, *Chemom. Intell. Lab. Syst.*, 33, (1996), 17.
- [27] N. Nomura, A. Taira, T. Tomioka, and M. Okada, *Macromolecules*, 33, (2000), 1497.

Appendix

Additional information: Synchronous and asynchronous PCMW2D spectra for 1070 and 1130 cm^{-1} characteristic of ether group present in transient specie and product, see Figures A-1 and A-2. Spectra retrieved $\mathbf{S}^{\text{T}'}$ from $\mathbf{D}' = \text{der}[\mathbf{D}]$, for different species (reagent, transient specie and product) in Figure A-3.

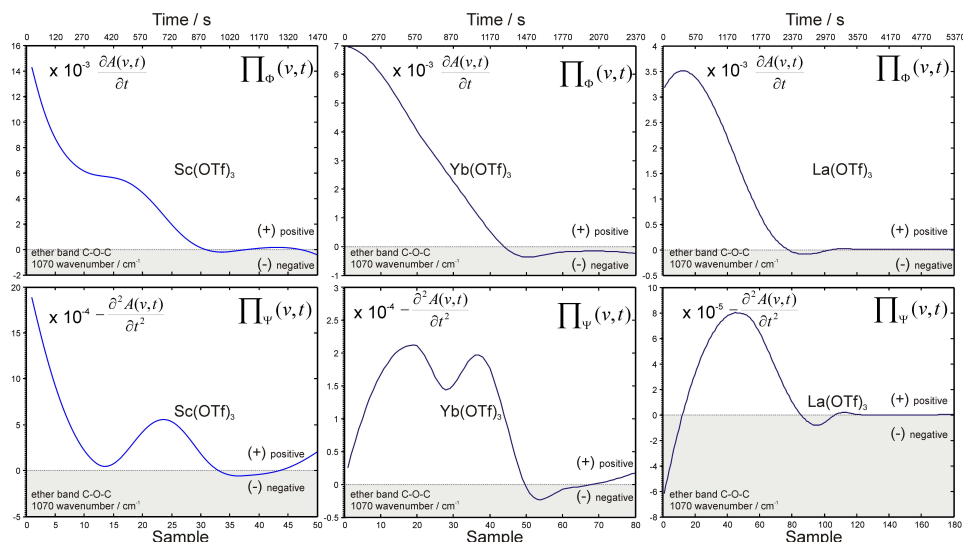


Figure A-1: Slices spectra taken from the synchronous and asynchronous PCMW2D correlation spectra, for the epoxy band 1070 cm^{-1} , for each initiator: $\text{Sc}(\text{OTf})_3$, $\text{Yb}(\text{OTf})_3$ and $\text{La}(\text{OTf})_3$.

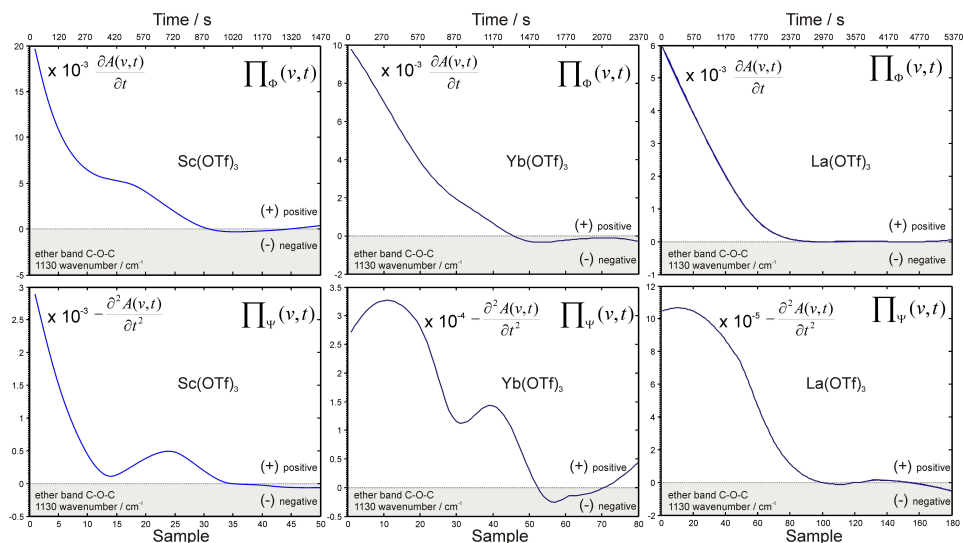


Figure A-2: Slices spectra taken from the synchronous and asynchronous PCMW2D correlation spectra, for the epoxy band 1130 cm^{-1} , for each initiator: $\text{Sc}(\text{OTf})_3$, $\text{Yb}(\text{OTf})_3$ and $\text{La}(\text{OTf})_3$.

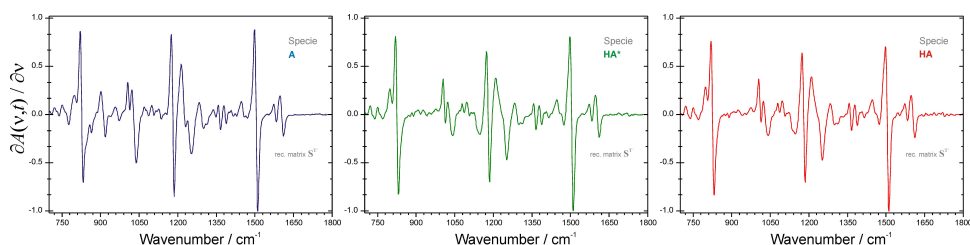


Figure A-3: First derivate spectra recovered by MCR-ALS, for the reactive chemical species: A, HA^* and PHA^* .

UNIVERSITAT ROVIRA I VIRGILI

TWO-DIMENSIONAL INFRARED CORRELATION SPECTROSCOPY AND MULTIVARIATE CURVE RESOLUTION

METHODS: APPLICATION TO QUANTITATIVE MONITORING OF CURING PROCESS

Nicolas Spegazzini

ISBN:978-84-693-4049-3/DL:T.998-2010

Chapter 4

CONCLUSIONS

UNIVERSITAT ROVIRA I VIRGILI

TWO-DIMENSIONAL INFRARED CORRELATION SPECTROSCOPY AND MULTIVARIATE CURVE RESOLUTION

METHODS: APPLICATION TO QUANTITATIVE MONITORING OF CURING PROCESS

Nicolas Spegazzini

ISBN:978-84-693-4049-3/DL:T.998-2010

Because each paper presented in **Chapter 3** contains its own **conclusion** section, this chapter emphasizes the thesis conclusions according to the goals set out in the **Scope** section. The first and most general conclusion is that multidimensional correlation spectroscopy and the multivariate curve resolution method are useful chemometric methods for quantitatively monitoring a curing process using infrared spectroscopy.

Specifically, we can also state that:

- Generalized and perturbation-correlation moving-windows two-dimensional correlation spectroscopy, are valuable methods for obtaining information about the reaction pathway in the case studied, which was representative of a curing process.
- Sample-sample two-dimensional correlation spectroscopy is a very useful method for obtaining concentration profiles of the chemical species involved in the curing process.
- And finally, MCR-ALS is a very useful method for the quantitative resolution of the curing process.

UNIVERSITAT ROVIRA I VIRGILI

TWO-DIMENSIONAL INFRARED CORRELATION SPECTROSCOPY AND MULTIVARIATE CURVE RESOLUTION

METHODS: APPLICATION TO QUANTITATIVE MONITORING OF CURING PROCESS

Nicolas Spegazzini

ISBN:978-84-693-4049-3/DL:T.998-2010

REFERENCES

UNIVERSITAT ROVIRA I VIRGILI

TWO-DIMENSIONAL INFRARED CORRELATION SPECTROSCOPY AND MULTIVARIATE CURVE RESOLUTION

METHODS: APPLICATION TO QUANTITATIVE MONITORING OF CURING PROCESS

Nicolas Spegazzini

ISBN:978-84-693-4049-3/DL:T.998-2010

- [1] C.A. May, Epoxy resins:chemistry and technology, 2nd ed.; Marcel Dekker, New York, 1988.
- [2] B. Ellis, Chemistry and Technology of Epoxy Resins, Blackie Academic Professional, New York, 1993.
- [3] H. J. Flammersheim, *Thermochim. Acta*, 310, (1998), 153.
- [4] S. Swier, B. Van Mele, *Thermochim. Acta*, 411, 2004, 149.
- [5] P. Musto, G. Ragosta, P. Russo, L. Mascia, *Macromol. Chem. Phys.*, 202, (2001), 3445.
- [6] B. Strehmel, V. Strehmel, M. Younes, *J. Polym. Sci. Part B: Polym. Phys.*, 37, (1999), 1367.
- [7] R. E. Lyon, K. E. Chike, S. M. Angel, *J. Appl. Polym. Sci.*, 53, (1994), 1805.
- [8] R. E. Challis, M. E. Unwin, D. L. Chadwick, R. J. Freemantle, I. K. Partridge, D. J. Dare, P. I. Karkanias, *J. Appl. Polym. Sci.*, 88, (2003), 1665.
- [9] M. Fedtke, J. Haufe, E. Kahler, G. Müller, *Angew. Makromol. Chem.*, 255, (1998), 53.
- [10] G. A. George, P. Cole-Clarke, N. St. John, G. Friend, *J. Appl. Polym. Sci.*, 42, 1991, 643.
- [11] V. Strehmel, T. Scherzer, *Eur. Polym. J.*, 30, 1994, 361.
- [12] Y. Du, J. Jiang, Y. Liang, T. Amari, Y. Ozaki, *Analyst*, 128, (2003), 1320.
- [13] S. Šašić, T. Amari, Y. Ozaki, *Anal. Chem.* 73, (2001), 5184.
- [14] L. Xu, J.H. Fu, J. Schlup, *Ind. Eng. Chem. Res.* 35, 1996, 963.

- [15] C. Billaud, M. Vandeuren, R. Legras, V. Carlier, *Appl. Spectrosc.* 56, 2002, 1413.
- [16] T. Amari, Y. Ozaki, *Appl. Spectrosc.* 56, 2002, 350.
- [17] K. Dean, W. Cook, L. Rey, J. Galy, H. Sautereau, *Macromolecules* 34, 2001, 6623.
- [18] Castan, P.; *Swiss Pat.* 211, 116 (1940).
- [19] P. Castell, M. Galià, A. Serra, J. M. Salla, X. Ramis, *Polymer*, 41, (2000), 8565.
- [20] C. Mas, X. Ramis, J. M. Salla, A. Mantecón, A. Serra, *J. Polym. Sci. Part A: Polym. Chem.*, 41, (2003), 2794.
- [21] L. González, X. Ramis, J. M. Salla, A. Mantecón, A. Serra, *J. Polym. Sci. Part A: Polym. Chem.*, 44, (2006), 6869.
- [22] S. González, X. Fernandez-Francos, J. M. Salla, A. Serra, A. Mantecón, X. Ramis, *J. Appl. Polym. Sci.*, 104, (2007), 3406.
- [23] J. Canadell, A. Mantecón, V. Cádiz, *J. Polym. Sci. Part A: Polym. Chem.*, 44, (2006), 4722.
- [24] S. Kobayashi, S. Nagayama, T. Busujima, *J. Am. Chem. Soc.*, 120, (1998), 8287.
- [25] S. Kobayashi, *Synlett*, 9, (1994), 689.
- [26] S. Kobayashi, I. Hachiya, M. Araki, H. Ishitani, *Tetrahedron Lett.*, 34, (1993), 3755.
- [27] A. De Nino, L. Maiuolo, M. Nardi, A. Procopio, A. Tagarelli, *Synthesis*, 4, (2004), 496.
- [28] H. Tsuruta, K. Yamaguchi, T. Imamoto, *Chem. Commun.*, (1999), 1703.
- [29] I. Noda, *Bull. Am. Phys. Soc.*, 31, (1986), 520.
- [30] I. Noda, *J. Am. Chem. Soc.*, 111, (1989), 8116.
- [31] I. Noda, *Appl. Spectrosc.*, 44, (1990), 550.

- [32] I. Noda, *Appl. Spectrosc.*, 47, (1993), 1329.
- [33] I. Noda, *Appl. Spectrosc.*, 54, (2000), 994.
- [34] S. Šašić, A. Muszynski, Y. Ozaki, *Appl. Spectrosc.*, 55, (2001), 343.
- [35] T. Isaksson, Y. Katsumoto, Y. Ozaki, I. Noda, *Appl. Spectrosc.*, 56, (2002), 1289.
- [36] I. Noda, A.E. Dowrey, C. Marcott, G. M. Story, Y. Ozaki, *Appl. Spectrosc.* 54 (2000) 236A.
- [37] I. Noda, Y. Ozaki, *Two-dimensional Correlation Spectroscopy-Applications in Vibrational and Optical Spectroscopy*, Wiley, Chichester, 2004.
- [38] M. Müller, R. Buchet, U. P. Fringeli, *J. Phys. Chem.* 100, (1996), 10810.
- [39] I. Noda, in: Y. Ozaki, I. Noda (Eds.) *Two-Dimensional Correlation Spectroscopy*, AIP Press, Melville, 2000, pp.201-204.
- [40] S. Morita, Y. Ozaki, I. Noda, *Appl. Spectrosc.* 55, (2001), 1618.
- [41] C. Zimba, Presented at the Second International Symposium on Advanced Infrared Spectroscopy (AIRS II), Durham, NC, 17 June 1996; and at the First International Symposium on Two-Dimensional Correlation Spectroscopy (2DCOS), Sanda, Japan, 30 August 1999.
- [42] S. Šašić, A. Muszynski, Y. Ozaki, *J. Phys. Chem. A* 104, (2000), 6380.
- [43] M. Thomas, H. Richardson, *Vib. Spectrosc.* 24, (2000), 137.
- [44] S. Morita, H. Shinzawa, I. Noda, Y. Ozaki, *Appl. Spectrosc.* 60, (2006), 398.
- [45] A. Watanabe, S. Morita, Y. Ozaki, *Appl. Spectrosc.* 60, (2006), 1054.
- [46] A. Watanabe, S. Morita, Y. Ozaki, *Biomacromolecules*, 8, (2007), 2969.

- [47] W. H. Lawton, E. A. Sylvestre, *Technometrics*, 13, (1971), 617.
- [48] E. J. Karjlainen, *Chemom. Intell. Lab. Syst.*, 14, (1989), 31.
- [49] R. Tauler, B. Kowalski, S. Fleming, *Anal. Chem.*, 65, (1993), 2040.
- [50] R. Tauler, *Chemom. Intell. Lab. Syst.*, 30, (1995), 133-146.
- [51] R. Tauler, A. K. Smilde, B. Kowalski, *J. Chemom.*, 9, (1995), 31-58.
- [52] A. de Juan, R. Tauler, *Anal. Chim. Acta*, 500, (2003), 195-210.
- [53] A. de Juan, Y. Vander Hieden, R. Tauler, D. L. Massart, *Anal. Chim. Acta*, 346, 1997, 307.
- [54] M. Maeder, *Anal. Chem.*, 59, (1987), 527.
- [55] W. Windig, J. Guilment, *Anal. Chem.*, 63, (1991), 1425.
- [56] F. Cuesta Sanchez, B. van den Bogaert, S.C. Rutan, D. L. Massart, *Chemom. Intell. Lab. Syst.*, 34 (1996) 139- 171.
- [57] H. R. Keller, D. L. Massart, *Chemom. Intell. Lab. Syst.*, 12, (1992), 209.
- [58] H. Shinsawa, M. Iwahashi, I. Noda, Y. Ozaki, *J. Mol. Struct.* 883-884, (2004), 73.
- [59] B. G. Osborne, T. Fearn, P. H. Hindle, *Practical NIR spectroscopy with application in food and beverage analysis*, Longman Scientific Technical, 2da Ed. Harlow, England, 1993.
- [60] H. Günzler, H. -U. Gremlich, *IR Spectroscopy An Introduction*, Wiley-VCH Verlag GmbH, Weinheim, 2002.

A

Appendix

UNIVERSITAT ROVIRA I VIRGILI

TWO-DIMENSIONAL INFRARED CORRELATION SPECTROSCOPY AND MULTIVARIATE CURVE RESOLUTION

METHODS: APPLICATION TO QUANTITATIVE MONITORING OF CURING PROCESS

Nicolas Spegazzini

ISBN:978-84-693-4049-3/DL:T.998-2010

A.1 Papers Presented

1. Two-dimensional fourier transform infrared correlation spectroscopy and evolving factor analysis in the study of cationic curing of DGEBA and γ -valerolactone mixtures.

N. Spegazzini, I. Ruisánchez, M. S. Larrechi, A. Serra, A. Mantecón.

Journal Polymer Science Part A: Polymer Chemistry 46, (2008), 3886.

Chemometrics, Qualimetrics and Nanosensors Group, Polymer's Research Group, Department of Analytical and Organic Chemistry, Rovira i Virgili University. Marcel·lí Domingo s/n, 43007, Tarragona, Spain.

2. Spectroscopic and quantitative analysis of the spiroorthoester synthesis by two-dimensional correlation and multivariate curve resolution methods of NIR data.

N. Spegazzini, I. Ruisánchez, M. S. Larrechi, V. Cádiz, J. Canadell

Analyst, 133, 1028 (2008)

Chemometrics, Qualimetrics and Nanosensors Group, Polymer's Research Group, Department of Analytical and Organic Chemistry, Rovira i Virgili University. Marcel·lí Domingo s/n, 43007, Tarragona, Spain.

3. MCR-ALS for sequential estimation of FTIR-ATR spectra to resolve a curing process using global phase angle convergence criterion

N. Spegazzini, I. Ruisánchez, M. S. Larrechi

Analytica Chimica Acta, 642, (2009), 155.

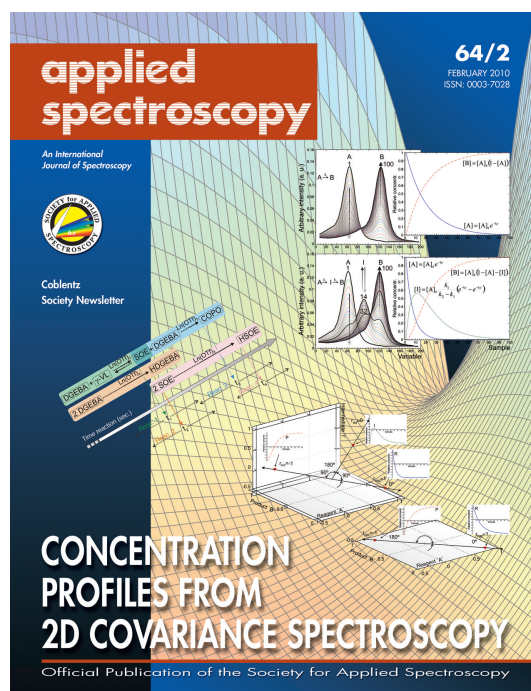
Chemometrics, Qualimetrics and Nanosensors Group, Department of Analytical and Organic Chemistry, Rovira i Virgili University. Marcel·lí Domingo s/n, 43007, Tarragona, Spain.

4. A methodology to estimate concentration profiles from 2D covariance spectroscopy applied to kinetic data.

N. Spegazzini, I. Ruisánchez, M. S. Larrechi, A. Serra, A. Mantecón.

Applied Spectroscopy 64, (2010), 177. (February-Cover).

Chemometrics, Qualimetrics and Nanosensors Group, Polymer's Research Group, Department of Analytical and Organic Chemistry, Rovira i Virgili University. Marcel·lí Domingo s/n, 43007, Tarragona, Spain.



5. Spectroscopic evidence of the mechanism involved in the cationic DGEBA curing with rare earth metal triflates.

N. Spegazzini, I. Ruisánchez, M. S. Larrechi, A. Serra, A. Mantecón.

Applied Spectroscopy 64, (2010), 104.

Chemometrics, Qualimetrics and Nanosensors Group, Polymer's Research Group, Department of Analytical and Organic Chemistry, Rovira i Virgili University. Marcel·lí Domingo s/n, 43007, Tarragona, Spain.

A.2 Meeting Contributions

Two-dimensional fourier transform infrared correlation spectroscopy and evolving factor analysis in the study of cationic curing of DGEBA and γ -valerolactone mixtures.

N. Spegazzini, I. Ruisánchez, M. S. Larrechi, A. Serra, A. Mantecón.

VII Colloquium Chemiometricum Mediterraneum
St. Maximin, France, September 5 - 7 (2007)

Poster communication

Sequential Estimation of IR Spectra of the Intermediate compounds obtained during the cationic curing of DGEBA and γ -valerolactone. A strategy to resolve several and parallel reactions by MCR-ALS.

N. Spegazzini, I. Ruisánchez, M. S. Larrechi, A. Serra, A. Mantecón.

“11 th International Conference on Chemometrics for Analytical Chemistry (CAC 2008)”
Montpellier, France, 30 June - 4 July (2008)

Poster communication

Sequential estimation of FTIR-ATR spectra of the intermediate compounds to resolve consecutives and sides reactions in cationic curing process by MCR-ALS. A strategy based on convergence criterion by global phase angle.

N. Spegazzini, I. Ruisánchez, M. S. Larrechi.

III Workshop of Chemometrics (III Workshop de Quimiometría)
Burgos, Spain, September 15 - 16 (2008)

Oral communication

Hybrid moving-windows two-dimensional correlation of IR spectra to analyze the effect of lanthanides triflates catalyst in the cationic curing process.

N. Spegazzini, I. Ruisánchez, M. S. Larrechi.

“12 th Conference on Instrumental Analysis”
Barcelona, Spain, October 21 - 23 (2008)

Poster communication

Quantitative analysis of DGEBA crosslinking with rare earth metal triflates using two-dimensional infrared correlation spectroscopy and multivariate curve resolution method.

N. Spegazzini, I. Ruisánchez, A. Serra, A. Mantecón, M. S. Larrechi.

“Fifth International Symposium on Two-Dimensional Correlation Spectroscopy (2DCOS-5)”
Wrocław, Poland, August 5 - 7 (2009)

Oral communication

A methodology to estimate concentration profiles from 2D covariance spectroscopy applied to kinetic data.

N. Spegazzini, I. Ruisánchez, M. S. Larrechi.

“Fifth International Symposium on Two-Dimensional Correlation Spectroscopy (2DCOS-5)”
Wrocław, Poland, August 5 - 7 (2009)

Poster communication (**3rd place in poster session**)

B

Predoctoral Formation

B.1 Master

Master's degree in Industrial Chemistry

Thesis: Two-Dimensional Correlation Spectroscopy for Monitoring a Polymerization Reaction

Universitat Rovira i Virgili
Tarragona, Spain, June 2007.

B.2 Stay Abroad

Objective: Learning and applying multivariate curve resolution methods combined with thermodynamic data to curing processes.

Three-months stay in the Automatic Control Laboratory, Swiss Federal Institute of Technology at Lausanne (EPFL), Switzerland, under the supervision of Dr. Michael Amrhein and Prof. Dominic Bonvin.

Supported by Ministry of Education and Science (MEC), Spain, September - November 2009.

**TWO-DIMENSIONAL INFRARED
CORRELATION SPECTROSCOPY
AND MULTIVARIATE CURVE
RESOLUTION METHODS**

Application to quantitative
monitoring of curing process

Doctoral thesis. Nicolas Spegazzini.

The curing process of epoxy resin directly affects the properties of the final polymer, so it is of great interest to develop analytical methods that make it possible to determine the pathway of the curing processes. Numerous studies have examined the evolution of the curing process and the quantification of the corresponding kinetic parameters using various techniques, such as differential scanning calorimetry (DSC), differential scanning calorimetry with temperature modulation (MTDSC), thermogravimetric analysis (TGA), fluorescence, Raman spectroscopy, nuclear magnetic resonance (NMR), high-resolution liquid chromatography (HPLC), infrared spectroscopy Fourier transform (FTIR) and near-infrared spectroscopy (NIR). Most studies use model reactions because it is very difficult, and sometimes even impossible, to isolate the intermediate products that are involved in the curing process. This thesis aims to explore the possibilities of multidimensional correlation spectroscopy for the quantitative monitorization of curing processes by means of infrared spectroscopy and curve resolution methods. The thesis focuses on a complex reaction in which several side reactions might take place, most or all of them almost simultaneously.

The thesis is structured in several chapters, as set out below.

Chapter 1 presents the background to this thesis, highlighting the current interest in studying epoxy resins. The theory of two-dimensional spectroscopy analysis is briefly reviewed and the relevant chemometric tools (multivariate curve resolution methods) are presented. This chapter also discusses the novelties introduced in the thesis and provides references for the underlying basic concepts.

Chapter 2 concerns the experimental work. The instrumental analytical techniques used to monitor the curing process are briefly described. The experimental conditions and setup of two main curing reactions are described: a reaction between phenylglycidylether (PGE) and γ -butyrolactone monitored by NIR, and copolymerization between diglycidyl ether of bisphenol A (DGEBA) and γ -valerolactone by FTIR/ATR. The conditions of the DGEBA homopolymerization are also presented. Finally, the ^1H and ^{13}C NMR experimental conditions for obtaining the spectrum of the final product in the first reaction between PGE and γ -butyrolactone are described.

Chapter 3 presents the results of the experimental work that has been carried out. This chapter cites five published works, each introduced with a brief description of the study's main goal and content. The five articles are presented in sequential order according to the main goal of the thesis.

Chapter 4 contains the conclusions and describes the goals achieved.